Acoustic scattering in waveguides with smoothly-varying or discontinuous elastic boundaries

A thesis submitted for the degree of Doctor of Philosophy

by

Andrew David Grant

Department of Mathematical Sciences, Brunel University

September 2001

Abstract

A method for solving boundary-value problems where a boundary parameter varies continuously in space is applied to some canonical waveguide problems. The method, previously employed by Roseau and Evans, generates a functional difference equation, the solution to which enables fluid velocity potential to be written as an explicit integral transform.

The two main problems to which the method is applied are a two-dimensional waveguide with a varying impedance condition and an elastic-walled waveguide with varying bending stiffness.

Limiting versions of the two problems are solved using the Wiener–Hopf technique. This provides a check on the varying-parameter solutions as well as being of interest in itself.

Acknowledgments I thank my supervisor, Dr Jane B Lawrie, for her expert guidance. I am also grateful to Dr Najla El-Sharif and Professor Edward Twizell for encouraging me to undertake this research.

Contents

List of Figures

Chapter 1

Introduction

Acoustic scattering by structures that have abrupt changes in either geometry or material properties pose many technical problems for scientists and engineers. For example welds, rivets and small physical variations in the properties of adjacent panels in an aircraft wing all give rise to scattering of fluid-coupled structural waves. It is essential for design engineers to understand the qualitative effects of, for example, sudden variation in panel depth or the presence of a weld. Presence of two or more such features gives rise to the possibility of resonance, which in turn could lead to structural fatigue. For these reasons, scattering by a wide variety of key structural features has been studied extensively.

Problems involving structures that have planar boundaries with abrupt change in material properties may be amenable to solution by the Wiener–Hopf technique. Recent work on examples of this type include Brazier-Smith [3], Norris and Wickham [19] and Cannell [4, 5]. For non-planar boundaries, there are no standard solution methods. Structures comprising two planar surfaces that are joined together to form a wedge may be solved by recourse to the Kontorovich–Lebedev transform [1, 22], or the Sommerfeld integral [2, 21]. Other geometric discontinuities that are amenable to analytic solution include problems involving wave propagation in a duct with abrupt change in height [25].

Scattering by structures in which the material properties vary smoothly in space as opposed to discontinuously have, for a variety of reasons, received little attention, although a finite transition region may be a better model of many real materials. Work by Roseau [23], Evans [8], and Fernyhough and Evans [9] applies one of the few mathematical techniques available for this kind of problem. Roseau solved a water-wave problem where the depth of water varied owing to a sloping bottom with a continuous, non-linear profile. By representing the fluid velocity potential as a Fourier integral, Roseau was able to recast the boundary-value problem as a functional difference equation of a well-known class. Evans was able to employ the same technique to solve another water-wave problem in which particles of varying density float on the surface of a body of water of constant depth. Evans and Fernyhough then extended the method to deal with the problem of scattering in an acoustic waveguide in which the bounding surface had smoothly varying impedance.

In this thesis the functional difference equation method is applied to a waveguide in which the bounding surface is an elastic plate. The elastic properties of the plate vary continuously, giving rise to a fourth-order boundary condition with space-dependent parameters. Related problems also investigated here include the impedance problem mentioned above (dealt with here in more detail than in the published work of Evans and Fernyhough) and limiting cases of the waveguide problems in which material properties change abruptly at some point in space.

Chapter 2 reviews linear functional difference equations, mainly of the first order, and the Wiener–Hopf method, as both of these techniques are fundamental to the solution of boundary-value problems in later chapters. In §2.2–§2.10 first-order functional difference equations are categorised and examples of their solution by means of the gamma function, infinite products, Mittag-Leffler series and integrals are given. In §2.11 the Wiener–Hopf method is reviewed and demonstrated by means of an example involving a duct with an elastic plate wall.

In chapter 3 a boundary-value problem with an impedance boundary condition varying in space is solved. Two methods are used, one in the case of smoothly-varying impedance and the other for abrupt variation. It is demonstrated that the two methods agree by comparing results for the limiting case of smoothly-varying impedance with those for abrupt change. The smoothly-varying impedance problem has been solved by Fernyhough and Evans [9], but it is included here because it was original at the time of execution, and the related Wiener–Hopf problem which is solved here is not included in their work.

In chapters 4 and 5, the duct wall with impedance boundary condition is replaced by an elastic plate. Solutions to the smoothly-varying case (chapter 4) and abruptly-varying case (chapter 5) are developed in a way which parallels the work in chapter 3, although there are extra complications due to the higher-order boundary condition and the fact that energy is propagated in elastic waves in the plate as well as in the fluid. In the case of a thin elastic-plate wall, a varying thickness model may be the most obviously practical one, but the mathematical analysis is equally applicable to a plate of constant thickness but varying material, such as an alloy containing changing proportions of metals, and to situations where both thickness and material vary in a suitable way.

All the analyses are for the steady state where wave motion is time harmonic. The velocity potential in such a two-dimensional problem has the form

$$\Phi(x,y,t) = \Re\{\phi(x,y)e^{-i\omega t}\}, \tag{1.1}$$

where ϕ is the complex potential in space variables only, and ω is the angular frequency, typically in radians per second. We separate the time and space variables, omitting the factor $e^{-i\omega t}$ and formulate the boundary-value problem to be solved in terms of $\phi(x,y)$ only. This convention is observed throughout.

Chapter 2

Mathematical methods

2.1 Introduction

This chapter reviews several techniques for solving functional difference equations for meromorphic functions, *ie* those which are analytic in the complex plane except for poles. The Wiener–Hopf technique is also illustrated and the relation between the two methods is discussed.

The meromorphic functions occur in the Fourier transforms of velocity potential fields, particularly in duct problems of the kind investigated in the thesis. Being meromorphic, they are free from branch points which are characteristic of fields which are not confined to ducts.

General references are Milne-Thompson, [16], for functional difference equations and Noble, [18], for the Wiener–Hopf method.

2.2 Types of functional difference equation

A functional difference equation method [23] is the key to solving the class of boundary-value problems considered in this thesis. Here the method is reviewed with reference to the particular kinds of functional difference equations (fdes) encountered in the thesis.

It is required to find a meromorphic function, $f(z)$, which satisfies an equation of one of the following types. Equations (2.1)–(2.4) have been written as relations between $f(z+1)$ and $f(z)$, but the methods of solution are easily extended to relations between $f(z+c)$ and $f(z)$ for any complex c. The solutions may be required to exist throughout the complex plane except at singularities. Further conditions, consequent upon the nature of the physical problem, will determine which of a family of solutions is chosen.

The first type of equation considered is the linear, constant-coefficient equation

$$f(z+1) - f(z) = h(z), \tag{2.1}$$

where $h(z)$ is a given meromorphic function. Related to this is the linear, variable-coefficient, homogeneous equation

$$\frac{f(z+1)}{f(z)} = g(z), \tag{2.2}$$

which may be derived from an equation of type (2.1) by taking the exponential function of both sides. A non-homogeneous generalisation of (2.2) is

$$f(z+1) - g(z)f(z) = h(z), \tag{2.3}$$

where $g(z)$ and $h(z)$ are two given meromorphic functions. Higher-order equations, such as the second-order

$$f(z+2) + g_1(z)f(z+1) + g_2(z)f(z) = h(z), \tag{2.4}$$

may also arise.

2.3 Solutions of simple constant-coefficient equations

A simple case of equation (2.1) is where $h(z) = z^k$, k being a non-negative integer. The general solution of this type of equation is given in [16]. There is a solution in terms of the Bernoulli polynomial $B_{k+1}(z)$,

$$f(z) = \frac{B_{k+1}(z)}{k+1}. \tag{2.5}$$

If $h(z) = z^{-k}$, where k is a positive integer, it is shown in [16] that there is a solution in terms of a derivative of the digamma function $\Psi(z) = \Gamma'(z)/\Gamma(z)$,

$$f(z) = \frac{(-1)^{k-1}}{(k-1)!}\Psi^{(k-1)}(z). \tag{2.6}$$

From (2.5) and (2.6), a solution to (2.1) can be constructed for any rational function $h(z)$, by writing

$$h(z) = p(z) + \sum_j q_j(z)^{-b_j}, \tag{2.7}$$

where $p(z)$ is a polynomial, $q_j(z)$ are first-degree polynomials and b_j are positive integers. Equation (2.1) is then solved with $h(z)$ replaced by each term of (2.7) in turn and the resulting solutions are combined by using the additivity and translation properties of (2.1).

Additivity: If $f_1(z)$ and $f_2(z)$ satisfy

$$f_1(z+1) - f_1(z) = h_1(z)$$

and

$$f_2(z+1) - f_2(z) = h_2(z),$$

then $f_3 = f_1(z) + f_2(z)$ satisfies

$$f_3(z+1) - f_3(z) = h_1(z) + h_2(z).$$

Translation: If $f(z)$ satisfies (2.1), then $f_\alpha(z) = f(z+\alpha)$ satisfies

$$f_\alpha(z+1) - f_\alpha(z) = h(z+\alpha).$$

Example 2.3.1 *It is convenient to use the function occurring in (3.19), but in an equation of type (2.1),*

$$f(s+1) - f(s) = \frac{s^2-\alpha_0^2}{s^2-\beta_0^2}. \tag{2.8}$$

The partial fraction representation (2.7) is, in this case,

$$\frac{s^2-\alpha_0^2}{s^2-\beta_0^2} = 1 + \frac{\beta_0^2-\alpha_0^2}{2\beta_0}\left(\frac{1}{s-\beta_0} - \frac{1}{s+\beta_0}\right),$$

and the solution to (2.8) is

$$f(s) = B_1(s) + \frac{\beta_0^2-\alpha_0^2}{2\beta_0}\{\Psi(s-\beta_0) - \Psi(s+\beta_0)\}, \tag{2.9}$$

where $B_1(s) = s - \frac{1}{2}$. In (2.9) the Ψ functions both give rise to sequences of poles, of which infinitely many are negative. It may be preferable to have infinite numbers of both negative and positive poles. This can be achieved by making use of the identity $\Psi(z) + \pi\cot\pi z = \Psi(1-z)$. If the periodic function $\pi\cot\{\pi(s-\beta_0)\}$, which has period 1, is added to the first Ψ function the alternative solution

$$f(s) = s - \frac{1}{2} + \frac{\beta_0^2-\alpha_0^2}{2\beta_0}\{\Psi(1+\beta_0-s) - \Psi(s+\beta_0)\}$$

is obtained. This has a sequence of negative poles at $-\beta_0 - m$ and a sequence of positive poles at $1+\beta_0+m$, in each case for $m = 0, 1, 2, \ldots$.

If $h(z)$ is identically zero, (2.1) is satisfied by any periodic function with period 1, for example $f(z) = \sin 2\pi z$. By the additivity property, any number of solutions can be obtained by combining a single known solution with periodic functions.

Equation (2.6) exemplifies a general property of solutions of (2.1), that a single pole of $h(z)$ requires an infinite sequence of poles in $f(z)$. It follows from (2.1) that if $h(z)$ has a pole at a, then $f(z)$ has poles either at $z = a+n$, $n = 1, 2, 3, \ldots$, or at $z = a - n$, $n = 0, 1, 2, \ldots$. It is also possible for both sequences to coexist provided that the residues have suitable values. These possibilities are illustrated in Figure 2.1.

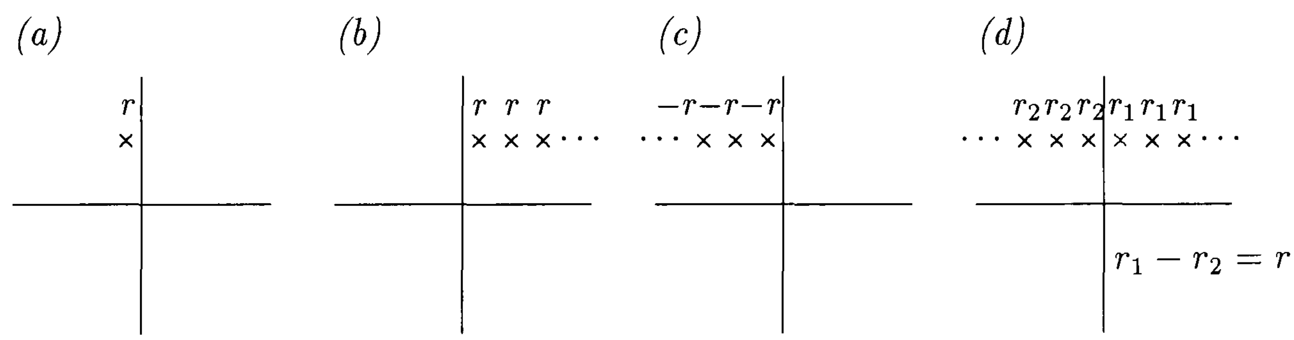

Figure 2.1: *(a) Pole of $h(z)$ at a with residue r. (b) Poles of $f(z)$ at $a+1, a+2, \ldots$ with residues r. (c) Poles of $f(z)$ at $a, a-1, \ldots$ with residues $-r$. (d) Poles of $f(z)$ at $\ldots, a-1, a, a+1, \ldots$ with residues r_1 and r_2, $r_1 - r_2 = r$.*

2.4 Solutions of simple variable-coefficient equations

If $g(z) = z^k$ in (2.2), a solution is given by $f(z) = \Gamma(z)^k$. More generally, if $g(z)$ is any rational function, a solution can be constructed using the multiplicative and translation properties of (2.2). It follows that

$$\frac{f(z+1)}{f(z)} = a\prod_{j=1}^{n}(z-b_j)^{m_j} \tag{2.10}$$

has a solution

$$f(z) = a^{B_1(z)}\prod_{j=1}^{n}\Gamma(z-b_j)^{m_j}, \tag{2.11}$$

where the m_j are integers and $B_1(z) = z - \frac{1}{2}$ is the Bernoulli polynomial.

When $g(z) = 1$ for all z, (2.2) is satisfied by any function with period 1, and such periodic functions can be combined with other solutions by means of the multiplicative property. With reference to the first example in this section, if $g(z) = z$, two solutions of (2.2) are

$$f(z) = \Gamma(z) \tag{2.12}$$

and

$$f(z) = \sin 2\pi z\ \Gamma(z). \tag{2.13}$$

The solution (2.12) has poles at $0, -1, -2, \ldots$, whereas (2.13) is an entire function with zeros at $1, 2, 3, \ldots$.

Example 2.4.1 *The same function as in Example 2.3.1 is used, but this time in an equation of type (2.2),*

$$\frac{f(s+1)}{f(s)} = \frac{s^2-\alpha_0^2}{s^2-\beta_0^2}. \tag{2.14}$$

This has the rational function form (2.10), and the solution to (2.14) in the form (2.11) is

$$f(s) = \frac{\Gamma(s-\alpha_0)\Gamma(s+\alpha_0)}{\Gamma(s-\beta_0)\Gamma(s+\beta_0)}. \tag{2.15}$$

As in Example 2.3.1, it may be desirable to have the zeros and poles in an symmetrical arrangement ie *with approximately the same number of negative and positive ones, and this can be achieved by multiplying by the function*

$$\frac{\sin\{\pi(s-\alpha_0)\}}{\sin\{\pi(s-\beta_0)\}},$$

which is periodic with period 1, giving the alternative solution

$$f(s) = \frac{\Gamma(1+\beta_0-s)\Gamma(s+\alpha_0)}{\Gamma(1+\alpha_0-s)\Gamma(s+\beta_0)}. \tag{2.16}$$

This has a sequence of real positive poles, another of real negative poles, and a similar pair of sequences of real zeros.

In general, if $g(z)$ has a zero at a, $f(z)$ will have a sequence of zeros at $z = a+n$; $n = 1, 2, 3, \ldots$; or a sequence of poles at $z = a-n$; $n = 0, -1, -2, \ldots$. A combination of the two sequences is also possible. If $g(z)$ has a pole at a, the same applies but with the roles of zeros and poles reversed. These possibilities are illustrated in Figure 2.2. The solution $f(z)$ can be chosen to have no zeros

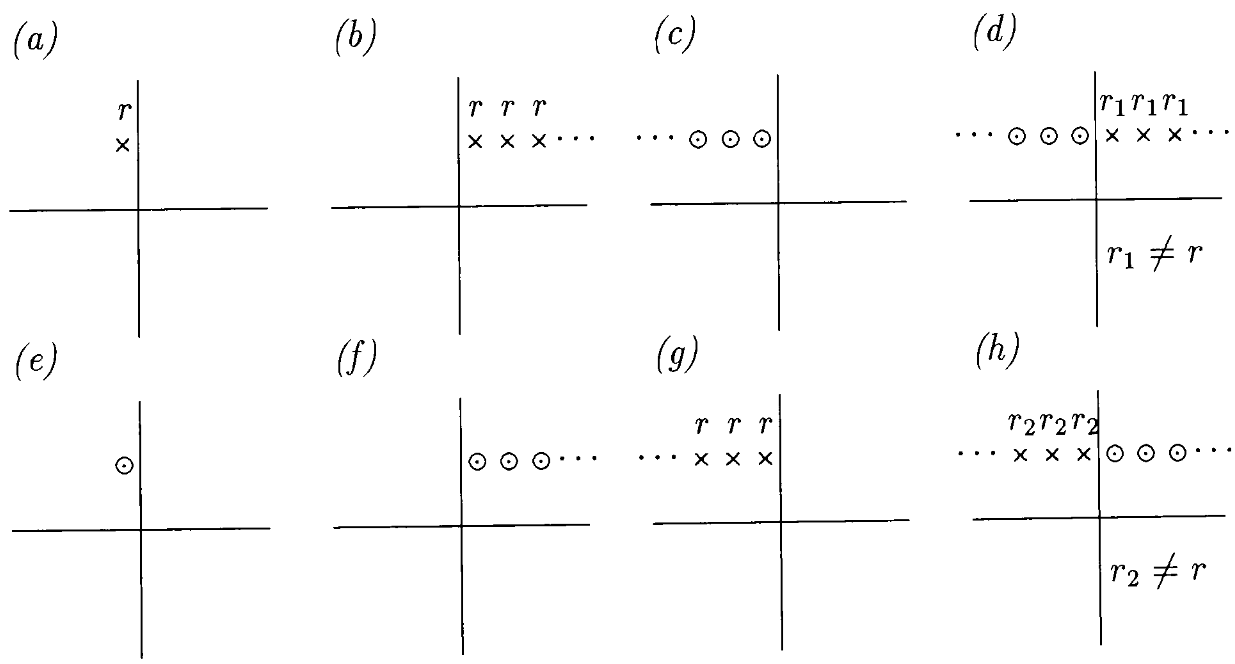

Figure 2.2: *(a) Pole of $h(z)$ at a with residue r. (b) Poles of $f(z)$ at $a+1, a+2, \ldots$ with residues r. (c) Zeros of $f(z)$ at $a, a-1, \ldots$. (d) Poles of $f(z)$ at $a+1, a+2, \ldots$ with residues r_1 and zeros at $a, a-1, \ldots$. $r_1 \neq r$. (e) Zero of $h(z)$ at a. (f) Zeros of $f(z)$ at $a+1, a+2, \ldots$. (g) Poles of $f(z)$ at $a, a-1, \ldots$ with residues r. (h) Zeros of $f(z)$ at $a+1, a+2, \ldots$ and poles at $a, a-1, \ldots$ with residues r_2. $r_2 \neq r$.*

or poles in a strip of the complex z-plane, $b < \Re(z) \leq b+1$, by making an appropriate choice of either *(b)* or *(c)* for each pole of $g(z)$, and either *(f)* or *(g)* for each zero. This principle was used in the construction of Figure 4.4.

2.5 Solutions using the Alexeiewsky G-function

The G-function satisfies

$$\frac{G(z+1)}{G(z)} = \Gamma(z) \tag{2.17}$$

([26]), from whence it follows that if $g(z) = \Gamma(z+a)$ in (2.2) a solution is given by

$$f(z) = G(z+a), \tag{2.18}$$

and that if $g(z) = \Gamma(a-z)$ a solution is given by

$$f(z) = \frac{1}{G(1+a-z)}. \tag{2.19}$$

Example 2.5.1 *Koiter [13] derives the equation*

$$T_0(s+1) = -2s\cot(\pi s)T_0(s) \tag{2.20}$$

in the course of solving a problem which models the diffusion of a load from a stiffener into an infinite or semi-infinite sheet. The standard result $\sin\pi s = \pi/\{\Gamma(s)\Gamma(1-s)\}$ *implies that*

$$\cot\pi s = \frac{\Gamma(s)\Gamma(1-s)}{\Gamma(\frac{1}{2}-s)\Gamma(\frac{1}{2}+s)}.$$

Equation (2.20) is therefore a case of (2.2) with

$$g(z) = \frac{-2z\Gamma(z)\Gamma(1-z)}{\Gamma(\frac{1}{2}-z)\Gamma(\frac{1}{2}+z)}. \tag{2.21}$$

The multiplicative property, together with (2.11), (2.18) and (2.19), allows the following solution to (2.2) to be written down.

$$f(z) = \frac{I(z)2^{z-\frac{1}{2}}\Gamma(z)G(z)G(\frac{3}{2}-z)}{G(2-z)G(\frac{1}{2}+z)},$$

where $I(z)$ is any function such that $I(z+1) + I(z) = 0$. This is the same as Koiter's solution,

$$T_0(s) = \frac{2^{s-1}G(s+1)G(\frac{5}{2}-s)}{\Gamma(\frac{1}{2})G(s-\frac{1}{2})G(2-s)}$$

provided that $I(z)$ is chosen to be $-\pi/\{2^{\frac{1}{2}}\Gamma(\frac{1}{2})\cos \pi z\}$.

2.6 Solutions of non-homogeneous equations

If a solution, $f_0(z)$, to equation (2.2) has been found, let $f(z) = f_0(z)f_1(z)$ satisfy (2.3). It follows that

$$f_0(z+1)f_1(z+1) - g(z)f_0(z)f_1(z) = h(z),$$

$$f_1(z+1) - f_1(z) = \frac{h(z)}{f_0(z)g(z)}. \tag{2.22}$$

Hence $f_1(z)$ satisfies the equation (2.22), which is of type (2.1). Thus, a solution of (2.3) can be found by first solving an equation of type (2.2) and then one of type (2.1).

Example 2.6.1 *The following non-homogeneous form of (2.14) is used as an example of the method:*

$$f(s+1) - \frac{s^2-\alpha_0^2}{s^2-\beta_0^2}f(s) = \pi \cot \pi s. \tag{2.23}$$

The function denoted by f_0 above is, in this case,

$$f_0(s) = \frac{\Gamma(1+\beta_0-s)\Gamma(s+\alpha_0)}{\Gamma(1+\alpha_0-s)\Gamma(s+\beta_0)}, \tag{2.24}$$

from (2.16). The required function $f_1(s)$ satisfies the equation corresponding to (2.22) which is

$$f_1(s+1) - f_1(s) = \frac{\pi\cot(\pi s)\Gamma(\alpha_0-s)\Gamma(s+\beta_0+1)}{\Gamma(\beta_0-s)\Gamma(s+\alpha_0+1)}. \tag{2.25}$$

This can be solved by the Mittag-Leffler sum method of §2.9. This is not done here, but a simpler example using the same method is given as Example 2.9.1.

2.7 Solutions of higher-order equations

Higher-order equations only occur in this thesis in the discussion in §4.6, and in chapter 6. The reader is referred to those sections for examples. The principle used in §4.6 is to find some substitution of the type $F(z) = p(z)f(z) + f(z+1)$ which yields a difference equation in $F(z)$ of lower order than the one in $f(z)$. This method amounts to factorising the difference operator. In chapter 6 a second-order linear equation is reduced to a first-order non-linear one by a substitution.

2.8 Infinite product methods

If $g(z)$ in (2.2) is not a rational function, the following approach may give a solution if it is possible to arrange for the infinite products involved to be convergent.

Let the known meromorphic function $g(z)$ in (2.2) have a representation in the canonical form (see [26])

$$g(z) = e^{H(z)} z^k \prod_{m=1}^{\infty} E\left(\frac{z}{a_m}, p\right)^{j_m}, \tag{2.26}$$

where the product has finite genus p. The genus is the polynomial degree in the expression for $E(u,p)$, namely

$$E(u,p) = (1-u)\exp\left(u + \frac{u^2}{2} + \frac{u^3}{3} + \cdots + \frac{u^p}{p}\right), E(u,0) = 1-u.$$

In the above, $H(z)$ is an entire function and k and j_m integers. The complex numbers a_m are the non-zero zeros and poles of $g(z)$. The factors of the right-hand side of (2.26) can be considered individually because of the multiplicative property of solutions of (2.2).

The equation $f(z+1)/f(z) = e^{H(z)}$ can be solved by transforming it into

$$\log f(z+1) - \log f(z) = H(z),$$

where $H(z)$ is an entire function. In general this is best solved by the integral methods of §2.10.

The equation $f(z+1)/f(z) = z^k$ has been discussed in §2.4.

When $g(z)$ in (2.2) is equal to the infinite product in (2.26), the following method is useful in boundary-value problems in this thesis. It can yield a solution in the form of a convergent infinite product, with zeros and poles distributed in the ways illustrated in Figure 2.2.

First we note that if $g(z) = g_1(z)g_2(z)$, (2.2) has the formal solution

$$f(z) = \frac{1}{g_2(z)} \prod_{n=1}^{\infty} \frac{g_1(z-n)}{g_2(z+n)}, \tag{2.27}$$

which can be checked by substitution. See also Appendix A. This might be used in the case where all the poles and/or zeros of g_1 are to the right of all those of g_2 in the complex plane. When $g(z) = \prod_{m=1}^{\infty} E(z/a_m, p)^{j_m}$, let l be a real number such that $\Re(a_m) \neq l$ holds for all m. Let (b_m) be the subsequence comprising those a_m with $\Re(a_m) > l$, and (c_m) the complementary subsequence. The set of numbers

$$\{b_m + n : m, n \geq 1\} \cup \{c_m + n : m, n \geq 1\}$$

has density, or exponent of convergence, at most $p+1$, so we can write

$$g(z) = \left(\exp \sum_{m=1}^{\infty} \frac{-j_m z^{p+1}}{(p+1)a_m^{p+1}}\right) \prod_{m=1}^{\infty} E\left(\frac{z}{a_m}, p+1\right)^{j_m},$$

where the sum and product both converge. Thus

$$g(z) = e^{-Sz^{p+1}} g_1(z) g_2(z), \tag{2.28}$$

say, with

$$g_1(z) = \prod_{m=1}^{\infty} E(z/b_m, p+1)^{k_m}$$

and

$$g_2(z) = \prod_{m=1}^{\infty} E(z/c_m, p+1)^{l_m}.$$

By the multiplicative property of (2.2), $g(z)$ can first be put equal to the exponential factor in (2.28). Then equation (2.2) can be converted to type (2.1) by taking logarithms, and the solution (2.5) can be used. Finally, the solution (2.27), with $g(z) = g_1(z)g_2(z)$ from (2.28), may be used in (2.2).

Example 2.8.1 *Example 2.5.1 may be solved by this method. The difference equation is (2.20),*

$$T_0(s+1) = -2s\cot(\pi s)T_0(s) \tag{2.29}$$

The expansion (2.26) may be obtained from the product

$$\pi s \cot \pi s = \prod_{n=1}^{\infty} \frac{1 - s^2/(n-\frac{1}{2})^2}{1 - s^2/n^2},$$

so that

$$-2s\cot\pi s = \frac{-2}{\pi}\prod_{j=1}^{\infty}\left\{\frac{1 - s/(j-\frac{1}{2})}{1 - s/j} e^{\frac{s}{j(2j-1)}}\right\}\prod_{k=1}^{\infty}\left\{\frac{1 + s/(k+\frac{1}{2})}{1 + s/k} e^{\frac{s}{k(2k+1)}}\right\}. \tag{2.30}$$

The two infinite products may serve as g_1 and g_2 and a solution is in this case

$$f(s) = \left(\frac{2}{\pi}\right)^{s-\frac{1}{2}} \sin(\pi s) \prod_{k=1}^{\infty}\left\{\frac{1 + s/k}{1 + s/(k+\frac{1}{2})} e^{-\frac{s}{k(2k+1)}}\right\}$$

$$\times \prod_{n=1}^{\infty}\prod_{m=1}^{\infty}\left\{\frac{1 - \dfrac{s-n}{m-\frac{1}{2}}}{1 - \dfrac{s-n}{m} e^{\frac{s-n}{m(2m-1)}}}\right\} \frac{1 + \dfrac{s+n}{m}}{1 + \dfrac{s+n}{m+\frac{1}{2}}} e^{\frac{s+n}{m(2m+1)}}$$

$$= \prod_{n=1}^{\infty}\prod_{m=1}^{\infty}\left\{\frac{m - \frac{1}{2} - s + n}{m - s + n} \cdot \frac{m + s + n}{m + \frac{1}{2} + s + n} \cdot \frac{m + \frac{1}{2}}{m - \frac{1}{2}} e^{\frac{2(2ms-n)}{(2m-1)(2m+1)}}\right\}.$$

The last form shows clearly the location of the zeros and poles at integers and halfway between integers; and their multiplicities.

2.9 Mittag-Leffler sum methods

The infinite-product method for equation (2.2) has an analogue in the following method for equation (2.1). Let $h(z) = h_1(z) + h_2(z)$. Then a formal solution of

(2.1) is

$$f(z) = -h_2(z) + \sum_{n=1}^{\infty}\{h_1(z-n) - h_2(z+n)\}. \tag{2.31}$$

Let $h(z)$ have a Mittag-Leffler expansion

$$h(z) = \sum_{m=1}^{\infty} \frac{\beta_m}{\alpha_m} L\left(\frac{z}{\alpha_m}, p\right), \tag{2.32}$$

where $L(\omega, p) = w^p/(w-1)$, and p is a non-negative integer. The complex numbers α_m are the poles of $f(z)$, which are assumed to be simple. Let l be a real number such that $\Re(\alpha_m) \neq l$ for all m. Let (γ_m) be the subsequence of those α_m with $Re(\alpha_m) < l$, and (δ_m) the complementary subsequence. Then $h(z)$ can be expressed as

$$h(z) = -\sum_{m=1}^{\infty} \frac{\beta_m z^p}{\alpha_m^{p+1}} + \sum_{m=1}^{\infty} \frac{\beta_m}{\alpha_m} L\left(\frac{z}{\alpha_m}, p+1\right),$$

where the sums converge,

$$= Sz^p + h_1(z) + h_2(z), \tag{2.33}$$

say, with

$$h_1(z) = \sum_{m=1}^{\infty} \frac{\gamma_m}{b_m} L\left(\frac{z}{b_m}, p+1\right) \text{ and } h_2(z) = \sum_{m=1}^{\infty} \frac{\delta_m}{c_m} L\left(\frac{z}{c_m}, p+1\right).$$

In (2.33), the first term can be dealt with as in (2.5). On using additivity of (2.1), the solution (2.5) can be combined with a solution (2.31) corresponding to $h(z) = h_1(z) + h_2(z)$ in (2.1).

Example 2.9.1 *As an example, consider*

$$f(s+1) - f(s) = \pi \cot \pi s, \tag{2.34}$$

which is a simplified form of (2.25). There is no difference of principle in solving (2.25) itself by this method, although the details are more complicated. In this case the expansion (2.32) has the form

$$\pi \cot \pi s = \frac{1}{s} + \sum_{m \neq 0} \left(\frac{1}{s-m} + \frac{1}{m}\right).$$

The terms of (2.33) are

$$h_1(s) = \sum_{m=1}^{\infty} \left(\frac{1}{s-m} + \frac{1}{m} + \frac{s}{n^2} \right),$$

$$h_2(s) = \sum_{m=1}^{\infty} \left(\frac{1}{s+m} - \frac{1}{m} + \frac{s}{n^2} \right),$$

$$S = -2s \sum_{m=1}^{\infty} \frac{1}{m^2} = -2\zeta(2)s,$$

where $\zeta(s)$ *is Riemann's zeta function, and there is an extra term,* $1/s$*. The term containing* $\zeta(2) = \pi^2/s$*, arises because the order* p *in (2.32) is 1. When* $p > 1$*, coefficients* $\zeta(3)$*,* $\zeta(4)$ *and so on will occur. A solution to (2.34) is obtained by means of (2.5), (2.6) and (2.31) as*

$$f(s) = -\zeta(2)B_2(s) + \Psi(s) - \sum_{m=1}^{\infty} \left(\frac{1}{s+m} - \frac{1}{m} + \frac{s}{m^2} \right)$$

$$+ \sum_{n=1}^{\infty} \left\{ \sum_{m=1}^{\infty} \left(\frac{1}{s-n-m} + \frac{1}{m} + \frac{s-n}{m^2} \right) - \sum_{m=1}^{\infty} \left(\frac{1}{s+n-m} - \frac{1}{m} + \frac{s+n}{m^2} \right) \right\}.$$

These sums can be rearranged in various ways, but the above form makes the location of poles clear.

2.10 Integral methods

Solutions to (2.1) may be written as definite integrals in the ways outlined below. These methods are used in chapter 3, but the infinite product method of §2.8 is exploited in other parts of the thesis. The problems of convergence, asymptotic behaviour and location of singularities are not dealt with fully here, but are of primary importance in applications.

In equation (2.1), let $h(z)$ have the Fourier transform

$$H(w) = \int_{-\infty}^{\infty} h(z) e^{iwz}\, dz. \tag{2.35}$$

Then a solution, $f(z)$, is given by

$$f(z) = \frac{1}{2\pi} \int_{-\infty}^{\infty} \frac{e^{-izw} - 1}{e^{iw} - 1} H(w)\, dw, \tag{2.36}$$

provided that both of the defining integrals (2.35) and (2.36) exist. This method is used by Evans [8] in solving a problem where water waves propagate in a shallow region of constant depth and particles having density which varies continuously in space float on the surface. A limitation of this method is that the Fourier transform, $H(z)$, has to exist, at least for real z, in order that the integral (2.36) be defined.

A similar method is given in terms of the Mellin transform of $h(z)$,

$$H(r) = \frac{1}{2\pi i} \int_{\nu - i\infty}^{\nu + i\infty} h(z) r^{-z}\, dz, \tag{2.37}$$

where $\nu > \Re(a)$ for every pole, a, of $h(z)$. A solution of (2.1) is given by

$$f(z) = \int_{0}^{\infty} \frac{H(r)}{1 - r} r^{z-1}\, dr. \tag{2.38}$$

This method is employed by Abrahams and Lawrie [2] when investigating the reflection and transmission of waves in a wedge of fluid contained by two plane membrane surfaces. This form of solution requires the existence of $H(r)$ for positive r and the convergence of (2.31), at least for z in some region of interest.

Another general method, applicable to equation (2.1), is by means of Nörlund's *principal solution* [16]. The principal solution to (2.1) is

$$f(z) = \int_{c}^{\infty} h(t)\, dt - \sum_{s=0}^{\infty} h(z + s), \tag{2.39}$$

if the integral and series both converge, where c is an arbitrary real number. If they do not converge, it may be possible to find a function $\phi(z, \mu)$ such that

i) $\lim_{\mu \to 0} \phi(z, \mu) = h(z)$,

ii) $\int_{c}^{\infty} \phi(t, \mu)\, dt$ and $\sum_{s=0}^{\infty} \phi(z + s, \mu)$ both converge.

Then let $F(z,\mu)$ be the principal solution of $f(z+1) - f(z) = \phi(z,\mu)$. If the limit

$$f(z) = \lim_{\mu \to 0} F(z,\mu) \tag{2.40}$$

exists uniformly and is independent of the choice of $\phi(z,\mu)$, it is the principal solution of (2.1).

If $h(z)$ is an entire function of order 1, the expression (2.39) can be replaced by one involving only integration. In this case, let

$$H(\zeta) = \int_c^\zeta h(z)\,dz.$$

The principal solution to (2.1) is then

$$f(z) = \frac{1}{2\pi i}\int_{-\alpha-i\infty}^{-\alpha+i\infty} H(z+\zeta)\left(\frac{\pi}{\sin\pi\zeta}\right)^2 d\zeta,$$

if α is chosen so that, for $\Re(z) \geq \alpha$, $|g(z)| < Ce^{(k+\epsilon)|z|}$ for some positive constants C, k and ϵ with $C > 0$ and $0 < k < 2\pi$.

2.11 The Wiener–Hopf method

This technique is described in detail by Noble [18]. The exposition here is an introduction to those applications which occur in this thesis. To quote from Noble's preface, "A typical problem [to which the technique might be applied] requires solution of the steady-state wave equation in free space when semi-infinite boundaries are present."

The method used in this thesis is that described by Noble as "Jones's method," and involves the following steps:

(a) Take half-range Fourier transforms of boundary conditions;

(b) Eliminate some of the unknown half-range transform functions;

(c) Write the relation between the remaining functions in a form where the "Wiener–Hopf kernel" multiplies a "plus function";

(d) Perform a product split on the Wiener–Hopf kernel;

(e) Rearrange the equation so that plus functions are on one side and "minus functions" on the other. This necessitates performing a "sum split" on one function;

(f) Determine the (polynomial) growth rate of the plus and minus members;

(g) Apply the extended form of Liouville's theorem to justify analytic continuation;

(h) Determine any arbitrary coefficients which were introduced because of the polynomial growth.

The process is illustrated here with a boundary-value problem which is a limiting case of that considered in chapter 5. The elastic plate in $x < 0$ is replaced by a rigid wall in the limiting case studied here. This provides an example which illustrates all of the steps *(a)–(h)* mentioned above. Noble's book contains many other examples, but the following one is typical of this thesis as it involves a duct with a wall which is partly made of an elastic plate, resulting in a fourth-order boundary condition.

The formulation of the problem is similar to that of §5.2, but the elastic plate boundary condition for $x < 0$ is replaced by

$$\phi_y(x, h) = 0; \; x < 0, \tag{2.41}$$

in non-dimensional coordinates. The incident wave in the rigid-walled duct is

$$Ae^{ix},$$

and the total potential will be denoted by

$$\phi^{\text{tot}} = \phi + Ae^{ix}. \tag{2.42}$$

The Fourier transform of the scattered potential takes the form

$$\Phi(s,y) = \Phi^{+}(s,y) + \Phi^{-}(s,y) = \int_{-\infty}^{\infty} \phi(x,y)e^{isx}\,dx,$$

where Φ^+ and Φ^- are the half-range transforms defined by $\int_0^\infty$ and $\int_{-\infty}^0$ respectively. The scattered potential ϕ satisfies (2.41) provided that ϕ^{tot} does. If ϕ^{tot} also satisfies the half-boundary condition

$$\left(\frac{\partial^4}{\partial x^4} - \mu_2^4\right)\phi_y^{\text{tot}}(x,h) - \alpha_2\phi^{\text{tot}}(x,h) = 0;\ x \geq 0, \tag{2.43}$$

then, for $x \geq 0$ and $y = h$,

$$\phi_{yxxxx} - \mu_2^4\phi_y - \alpha_2\phi - \alpha_2 Ae^{ix} = 0. \tag{2.44}$$

The boundary-value problem in non-dimensional form for the scattered potential is

$$\left(\frac{\partial^2}{\partial x^2} + \frac{\partial^2}{\partial y^2} + 1\right)\phi = 0;\ 0 < y < h,$$

$$\phi_y(x,0) = 0,$$

$$\phi_y(x,h) = 0;\ x < 0,$$

$$\left(\frac{\partial^4}{\partial x^4} - \mu_2^4\right)\phi_y - \alpha_2(\phi + Ae^{ix}) = 0;\ x \geq 0, y = h, \tag{2.45}$$

$$\phi(x,y) = \begin{cases} R_0 e^{-ix} \text{ as } x \to -\infty, \\ T_0 e^{i\nu_0 x}\cosh(\lambda_0 y) \text{ as } x \to +\infty. \end{cases}$$

The wavenumbers ν_0 and λ_0 are defined in chapter 5. For the present purpose of illustrating the technique, it is not necessary to define them. Edge conditions of various kinds may be imposed as in the related problem in chapter 5. These take the form of relations between the left and right x-derivates of $\phi_y(x,y)$ at x=0 and y=h. Their application is briefly mentioned at the end of this section.

The Fourier transform with respect to x of the governing equation is

$$\left(\frac{\partial^2}{\partial y^2} - \gamma^2\right)\Phi = 0, \tag{2.46}$$

where $\gamma = (s^2-1)^{\frac{1}{2}}$, and that of the rigid boundary condition is

$$\Phi_y(s,0) = \Phi_y^+(s,0) + \Phi_y^-(s,0) = 0. \tag{2.47}$$

The form

$$\Phi(s,y) = C(s)\cosh(\gamma y)$$

is appropriate in order that the boundary condition $\phi_y(x,0) = 0$ be satisfied. So,

$$\Phi_y(s,y) = \gamma C(s)\sinh(\gamma y).$$

When the half-range transform of (2.45) is taken, integration by parts gives

$$\int_0^\infty \phi_{yxxxx} e^{isx}\, dx = p_2(s,y) + s^4\Phi_y^+(s,y).$$

The function p_2 is a cubic polynomial in s, and is the same as the p_2 given in full in (5.18). Its coefficients are edge values which can be determined from the edge conditions of the problem and consideration of the asymptotic properties of the transformed potential Φ for large s.

The following relations between the half-range transforms of the scattered potential, ϕ, are obtained. These represent step *(a)* of the steps *(a-h)* listed in the second paragraph of this section.

$$\Phi^+(s,h) + \Phi^-(s,h) = C(s)\cosh(\gamma h), \tag{2.48}$$

$$\Phi_y^+(s,h) + \Phi_y^-(s,h) = \gamma C(s)\sinh(\gamma h), \tag{2.49}$$

$$\Phi_y^-(s,h) = 0, \tag{2.50}$$

$$(s^4 - \mu_2^4)\Phi_y^+(s,h) - \alpha_2\Phi^+(s,h) + p_2(s,h) = -\frac{i\alpha_2 A}{1+s}. \tag{2.51}$$

For step *(b)*, it is convenient to follow Cannell [5] and eliminate $C(s)$, $\Phi_y^-(s,h)$ and $\Phi^+(s,h)$ from (2.48-2.51) to get the single relation

$$\begin{aligned} &\alpha_2\gamma\tanh(\gamma h)\Phi^-(s,h) + \{(s^4-\mu_2^4)\gamma\tanh(\gamma h) - \alpha_2\}\Phi_y^+(s,h) \\ = &\ -\gamma\tanh(\gamma h)p_2(s,h) - \frac{i\alpha_2\gamma\tanh(\gamma h)}{1+s}. \end{aligned} \tag{2.52}$$

The Wiener–Hopf kernel (step *(c)*) is

$$L(s) = \frac{(s^4-\mu_2^4)\gamma\tanh(\gamma h) - \alpha_2}{\alpha_2\gamma\tanh(\gamma h)} = \frac{(s^4-\mu_2^4)K(s)}{\alpha_2}, \tag{2.53}$$

where

$$K(s) = \frac{(s^4-\mu_2^4)\gamma\tanh(\gamma h) - \alpha_2}{(s^4-\mu_2^4)\gamma\tanh(\gamma h)} \tag{2.54}$$

is a function of a type arising elsewhere in this thesis and amenable to the infinite-product method of factorisation into plus and minus functions. If $L(s)$ is compared with Cannell's kernel function (A1) in [5] it will be seen that the duct problem introduces the non-rational function $\tanh(\gamma h)$, which is an apparent complication, but on the other hand the branch point of the function γ is eliminated. This accounts for the difference in treatment. Cannell, in his Appendix A, uses logarithmic differentiation because of the branch point, while here we use the infinite product method because of the infinite sequence of zeros and poles due to the tanh function.

The function $K(s)$ in (2.54) has a convergent infinite-product representation

$$K(s) = K(0)\prod_{n=0}^{\infty}\frac{1-s^2/\eta_n^2}{1-s^2/\zeta_n^2} = \prod_{n=0}^{\infty}\frac{s^2-\eta_n^2}{s^2-\zeta_n^2}, \tag{2.55}$$

where $\pm\eta_n$ are the zeros of the numerator of (2.54), and $\pm\zeta_n$ are the zeros of the denominator, in each case for $n = 0,1,2,\ldots$. The ζ_n are readily seen to be $\pm\mu_2$, $\pm i\mu_2$, $\pm\sqrt{1-\pi^2m^2/h^2}$; $m = 0,1,2,\ldots$. By substitution in (2.54),

$$K(0) = \frac{\mu_2^4\tan h - \alpha_2}{\mu_2^4\tan h} = \prod_{n=0}^{\infty}\frac{\eta_n^2}{\zeta_n^2}. \tag{2.56}$$

The convergence of the infinite products in (2.55) and (2.56) follows from the results in Appendix B. The representation (2.55) is combined with (2.53) to give

$$L(s) = \frac{(s^2-\eta_0^2)(s^2-\eta_1^2)}{\alpha_2}\prod_{n=2}^{\infty}\frac{s^2-\eta_n^2}{s^2-\zeta_n^2}.$$

A product split into plus and minus functions, step *(d)*, is

$$L^{\pm}(s) = \frac{(s\pm\eta_0)(s\pm\eta_1)}{\sqrt{\alpha_2}}\prod_{n=2}^{\infty}\frac{s\pm\eta_n}{s\pm\zeta_n}. \tag{2.57}$$

The convergence of the infinite products in (2.57) follows from the asymptotic representation (B.6). The factorisation $L(s) = L^+(s)L^-(s)$, when substituted in the Wiener–Hopf equation (2.52), gives

$$\frac{\Phi^-(s,h)}{L^-(s)} + \Phi_y^+(s,h)L^+(s) = \frac{-p_2(s,h) - \frac{iA\alpha_2}{1+s}}{L^-(s)}. \tag{2.58}$$

This is rearranged, as step *(e)*, to give

$$\begin{aligned} &\frac{\Phi^-(s,h)}{L^-(s)} + \frac{p_2(s,h)}{L^-(s)} + \frac{iA\alpha_2}{L^-(-k)(1+s)} \\ &= -\Phi_y^+(s,h)L^+(s) - \frac{iA\alpha_2}{1+s}\left(\frac{1}{L^-(-1)} - \frac{1}{L^-(s)}\right), \end{aligned} \tag{2.59}$$

where an elementary sum split has been done on the right-hand side of (2.58). The left-hand side is analytic in the lower half s-plane, and the right-hand side in the upper half plane. The upper and lower half planes can be made to overlap by giving k, the wavenumber in the dimensional formulation, a small positive imaginary part (see (5.4)). Let $J(s)$ be the entire function obtained by analytic continuation of each member of (2.59). Its growth for large s can be deduced from the asymptotic behaviour of the terms of (2.59). Firstly, finite pressure at $x = y = 0$ requires that

$$\phi_y \sim \phi_y^0 + x\phi_{yx}^0 + O(x^4) \text{ as } x \to 0_+,$$

and it follows that

$$\Phi_y(s,y) \sim \frac{i\phi_y^0}{s} - \frac{\phi_{xy}^0}{s^2} + O(s^{-5}) \tag{2.60}$$

as $s \to -\infty$ in the upper half plane (*cf* Cannell [5] (3.20-21)). It can be shown, as in appendix D, that $L^+(s) = O(s^2)$ as $s \to \infty$ in the upper-half plane. Since $\Phi_y^- = O(s^{-\epsilon})$ as $s \to \infty$, it follows that both members of (2.59) are $O(s)$ as $s \to \infty$, and this completes step *(f)* of the procedure.

By the extended form of Liouville's theorem, $J(s)$ must be a polynomial of degree 1 (step *(g)*), and we write

$$\Phi_y^+(s,y)L^+(s) + \frac{iA\alpha_2}{1+s}\left(\frac{1}{L^-(-1)} - \frac{1}{L^-(s)}\right) = qs + r, \tag{2.61}$$

where q and r are constants to be determined. They can be found by examining the asymptotic form of (2.61) as $s \to \infty$ in the upper half plane. The second term on the left-hand side of (2.61) is $O(s^{-1})$. In the first term,

$$L^+(s) = \frac{s^2 + (\eta_0 + \eta_1)s + \eta_0\eta_1}{\sqrt{\alpha_2}} \prod_{n=2}^{\infty} \frac{s+\eta_n}{s+\zeta_n}. \tag{2.62}$$

As is shown in appendix D, the infinite product has the asymptotic expansion

$$1 + \frac{b_1}{s} + \frac{b_2}{s^2} + \frac{b_3}{s^3} + O(s^{-4}), \tag{2.63}$$

with $b_1 = a_1$, $b_2 = a_2 + a_1^2/2$, $b_3 = a_3 + a_1a_2 + a_1^3/6$, and

$$a_r = (-1)^{r-1} \sum_{n=2}^{\infty} \frac{\zeta_n^r - \eta_n^r}{r}; \ r = 1, 2, 3.$$

Hence, by (2.61),

$$L^+(s) = \frac{s^2 + (b_1 + \eta_0 + \eta_1)s}{\sqrt{\alpha_2}} + O(1) \text{ as } s \to \infty.$$

when this is combined with (2.60), the following asymptotic expression is obtained,

$$\Phi_y^+(s,h)L^+(s) = \frac{i\phi_y^0}{\sqrt{\alpha_2}}s + \frac{i\phi_y^0(b_1 + \eta_0 + \eta_1) - \phi_{xy}^0}{\sqrt{\alpha_2}} + O(s^{-1}).$$

Consequently, step *(h)* of the procedure yields

$$q = \frac{i\phi_y^0}{\sqrt{\alpha_2}}, \ r = \frac{i\phi_y^0(b_1 + \eta_0 + \eta_1) - \phi_{xy}^0}{\sqrt{\alpha_2}}.$$

The edge values ϕ_y^0 and ϕ_{xy}^0 are determined according to the edge conditions which represent the type of join between the plate and rigid wall. Some edge conditions would make b_1 and/or b_2 zero, and in that case q and r would depend on higher-order edge values and further terms of the series (2.63).

This completes the calculations which are characteristic of the Wiener–Hopf method. The problem is now solved in that the velocity potential is given by the inverse transform

$$\phi(x, y) = \frac{1}{2\pi} \int_{-\infty}^{\infty} \Phi(s, y) e^{-ixs}\, ds.$$

The transforms $\Phi^+(s, y)$ and $\Phi_y^-(s, h)$ can be obtained by equating the left- and right-hand members of (2.59) to $qs+r$ in turn. It only remains to express $\Phi^+(s, h)$ in terms of $\Phi_y^+(s, h)$, which can be done by using the last equation of (2.48).

Chapter 3

A boundary-value problem with smoothly-varying impedance boundary condition

3.1 Introduction

The boundary value problem considered here relates to a two-dimensional waveguide with continuously-varying impedance on one surface. The method of solution is that used by Evans [8], that is the difference-equation technique due to Roseau, [23]. The reflection and transmission coefficients are obtained directly from the velocity potential and a power balance is performed. In addition, the solution is shown to be equivalent, in a limiting case, to that for a standard Wiener–Hopf problem.

This problem is mentioned briefly by Fernyhough and Evans, [9], where the moduli of the reflection and transmission coefficients, $|R|$ and $|T|$ are given. They do not present details of the solution, as the method is similar to that of the related cylindrical problem which is the main topic of the paper, but the reader is referred to Fernyhough's PhD thesis [10].

3.2 The boundary value problem

The model problem consists of a two-dimensional infinite duct occupying the region $0 \le y \le h$ of a Cartesian coordinate system (x, y, z) (Figure 3.1). The

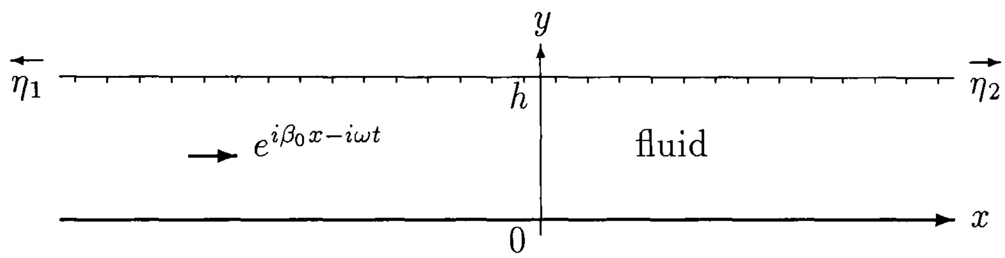

Figure 3.1: *The duct*

lower duct wall, that is at $y = 0$, is rigid whilst the upper wall is partially absorbent having a specific acoustic admittance, η, which depends on x and is such that $\eta \to \eta_1(\eta_2)$ as $x \to -\infty(+\infty)$. A compressible fluid of mean density ρ_0 and sound speed c occupies the interior of the duct whilst the exterior region is *in vacuo*. The analysis is also applicable to the symmetrical problem obtained by reflecting the configuration in the plane $y = 0$ and removing the rigid surface there. The incident forcing has the form

$$\phi_0(x, y, t) = A\cosh(\tau_0 y)e^{i\beta_0 x - i\omega t} \tag{3.1}$$

where the wavenumbers τ_0 and β_0 will be defined later and the amplitude A will be chosen to give a simple expression for the power input. This plane wave has harmonic time dependence, of angular frequency ω. Both the incident wave and $\eta(x)$ are independent of z and thus fluid velocity potential may be written as

$\Phi(x, y, t)$. The fluid pressure is related to the velocity potential by

$$p(x, y, t) = -\rho_0 \frac{\partial \Phi}{\partial t}(x, y, t). \tag{3.2}$$

As mentioned in the introduction a steady state solution is sought and thus the acoustic field may be expressed as

$$\Phi(x, y, t) = \Re\{\phi(x, y)e^{-i\omega t}\}. \tag{3.3}$$

For convenience, the harmonic time factor is henceforth suppressed.

The time-independent potential ϕ satisifies the Helmholtz equation

$$\left(\frac{\partial^2}{\partial x^2} + \frac{\partial^2}{\partial y^2} + k^2\right)\phi = 0; \quad \Re(k) > 0, \ \Im(k) \geq 0. \tag{3.4}$$

The condition on $Re(k)$ is to give the wavenumber the conventional positive sign, while its imaginary part is positive if there is any attenuation in the system, otherwise zero. The lower bounding surface gives rise to the boundary condition

$$\phi_y(x, 0) = 0, \tag{3.5}$$

and the upper one to the condition

$$\phi_y - i\eta k\phi = 0; \quad y = h, \ \Re(\eta) \geq 0 \tag{3.6}$$

where we assume the space-dependent form

$$\eta = \eta(x) = \frac{\eta_1 + \eta_2 e^{x/a}}{1 + e^{x/a}}, \quad a > 0. \tag{3.7}$$

The specifice acoustic admittance, η, is purely imaginary although a small non-zero real part may be useful for mathematical reasons. Small values of a represent a rapid transition from $\eta(x) \simeq \eta_1$ to $\eta(x) \simeq \eta_2$ near $x = 0$; thus, in the limit $a \to 0$ the problem is equivalent to one of standard Wiener–Hopf type.

A radiation condition incorporating the incident wave, a reflected mode with the same wave number and a transmitted mode (all other modes being assumed to be attenuated as $x \to \pm\infty$) is

$$\phi(x,y) \sim \begin{cases} (Ae^{i\beta_0 x} + Re^{-i\beta_0 x})\cosh(\tau_0 y), & x \to -\infty, \\ Te^{i\alpha_0 x}\cosh(\lambda_0 y), & x \to \infty, \end{cases} \tag{3.8}$$

where β_0 and α_0 are wave numbers satisfying the dispersion relation (3.12) below, $\tau_0 = \gamma(\beta_0)$ and $\lambda_0 = \gamma(\alpha_0)$. (It will emerge later that $\gamma(s)$ is an even function.)

Henceforth, except where otherwise stated, it is assumed that $\Im(k) = \Re(\eta_1) = \Re(\eta_2) = 0$.

We assume a solution of the form

$$\phi(x,y) = \frac{1}{2\pi}\int_C \Phi(s,y)e^{-isx}\,ds, \tag{3.9}$$

where the wavenumber s is regarded as a complex variable and C is a contour extending from $-\infty$ to ∞ to be specified in more detail later. This satisfies (3.4) provided that

$$\Phi_{yy}(s,y) - (s^2 - k^2)\Phi(s,y) = 0. \tag{3.10}$$

On assuming the form $\Phi(s,y) = A(s)e^{\gamma y} + B(s)e^{-\gamma y}$, where γ is a complex variable depending on s, the boundary condition (3.5) implies that

$$\gamma A(s) - \gamma B(s) = 0,$$

so that

$$\Phi(s,y) = 2A(s)\cosh(\gamma y) \tag{3.11}$$

which has to satisfy the boundary condition (3.6), leading to

$$L_1(s) = \gamma\sinh(\gamma h) - i\eta_1 k\cosh(\gamma h) = 0, \quad \eta_1 = \eta_2; \tag{3.12}$$

with $\gamma^2 = s^2 - k^2$ from (3.10). This dispersion relation is satisfied if s is a root of (3.12). To ensure that there is exactly one pair of real roots, the conditions

$hk < 3\pi/2$ and $\Im(\eta) < k \tan hk$ are imposed. The roots of (3.12) are then $\pm s_0$, $\pm s_1$, $\pm s_2$, ..., where s_0 is real and positive, whilst s_1, s_2, ... are purely imaginary with argument $\pi/2$. Two physical cases can be distinguished: $\Im(\eta) < 0$ (springlike susceptance), in which case $s_0 > k$; and $\Im(\eta) > 0$ (masslike susceptance), in which case $s_0 < k$ ([17] p1522). The transitional case, $\eta = 0$, represents a rigid upper boundary with $s_0 = k$.

Only even functions of $\gamma = (s^2 - k^2)^{1/2}$ will appear in the analysis because the duct does not admit any radiation as $y \to \infty$. However to be definite it is deemed to be evaluated with respect to the branch cut shown in Figure 3.2 so

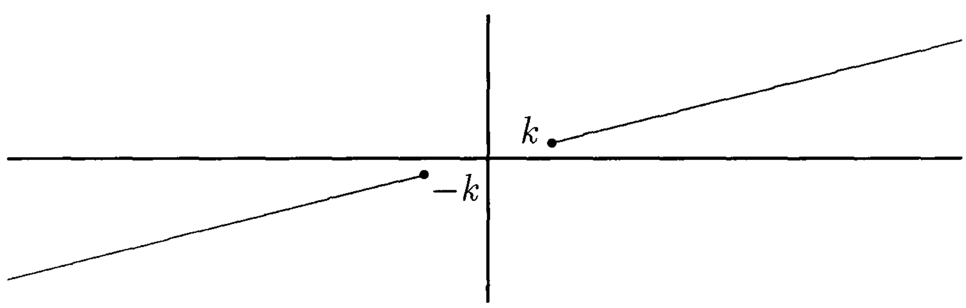

Figure 3.2: *Branch cut*

that for real s, $\gamma = |s| + o(1)$ as $s \to \pm\infty$, whilst $\gamma = -ik$ if $s = 0$.

Note that in the following analysis $\eta_1 \neq \eta_2$ and both the functions $L_1(s)$ and $L_2(s)$ will be required (where $L_2(s)$ is defined as in (3.12) but with η_1 replaced by η_2). To distinguish between the two sets of roots, the notation $s_i = \beta_i$ will be used for the solutions to $L_1(s) = 0$ and $s_i = \alpha_i$ for the solutions to $L_2(s) = 0$.

In the general case where $\eta_2 \neq \eta_1$, assume that the velocity potential has the form

$$\phi(x, y) = \frac{1}{2\pi} \int_C \frac{f(s) \cosh(y\gamma) \, e^{-isx}}{\gamma \sinh(h\gamma) - i\eta_1 k \cosh(h\gamma)} \, ds, \tag{3.13}$$

where C is a contour extending from $-\infty$ to ∞ to be defined later. The governing equation (3.4) still holds, as does the boundary condition (3.5). The denominator has been chosen for convenience and $f(s)$, determined by the need to satisfy (3.6), is expected to reveal the properties of the transmitted mode by its contribution to the evaluation of the integral by the method of residues.

3.3 A solution of the boundary value problem

In the expression (3.13) for the velocity potential, it remains to choose $f(s)$ so that the impedance and radiation boundary conditions, (3.6) and (3.8), are satisfied.

Boundary condition (3.6), together with (3.7), can be arranged as

$$\{\phi_y - i\eta_1 k\phi + e^{x/a}(\phi_y - i\eta_2 k\phi)\} = 0, \quad \text{on } y = h. \tag{3.14}$$

On substituting (3.13) into (3.14), it is found that

$$\frac{1}{2\pi}\int_C f(s)e^{-isx}\,dx + \frac{1}{2\pi}\int_C \frac{\gamma\sinh h\gamma - i\eta_2 k\cosh h\gamma}{\gamma\sinh h\gamma - i\eta_1 k\cosh h\gamma} f(s)e^{-ix(s+i/a)}\,ds = 0. \tag{3.15}$$

In the first integral, put $t = s - i/a$ to get

$$\frac{1}{2\pi}\int_{C'} f\left(t + \frac{i}{a}\right)e^{-ix(t+i/a)}\,dt, \tag{3.16}$$

where C' is the contour which is everywhere a distance $1/a$ below C. Expression (3.15), which holds for all x, will be satisfied if C' can be translated to C without crossing any poles and $f(s)$ satisfies

$$(\gamma\sinh h\gamma - i\eta_2 k\cosh h\gamma)f(s) + (\gamma\sinh h\gamma - i\eta_1 k\cosh h\gamma)f(s + i/a) = 0,$$

equivalently

$$\frac{f(s+i/a)}{f(s)} = -\frac{\gamma\tanh h\gamma - i\eta_2 k}{\gamma\tanh h\gamma - i\eta_1 k} = -p(s), \tag{3.17}$$

say, where $f(s)$ is meromorphic. If $s = \beta_n$ is a zero of $\gamma\tanh h\gamma - i\eta_1 k$, it is to be a zero of $f(s)$ or a pole of $f(s + i/a)$. Similarly, a zero of $\gamma\tanh h\gamma - i\eta_2 k$ must be a zero of $f(s + i/a)$ or a pole of $f(s)$. Note that $p(s)$ is even.

The zeros and poles of $p(s)$ have already been denoted by $\pm\alpha_0$, $\pm\alpha_1$, ... and $\pm\beta_0$, $\pm\beta_1$, ... in §3.2. It is preferable to have a right-hand side which has no real zeros or poles, so write $f(s) = f_0(s)f_1(s)f_2(s)$, where f_0, f_1 and f_2 satisfy

$$\frac{f_0(s+i/a)}{f_0(s)} = -1, \tag{3.18}$$

$$\frac{f_1(s+i/a)}{f_1(s)} = \frac{s^2-\alpha_0^2}{s^2-\beta_0^2} \tag{3.19}$$

and

$$\frac{f_2(s+i/a)}{f_2(s)} = \frac{\gamma\tanh h\gamma - i\eta_2 k}{\gamma\tanh h\gamma - i\eta_1 k}\cdot\frac{s^2-\beta_0^2}{s^2-\alpha_0^2} = h(s), \tag{3.20}$$

$h(s)$ having only the purely imaginary zeros α_1, α_2, ...and poles β_1, β_2, ... Solutions of (3.18) include $\sinh\{(2n-1)bs+c\}$ and $\operatorname{cosech}\{(2n-1)bs+c\}$ for any constant c, and $b = \pi a$; and integers n as well as polynomials of odd degree in these functions.

A solution of (3.19) can be obtained by using properties of the gamma-function. A similar equation was solved in example 2.4.1. It is found that

$$f_1(s) = \frac{\Gamma\{-ia(s-\alpha_0)\}\,\Gamma\{-ia(s+\alpha_0)\}}{\Gamma\{-ia(s-\beta_0)\}\,\Gamma\{-ia(s+\beta_0)\}}. \tag{3.21}$$

In order to solve (3.20) it is necessary to take logarithms of both sides, giving

$$g\left(s+\frac{i}{a}\right) - g(s) = \log h(s), \tag{3.22}$$

where $g(s) = \log f_2(s)$. This functional difference equation can be solved by assuming an integral expression for $g(s)$ of the form

$$g(s) = \frac{1}{2\pi}\int_{-\infty}^{\infty}\frac{e^{-isw}-1}{e^{w/a}-1}G(w)\,dw, \tag{3.23}$$

The function $G(w)$ may be defined as the inverse transform

$$G(w) = \int_{-\infty}^{\infty}\log h(s)\,e^{iws}\,ds, \tag{3.24}$$

corresponding to

$$\log h(s) = \frac{1}{2\pi}\int_{-\infty}^{\infty} G(w)e^{-isw}\,dw. \tag{3.25}$$

By substituting (3.23) in (3.22) and using (3.25), it may be seen that the difference equation (3.22) is indeed satisfied.

It is now necessary to investigate the growth properties of $G(w)$ in order to show how $g(s)$, defined by (3.23), behaves for large s. The two are related by an Abelian theorem which depends on the singularity of $G(\omega)$ at $\omega = 0$ and the rate of decay of $G(\omega)$ as ω becomes large through positive and negative real values. On expanding (3.17) for $|s| >> 1$ it can be shown that $p(s)$ has the asymptotic form

$$p(s) \sim 1 + i(\eta_1 - \eta_2)k|s|^{-1} + \frac{1}{2}ik^3(\eta_1 - \eta_2)|s|^{-3} + O(|s|^{-5}) \text{ as } s \to \pm\infty. \tag{3.26}$$

Hence, using (3.20) and (3.26) it is found that

$$\log h(s) \sim i(\eta_1 - \eta_2)k|s|^{-1} \text{ as } s \to \pm\infty. \tag{3.27}$$

On substituting (3.27) into (3.24) it transpires that

$$G(w) \sim -2i(\eta_1 - \eta_2)k \log|w| \text{ as } w \to 0. \tag{3.28}$$

The asymptotic behaviour of $G(w)$ for small w is given by (3.28), whilst for large w, it is necessary to note that $\log h(s)$ is even. Integration of (3.24) by parts leads to

$$G(w) = -\frac{2}{w}\int_0^{\infty} \frac{h'(s)}{h(s)} \sin ws\,ds.$$

The Mittag-Leffler expansion

$$\frac{h'(s)}{h(s)} = \sum_{n=1}^{\infty}\left(\frac{1}{s-\alpha_n} + \frac{1}{\alpha_n} + \frac{1}{s+\alpha_n} - \frac{1}{\alpha_n} + \frac{1}{s-\beta_n} + \frac{1}{\beta_n} + \frac{1}{s+\beta_n} - \frac{1}{\beta_n}\right)$$

is valid so that

$$G(w) = -\frac{2}{w}\int_0^{\infty}\sum_{n=1}^{\infty}\left(\frac{2s}{s^2-\alpha_n^2} - \frac{2s}{s^2-\beta_n^2}\right)\sin ws\,ds.$$

The series can be integrated term by term ([14] 4.8-4(b)), giving

$$\begin{aligned} G(w) &= \frac{2\pi}{|w|}\sum_{n=1}^{\infty}\left(e^{i\beta_n|w|} - e^{i\alpha_n|w|}\right) \\ &= O\left(\frac{e^{-\mu|w|}}{w}\right) \quad \text{as } w \to \pm\infty, \end{aligned} \tag{3.29}$$

where $\mu = \min\{\Im(\alpha_1), \Im(\beta_1)\}$.

The integral (3.23) exists in the strip $-\mu < \Im(s) < 1/a + \mu$. Its behaviour as $s \to \infty$ with fixed imaginary part follows from the properties (3.28) and (3.29) of $G(w)$ found above. It turns out that $g(s)$, with $s = \sigma_1 + i\sigma_2$, is bounded as $\sigma_1 \to \pm\infty$ with $-\mu < \sigma_2 < 1/a + \mu$. Consequently, $f(s)$ has the same property provided that f_1 is defined by (3.21) and f_0 is chosen to be bounded. From (3.23),

$$\begin{aligned} \log f_2(s) &= \frac{1}{2\pi}\int_{-\infty}^{\infty}\frac{e^{-isw}-1}{e^{w/a}-1}G(w)\,dw \\ &= \sum_{n-1}^{\infty}\log f_{2n}(s), \end{aligned}$$

where

$$\log f_{2n}(s) = \int_{-\infty}^{\infty}\frac{e^{-ist}-1}{t(e^{t/a}-1)}(e^{i\beta_n|t|} - e^{i\alpha_n|t|})\,\mathrm{sgn}\,t\,dt. \tag{3.30}$$

Evans, in [8], uses the standard integral

$$\ln\Gamma(z) = \int_0^{\infty}\left\{(z-1)e^{-t} - \frac{e^{-t}-e^{-zt}}{1-e^{-t}}\right\}\frac{dt}{t},$$

given in [11], to show that (3.30) reduces to

$$f_{2n}(s) = \frac{\alpha_n\Gamma\{-ia(\alpha_n+s)\}\,\Gamma\{-ia(\beta_n-s)+1\}}{\beta_n\Gamma\{-ia(\beta_n+s)\}\,\Gamma\{-ia(\alpha_n-s)+1\}}.$$

Since $\sum_{n=1}^{\infty}\log f_{2n}(s)$ converges for each s in the horizontal strip, f_2 is given by the convergent product

$$f_2(s) = \prod_{n=1}^{\infty}\frac{\Gamma\{-ia(\beta_n-s)+1\}\,\Gamma\{-ia(\alpha_n+s)\}\alpha_n}{\Gamma\{-ia(\alpha_n-s)+1\}\,\Gamma\{-ia(\beta_n+s)\}\beta_n}. \tag{3.31}$$

The function $f_1(s)$ given by (3.21) has simple poles at $-in/a \pm \alpha_0$ and simple zeros at $-in/a \pm \beta_0$; $n = 0, 1, 2, \ldots$. Similarly, $f_2(s)$ given by (3.31) has simple poles at $i(n+1)/a+\beta_m$ and $-in/a-\alpha_m$; and simple zeros at $i(n+1)/a+\alpha_m$ and $-in/a-\beta_m$; $n=0,1,2,\ldots$; $m=1,2,3,\ldots$. Define

$$f_0(s)=\frac{H\sinh\{\pi a(s-\alpha_0)\}}{\sinh\{\pi a(s-\beta_0)\}\sinh\{\pi a(s+\beta_0)\}} \tag{3.32}$$

where H will be assigned so that the incident wave has the desired amplitude. This form of f_0 has been chosen to cancel the pole of f_1 at α_0, while introducing poles at $\pm\beta_0$. At the same time f_0 decays exponentially as $s\to\pm\infty$, ensuring that the integral in (3.13) converges and allowing some movement of the contour of integration without changing the value of the integral. It has poles at $\pm\beta_0\pm in/a$; $n=0,1,2,\ldots$ and zeros at $-\alpha_0\pm in/a$, some of these zeros and poles being cancelled by poles and zeros of f_1. Define the contour of integration C to pass above $\pm\alpha_0$ and below $\pm\beta_0$. The poles of the integrand in (3.16) are shown in Figure 3.3 together with the contours of integration C and C'. It can be seen

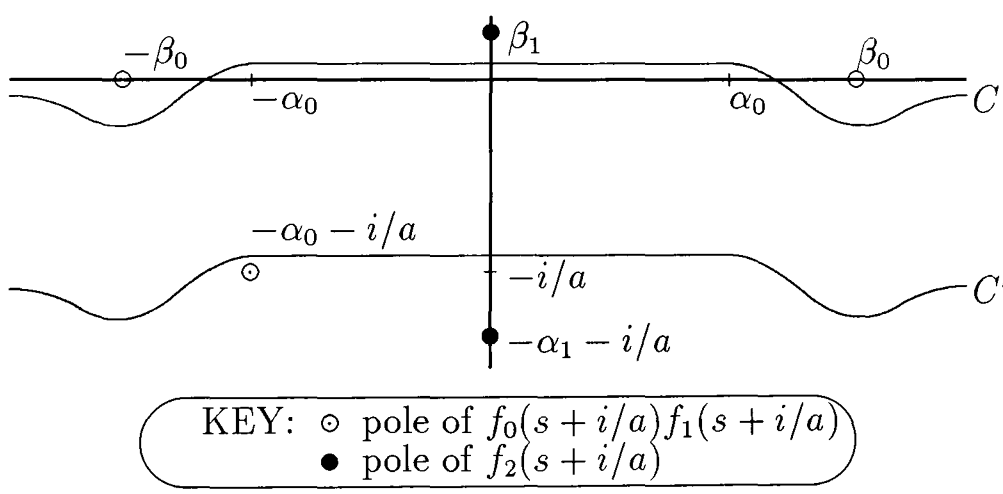

Figure 3.3: *Translation of the contour C*

that the region between C and C' is free from poles. Moreover, as $s\to\pm\infty$ within this region, $f_2(s)$ is bounded as shown above, $f_1(s)=1+O(|s|^{-1})$ by properties of the gamma-function and f_0 decreases exponentially. It is therefore permissible to move the contour.

The integrand in (3.13) has poles in the vicinity of the real line as shown in Figure 3.4. For $x < 0$, evaluating $\phi(x, y)$ by means of residues in the upper

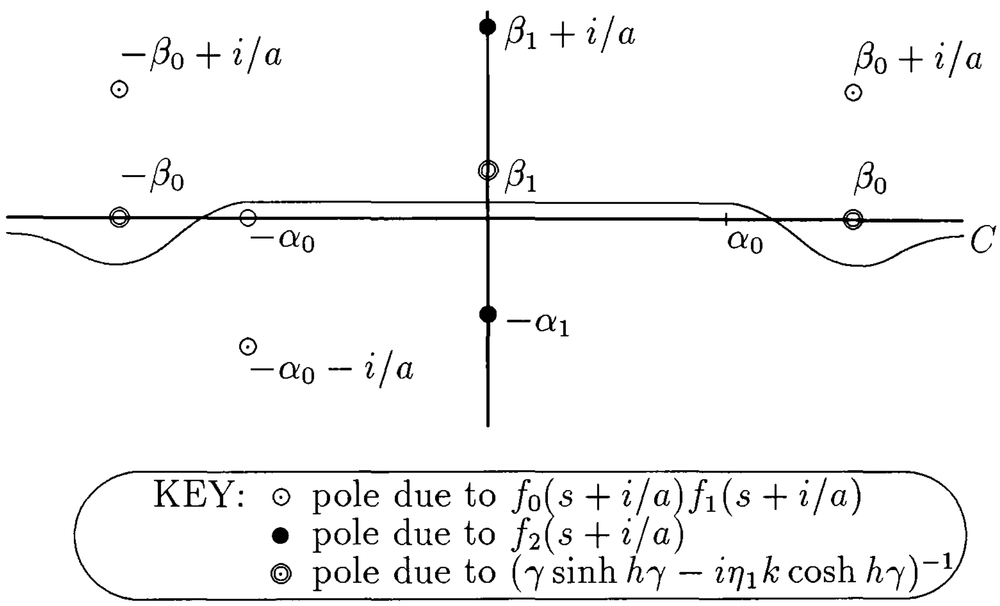

Figure 3.4: *Poles near the real line*

half-plane gives, from (3.13), incident and reflected waves from the poles $-\beta_0$ and β_0 respectively. For $x > 0$, evaluating $\phi(x, y)$ by means of residues in the lower half-plane gives the transmitted wave from the pole at $-\alpha_0$. The numerator in (3.32) was chosen so that there would be no pole at α_0.

Now, from (3.21) and (3.32),

$$f_0(s)f_1(s) = \frac{H(s-\beta_0)}{(s-\alpha_0)\sinh\{\pi a(s+\beta_0)\}}. \tag{3.33}$$

and on combining this with (3.31) it is found that

$$\begin{aligned} f(s) &= \frac{H}{\sinh\{\pi a(s+\beta_0)\}} \cdot \frac{\Gamma\{1+ia(s-\beta_0)\}\Gamma\{-ia(s+\alpha_0)\}}{\Gamma\{1+ia(s-\alpha_0\}\Gamma\{-ia(s+\alpha_0)\}} \\ &\quad \times \prod_{n=1}^{\infty} \frac{\alpha_n\Gamma\{1+ia(s-\beta_n)\}\Gamma\{-ia(s+\alpha_n)\}}{\beta_n\Gamma\{1+ia(s-\alpha_n)\}\Gamma\{-ia(s+\beta_n)\}}. \end{aligned} \tag{3.34}$$

The incident mode is given by the residue contribution to (3.13) at $s = -\beta_0$, where the contour is closed in the upper half plane.

$$I = ie^{i\beta_0 x} \lim_{s \to -\beta_0} \frac{(s+\beta_0)f(s)\cosh(\gamma y)}{\gamma \sinh(\gamma h) - i\eta_1 k \cosh(\gamma h)}$$

which, using (3.34) becomes

$$\begin{aligned} I = & \frac{H\gamma_1 \cosh(\gamma_1 y)e^{i\beta_0 x}}{\pi\{i\beta_0\eta_1 kh \sinh(\gamma_1 h) - \beta_0 \sinh(\gamma_1 h) - \gamma_1\beta_0 h \cosh(\gamma_1 h)\}} \\ & \times \frac{\Gamma(1-2ia\beta_0)\Gamma\{ia(\beta_0-\alpha_0)\}}{\Gamma\{1-ia(\alpha_0+\beta_0)\}} \\ & \times \prod_{n=1}^{\infty} \frac{\alpha_n \Gamma\{1-ia(\beta_o+\beta_n)\}\Gamma\{-ia(\alpha_n-\beta_0)\}}{\beta_n \Gamma\{1-ia(\beta_0+\alpha_n)\}\Gamma\{-ia(\beta_n-\beta_0)\}} \end{aligned} \tag{3.35}$$

Hence the solution is now known through (3.13) and (3.24). It remains to choose the constant H and this is done by specifying the amplitude of the incident wave. On closing the contour in the upper half plane (for $x < 0$) the incident mode is given by the residue at $s = -\beta_0$. The constant A in (3.1) is chosen so that the power across a surface perpendicular to the duct and at a remote distance in the negative x-direction is $\frac{1}{2}\rho_0\omega$. The power across a surface S is given by

$$P = \frac{\rho_0\omega}{2} \Re\left(i \int_S \phi \frac{\partial \overline{\phi}}{\partial n} \, dS \right). \tag{3.36}$$

In the case of the incident potential (3.1) this becomes

$$\frac{\rho_0\omega\beta_0|A|^2}{2}\left(\frac{\sinh 2h\gamma_1}{4\gamma_1} + \frac{h}{2}\right),$$

using the fact that $\gamma_1 = \gamma(\beta_0)$ is real or purely imaginary. Equating this to $\frac{1}{2}\rho_0\omega$ gives

$$A = \left\{\beta_0\left(\frac{\sinh 2h\gamma_1}{4\gamma_1} + \frac{h}{2}\right)\right\}^{-\frac{1}{2}}, \tag{3.37}$$

and substituting for A in (3.1) leads to

$$I = \frac{\cosh(\gamma_1 y)e^{i\beta_0 x}}{\{\beta_0(\sinh(2h\gamma_1)/(4\gamma_1) + h/2)\}^{\frac{1}{2}}}.$$

Comparing this with (3.35), it follows that

$$\begin{aligned} H &= \frac{\pi\beta_0\{i\eta_1 kh\sinh(\gamma_1 h) - \sinh(\gamma_1 h) - \gamma_1 h\cosh(\gamma_1 h)\}}{\gamma_1\{\beta_0(\sinh(2h\gamma_1)/(4\gamma_1) + h/2)\}^{\frac{1}{2}}} \\ &\times \frac{\Gamma\{1 - ia(\alpha_0+\beta_0)\}}{\Gamma(1-2ia\beta_0)\Gamma\{ia(\beta_0-\alpha_0)\}} \\ &\times \prod_{n=1}^{\infty} \frac{\beta_n\Gamma\{1-ia(\beta_0+\alpha_n\}\Gamma\{-ia(\beta_n-\beta_0)\}}{\alpha_n\Gamma\{1-ia(\beta_0+\beta_n)\}\Gamma\{-ia(\alpha_n-\beta_0)\}}. \end{aligned} \tag{3.38}$$

3.4 Reflection and transmission coefficients

On closing the contour (3.13) in the upper half plane the reflected mode is the residue at β_0,

$$R\cosh(y\tau_0)e^{-i\beta_0 x} = ie^{-i\beta_0 x}\lim_{s\to\beta_0}\frac{(s-\beta_0)f(s)\cosh(\gamma y)}{\gamma\sinh(\gamma h) - i\eta_1 k\cosh(\gamma h)},$$

and on substituting the expressions derived in §3.3 for $f(s)$ and H it can be written as

$$\begin{aligned} R &= \frac{i}{\{\beta_0(\sinh(2h\tau_0)/(4\tau_0) + \frac{h}{2}\}^{\frac{1}{2}}}\cdot\frac{(\alpha_0+\beta_0)\Gamma\{ia(\alpha_0+\beta_0)\}^2\Gamma(2ia\beta_0)}{(\alpha_0-\beta_0)\Gamma\{ia(\beta_0-\alpha_0)\}^2\Gamma(-2ia\beta_0)} \\ &\times\prod_{n=1}^{\infty}\frac{(\beta_0-\beta_n)(\beta_0+\alpha_n)\Gamma\{ia(\beta_0+\beta_n)\}^2\Gamma\{-ia(\beta_0-\alpha_n)\}^2}{(\beta_0+\beta_n)(\beta_0-\alpha_n)\Gamma\{-ia(\beta_0+\beta_n)\}^2\Gamma\{ia(\beta_0-\alpha_n)\}^2}. \end{aligned} \tag{3.39}$$

It can be seen from (3.8) that the reflection coefficient, *ie* the ratio of the amplitude of the only far-reflected mode to that of the incident wave, is $|R|/\{|A|\cosh(\tau_0 y)\}$. Since β_0 and α_0 are real with all other β_n and α_n purely imaginary, it follows from (3.39) that the reflection coefficient is

$$\left|\frac{\alpha_0+\beta_0}{\alpha_0-\beta_0}\cdot\frac{\Gamma\{ia(\alpha_0+\beta_0\}^2}{\Gamma\{ia(\beta_0-\alpha_0)\}^2}\right| = \left|\frac{\sinh\{\pi a(\alpha_0-\beta_0)\}}{\sinh\{\pi a(\alpha_0+\beta_0)\}}\right|, \tag{3.40}$$

in agreement with (4.10) in [9], where the notation is different.

Similarly the transmitted mode is given by closing the contour in the lower half plane in (3.13) and taking the residue at α_0. Accordingly, the mode is

$$T\cosh(y\lambda_0 y)e^{i\alpha_0 x} = ie^{i\alpha_0 x}\lim_{s\to-\alpha_0}\frac{(s+\alpha_0)f(s)\cosh(\gamma y)}{\gamma\sinh(\gamma h) - i\eta_1 k\cosh(\gamma h)},$$

which, using the expressions for $f(s)$ and H, becomes

$$\begin{aligned} T &= \frac{-i}{\alpha_0\beta_0^{\frac{3}{2}}} \cdot \frac{L_1'(-\beta_0)}{L_1(\alpha_0)} \cdot \frac{(\alpha_0^2-\beta_0^2)(\alpha_0+\beta_0)}{\sinh(2h\tau_0)/(2\tau_0)+h} \\ &\times \frac{\Gamma\{-ia(\alpha_0+\beta_0)\}^2}{\Gamma(-2ia\alpha_0)\Gamma(-2ia\beta_0)} \prod_{n=1}^{\infty} \left[\frac{(\beta_0+\alpha_n)(\alpha_0+\beta_n)\Gamma\{-ia(\beta_0+\alpha_n)\}}{(\beta_0+\beta_n)(\alpha_0+\alpha_n)\Gamma\{-ia(\beta_0+\beta_n)\}} \right. \\ &\times \left. \frac{\Gamma\{-ia(\beta_n-\beta_0)\}\Gamma\{-ia(\alpha_0+\beta_n)\}\Gamma\{ia(\alpha_0-\alpha_n)\}}{\Gamma\{-ia(\alpha_n-\beta_0)\}\Gamma\{-ia(\alpha_0+\alpha_n)\}\Gamma\{ia(\alpha_0-\beta_n)\}} \right], \end{aligned} \tag{3.41}$$

using the notation $L_1(s)$ for the denominator of the integrand in (3.13), a function closely related to the K_1 of (3.51).

The modulus of this expression simplifies when α_0 and β_0 are real but all other α_n and β_n are purely imaginary. In that case $-ia(\beta_0+\alpha_n)$ and $-ia(\alpha_n-\beta_0)$, for example, are complex conjugates. It follows that the gamma functions of these two quantities are also complex conjugates. The transmission coefficient, *ie* the ratio of the amplitude of the only far-transmitted mode to that of the incident wave, is $|T|/\{|A|\cosh(\tau_0 y)\}$, which, because of the real and imaginary nature of the α_n and β_n, simplifies to

$$\left\{ \frac{\eta_1}{\eta_2} \cdot \frac{\sinh(2h\lambda_0)/(2\lambda_0)+h}{\sinh(2h\tau_0)/(2\tau_0)+h} \left(1 - \left| \frac{\sinh\{\pi a(\alpha_0-\beta_0)\}}{\sinh\{\pi a(\alpha_0+\beta_0)\}} \right|^2 \right) \right\}^{\frac{1}{2}} = \frac{|T|}{|A|}, \tag{3.42}$$

again in agreement with [9]. The notation $\tau_0 = \gamma(\beta_0)$, $\lambda_0 = \gamma(\alpha_0)$ is used here.

3.5 Power balance

Denoting the power associated with the reflected and transmitted waves by $P(R)$ and $P(T)$ respectively, and using (3.36), the modes (3.39) and (3.41) give the expressions

$$\begin{aligned} P(R) &= \frac{\rho_0\omega}{2} \left(\frac{\alpha_0+\beta_0}{\alpha_0-\beta_0} \right)^2 \left| \frac{\Gamma\{ia(\alpha_0+\beta_0\}}{\Gamma\{ia(\alpha_0-\beta_0\}} \right|^4 \\ &= \frac{\rho_0\omega}{2} \cdot \frac{\sinh^2\{\pi a(\alpha_0-\beta_0)\}}{\sinh^2\{\pi a(\alpha_0+\beta_0)\}}, \end{aligned} \tag{3.43}$$

$$\begin{aligned} P(T) &= \frac{-\rho_0\omega\beta_0}{8\alpha_0}\left|\frac{L'(-\beta_0)}{L(\alpha_0)}\right|^2(\alpha_0+\beta_0)^4(\alpha_0-\beta_0)^2\frac{\sinh(2h\gamma_2)/(2\gamma_2)+h}{\sinh(2h\gamma_1)/(2\gamma_1)+h} \\ &\quad\times\left|\frac{\Gamma\{ia(\alpha_0+\beta_0)\}^2}{\Gamma(2ia\alpha_0)\Gamma(2ia\beta_0)}\right|^2\prod_{n=1}^{\infty}\frac{(\beta_0^2-\alpha_n^2)(\alpha_0^2-\beta_n^2)}{(\beta_0^2-\beta_n^2)(\alpha_0^2-\alpha_n^2)} \\ &= \frac{\rho_0\omega}{2}\left[1-\frac{\sinh^2\{\pi a(\alpha_0-\beta_0)\}}{\sinh^2\{\pi a(\alpha_0+\beta_0)\}}\right]. \end{aligned} \tag{3.44}$$

The power balance is now complete, since $P(R)+P(T)=\frac{1}{2}\rho_0\omega$, which is the input power associated with the incident wave.

3.6 The limiting case of discontinuous acoustic impedance

In the limiting case, $a \to 0$, the upper wall of the duct illustrated in Figure 3.1 has two halves, each with constant impedance. In this case those modes containing terms in/a ($n \neq 0$) (see Figure 3.4 and the preceding discussion) disappear to infinity and the remaining modes have x-wavenumbers $-\alpha_0$, $\pm\beta_0$, $-\alpha_1$, $-\alpha_2$, $\ldots$, β_1, β_2, $\ldots$. In the Wiener–Hopf formulation of the limiting case, which is related to (3.4), (3.5) and (3.6), the total velocity potential, ϕ, satisfies

$$\left(\frac{\partial^2}{\partial x^2}+\frac{\partial^2}{\partial y^2}+k^2\right)\phi=0; \quad \Re(k)>0,\ \Im(k)\geq 0 \tag{3.45}$$

and the boundary condition for the lower, rigid surface is

$$\phi_y(x,0)=0. \tag{3.46}$$

The impedance boundary condition takes the form

$$\phi_y - i\eta k\phi = 0; \quad y=h,\ \Re(\eta)\geq 0 \tag{3.47}$$

but with

$$\eta(x)=\begin{cases}\eta_1, & x<0,\\ \eta_2, & x\geq 0,\end{cases} \tag{3.48}$$

which is the limiting ($a \to 0$), discontinuous form of (3.7). The solution to the limiting problem depends on edge conditions at the discontinuity. A suitable condition is obtained by requiring that pressure be continuous in the fluid. In particular, $\phi_y(+0) = \phi_y(-0)$. On defining the total, time-harmonic velocity potential by

$$\phi(x,y) = \phi^{(s)} + \frac{\cosh(\tau_0 y)}{\cosh(\tau_0 h)} e^{i\beta_0 x}, \tag{3.49}$$

where $\phi^{(s)}$ denotes the scattered potential, the Fourier transforms of the governing equation and boundary conditions, evaluated at $y = h$, are

$$\begin{aligned} \Phi^+(s,h) + \Phi^-(s,h) &= C(s)\cosh(h\gamma), \\ \Phi_y^+(s,h) + \Phi_y^-(s,h) &= \gamma C(s)\sinh(h\gamma), \\ \Phi_y^+(s,h) - i\eta_1\Phi^-(s,h) &= 0, \\ \Phi_y^+(s,h) - i\eta_2\Phi^+(s,h) &= \frac{-iK_2(\beta_0)}{\beta_0 + s}. \end{aligned} \tag{3.50}$$

The functions K_2 of (3.50) and K_1 are defined by

$$K_j(s) = \gamma(s)\tanh\{h\gamma(s)\} - i\eta_j k; \quad j = 1,2, \tag{3.51}$$

which is consistent with (3.12). On eliminating $C(s)$, $\Phi_y^+(s,h)$ and $\Phi_y^-(s,h)$, it is found that

$$\Phi_y^+(s,h) + \frac{\eta_2 K_1(s)}{\eta_1 K_2(s)}\Phi_h^-(s,h) = \frac{-iK_2(\beta_0)}{K_2(s)(s+\beta_0)}\gamma\tanh(h\gamma)$$

which, on noting that

$$\gamma\tanh(h\gamma) = \frac{i\eta_1\eta_2\{K(s)-1\}}{\eta_1 K(s) - \eta_2}, \tag{3.52}$$

can be rearranged as

$$\frac{\Phi^+(s,h)}{K_+(s)} + \Phi^-(s,h)K_-(s) = \frac{K_2(\beta_0)\eta_1\eta_2 k\{K(s)-1\}}{(s+\beta_0)K_2(s)\{\eta_1 K(s) - \eta_2\}K_+(s)}. \tag{3.53}$$

Here $K(s)$ is the Wiener–Hopf kernel and is defined by

$$K(s) = \frac{\eta_2 K_1(s)}{\eta_1 K_2(a)} = K_+(s)K_-(s), \tag{3.54}$$

where the functions $K_+(s)$ and $K_-(s)$ are analytic and non-zero in the upper and lower half planes respectively. These are "plus" and "minus" functions such as have already been described in §2.11. Suitable functions K_+ and K_- can be constructed by starting from the infinite product representation

$$K(s) = K(0) \prod_{n=0}^{\infty} \frac{1 - s^2/\beta_n^2}{1 - s^2\alpha_n^2} = \frac{\eta_2}{\eta_1} \prod_{n=0}^{\infty} \frac{s^2 - \beta_n^2}{s^2 - \alpha_n^2}. \tag{3.55}$$

The infinite products converge because both α_n and β_n are asymptotically equal to $(\pi i n)/h$, whilst their difference is of order n^{-3} for large n. The plus and minus functions may be defined as

$$K_\pm(s) = \left(\frac{\eta_2}{\eta_1}\right)^{\frac{1}{2}} \prod_{n=0}^{\infty} \frac{s \pm \beta_n}{s \pm \alpha_n}. \tag{3.56}$$

These are analytic and non-zero in overlapping upper and lower half planes respectively, provided that all the α_n and β_n have positive imaginary parts, which can be ensured by giving k a small positive imaginary part, [18]. Alternatively, η_1 and η_2 can each be given a small positive real part (acoustic conductance, [17]). This will also ensure that $\Im(\alpha_n) > 0$ and $\Im(\beta_n) > 0$ for all large enough n. A finite number of factors can be transferred from K_+ to K_- and *vice versa* in (3.56) in order to define functions with the requisite "plus" and "minus" properties.

The right-hand side of (3.53) can be rearranged, with further application of the relation (3.52), into a form which is easily written as the sum of plus and minus functions. This form is

$$\frac{\Phi^+(s,h)}{K_+(s)} + \Phi^-(s,h)K_-(s) = -\left\{\frac{1}{K_+(s)} - K_-(s)\right\} \frac{i\eta_1 K_2(\beta_0)}{(\eta_1 - \eta_2)(s + \beta_0)},$$

and after performing the split, the resulting relation is

$$\frac{\Phi_y^+(s,h)}{K_+(s)} - \frac{i\eta_1 K_2(\beta_0)}{(\eta_2 - \eta_1)(s + \beta_0)} \left\{-\frac{1}{K_+(s)} + K_+(\beta_0)\right\} = E(s)$$

$$= -\Phi_y^-(s,h)K_-(s) + \frac{K_+(\beta_0) - K_-(s)}{s+\beta_0} \cdot \frac{i\eta_1 K_2(\beta_0)}{\eta_2 - \eta_1} \tag{3.57}$$

Note that, since the regions in which K_+ and K_- are analytic overlap, it follows by analytic continuation that both sides of (3.57) represent the same entire function, say $E(s)$. The rates of growth of the two sides can be deduced from those of Φ^+ and $1/K_+$ in the upper half plane, and Φ^- and K_- in the lower.

For Φ^+ and Φ^-, assume an integrable singularity at (0,h) in ϕ, that is

$$\phi(x,h) \sim Ax^{b_\pm}, \ b_\pm > -1 \text{ as } x \to \pm 0.$$

In fact, using the edge condition of continuous pressure, $b_\pm > 0$. On using the Abelian theorem given by Noble [18], $\Phi^+(s) \sim s^{-b_+-1}$ as $s \to \infty$ in the upper half plane, and $\Phi^-(s) \sim s^{-b_--1}$ as $s \to \infty$ in the lower half plane. The functions $\Phi_y^\pm(s)$ tend to zero as $|s| \to \infty$ because of the relation $\Phi_y^\pm(s) = \gamma \tanh(h\gamma)\Phi^\pm(s)$.

It can be shown that $1/K_+$ is bounded as $|s| \to \infty$ in the upper half plane. Equation (3.56) can be rearranged as

$$\frac{1}{K_+(s)} = \prod_{n=0}^{\infty} \frac{s+\alpha_n}{s+\beta_n} = \prod_{n=0}^{\infty} \left(1 + \frac{\alpha_n - \beta_n}{s+\beta_n}\right).$$

The right-hand product satisfies

$$\left|\prod_{n=0}^{\infty} \left(1 + \frac{\alpha_n - \beta_n}{s+\beta_n}\right)\right| \leq \prod_{n=0}^{\infty} \left(1 + \frac{|\alpha_n - \beta_n|}{|s+\beta_n|}\right)$$

which converges provided that s is not equal to any $-\beta_n$, a condition which holds in the half plane of interest, since $\beta_n = O(n)$ and $\beta_n - \alpha_n = O(n^{-1})$ as $n \to \infty$. Hence, $1/K_+(s) = O(1)$ as $|s| \to \infty$ in the upper half plane. An analogous result holds for $K_-(s)$ in the lower half plane.

It follows from Liouville's theorem that $E(s)$ is identically zero. Expressions for Φ_y^+ and Φ_y^- can now be obtained from (3.57). Thus

$$\Phi_y^+(s,h) = \frac{i\eta_1 K_2(\beta_0)}{\eta_2 - \eta_1} \left\{ \frac{1}{s+\beta_0} + \frac{K_+(s)K_+(\beta_0)}{s+\beta_0} \right\} \tag{3.58}$$

and

$$\Phi_y^-(s,h) = \frac{i\eta_1 K_2(\beta_0)}{\eta_2 - \eta_1} \frac{K_+(\beta_0) - K_-(s)}{(s+\beta_0)K_-(s)}. \tag{3.59}$$

An expression for $\Phi_y(s,h)$ is obtained by addition of (3.58) and (3.59). After simplification the result is

$$\Phi_y(s,h) = \frac{i\eta_1 K_2(\beta_0)}{(\eta_2 - \eta_1)(s+\beta_0)} K_+(\beta_0) \left\{ -K_+(s) + \frac{1}{K_-(s)} \right\}$$

Likewise, the transform of the velocity potential is obtained, after some manipulation, as

$$\Phi(s,h) = \frac{\Phi_y(s,h)}{\gamma \tanh(h\gamma)} = -\frac{iK_2(\beta_0)K_+(\beta_0)}{K_2(s)(s+\beta_0)K_-(s)}. \tag{3.60}$$

The inverse transform of (3.60) is the velocity potential,

$$\phi(x,y) = \frac{K_2(\beta_0)K_+(\beta_0)}{2\pi i} \int_{-\infty}^{\infty} \frac{\cosh(y\gamma)}{\cosh(h\gamma)} \cdot \frac{e^{-isx}\,dx}{K_2(s)(s+\beta_0)K_-(s)}. \tag{3.61}$$

The poles of the integrand are at $-\alpha_n$, β_n and $-\beta_0$, where $n = 0, 1, 2, \ldots$. These represent the incident wave mode ($-\beta_0$), the reflected modes (β_n) and transmitted modes ($-\alpha_n$). In accordance with the radiation condition (3.8) (which is enforced by restricting the duct height), all modes for $n > 0$ are imaginary and so not propagated for large positive or negative x.

The residue contribution to (3.61) from the simple pole at $-\beta_0$ gives the incident mode, with amplitude

$$\frac{\cosh(y\tau_0)}{\cosh(h\tau_0)},$$

while the amplitude of the reflected mode, from the residue contribution at β_0, is

$$\frac{\cosh(y\tau_0)}{\cosh(h\tau_0)} \frac{|\alpha_0 - \beta_0|}{|\alpha_0 + \beta_0|}.$$

The reflection coefficient is therefore

$$\frac{|\alpha_0 - \beta_0|}{|\alpha_0 + \beta_0|},$$

which is the same as (3.40) in the limit as $a \to 0$.

A similar computation for the transmission coefficient uses the residue contribution to (3.61) from the pole at $-\alpha_0$. The transmission coefficient, being the ratio of the amplitude of the transmitted mode, is

$$\frac{\cosh(y\lambda_0)}{\cosh(h\lambda_0)} \frac{\cosh(h\tau_0)}{\cosh(y\tau_0)} \frac{K_2(\beta_0)}{K_2'(\alpha_0)} \frac{K_+(\beta_0)}{(\alpha_0+\beta_0)K_+(\alpha_0)}. \tag{3.62}$$

The limiting form of (3.42) as $a \to 0$, with $y = h$, is

$$\frac{\cosh(h\lambda_0)}{\cosh(h\tau_0)} \frac{4\alpha_0\beta_0}{(\alpha_0+\beta_0)^2} \frac{\eta_1 K_2'(\beta_0)}{\eta_2 K_1'(\alpha_0)}. \tag{3.63}$$

It can be shown that (3.62) and (3.63) are equivalent by means of the infinite product representations already used in (3.41) and (3.44). It has now been shown that the transmission and reflection coefficients in the limiting case are the same as those obtained by letting $a \to 0$ in the expressions (3.40) and (3.41). This provides a check on the working and on the different solution techniques used for the smoothly-varying and discontinuous cases.

Chapter 4

Propagation of fluid-loaded structural waves along an elastic duct with smoothly-varying bending characteristics

4.1 Introduction

This chapter contains published material [12]. It deals with acoustic scattering by a duct in which one wall comprises an elastic plate with properties varying continuously in one space direction. Specific details as to which parameters vary are left until later in the text, however a simple example is smooth variation in plate thickness. The physical parameters are assumed to vary according to a simple heuristic mathematical law (*cf.* [23, 8]). The aim is to understand qualitatively the effects of a smooth change in material properties rather than quantify a specific physical situation.

4.2 The plate equation

Before formulating the boundary-value problem that describes the sound field within the duct it is necessary to derive the equation governing vibrations of a loaded plate with non-uniform elastic properties. The following is based on the theory in [24], where different notation is used.

Figure 4.1 shows a rectangular portion of a thin elastic plate which is subjected to pressure causing slight cylindrical bending; the broken lines indicate a strip of the plate with unit width in the z-direction. In any thin, narrow layer of the

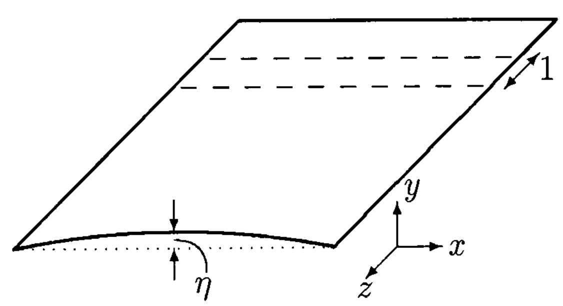

Figure 4.1: *Rectangular portion of bent plate, showing the strip of unit width.*

strip, located at a distance y from the neutral surface (see Figure 4.2 and the text below), the normal component of stress in the longitudinal direction of the layer, σ_x, can be expressed in terms of the Young's modulus $E(x)$, Poisson's ratio $\nu(x)$ and curvature, all of which are assumed to vary with x, as explained in the next paragraph.

The deflection of the plate is denoted by η and is taken as positive in the direction of increasing y. The curvature of the plate, regarded as positive when convex downwards, is approximated by $d^2\eta/dx^2$ so that the elongation in the x-direction of the layer under consideration is

$$\epsilon_x = -y\frac{d^2\eta}{dx^2}. \tag{4.1}$$

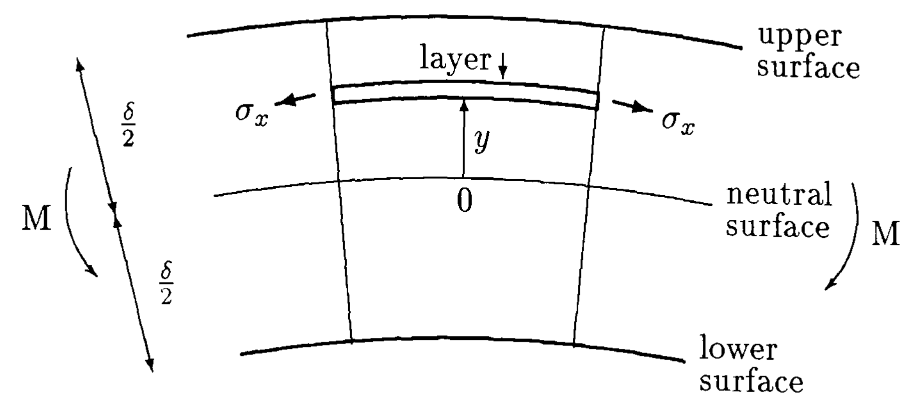

Figure 4.2: *Section of strip, showing neutral surface and thin layer.*

Hooke's law relates the normal stresses σ_x and σ_z to the unit elongations ϵ_x and ϵ_z by

$$\epsilon_x = \frac{\sigma_x}{E(x)} - \frac{\nu(x)\sigma_z}{E(x)}, \qquad \epsilon_z = \frac{\sigma_z}{E(x)} - \frac{\nu(x)\sigma_x}{E(x)} = 0.$$

In the second of these equations the lateral strain ϵ_z must be zero to preserve the cylindrical shape, so that

$$\epsilon_x = \frac{1-\nu(x)^2}{E(x)}\sigma_x,$$

and it follows from (4.1) that, for small deflections of the plate,

$$\sigma_x = -\frac{E(x)\,y}{1-\nu(x)^2}\frac{d^2\eta}{dx^2}. \tag{4.2}$$

It should be noted that for the purposes of this section, y is measured from the neutral surface, that is the plane which is subject to neither compression nor tension during deformation. The curvature of the plate as drawn in Figure 4.2 is negative; for $y > 0$ the stress on the indicated layer is positive, causing elongation. (In following sections of this chapter the dimensional co-ordinate $\hat{y}$ and its non-dimensional counterpart y are measured from the lower surface of the duct.) Equation (4.2) is an expression for the normal component of stress in the longitudinal direction in the case of varying Young's modulus (E) and Poisson ratio (ν). The reader is referred to [24] for further details.

The relation (4.2) is multiplied by y and integrated with respect to y through the thickness of the plate to give the equation of the deflection curve of the elemental strip, namely

$$B(x)\frac{d^2\eta}{dx^2} = -M(x), \tag{4.3}$$

where

$$B(x) = \frac{E(x)\delta^3}{12\{1-\nu(x)^2\}}$$

is the bending stiffness (flexural rigidity) of the plate material and $M(x)$ the bending moment per unit distance in the x-direction. With reference to Figure 4.2, positive M is in the sense depicted, causing tension in the upper surface of the plate and compression in the lower.

If the plate is subjected to a loading $q(x)$ acting from below, the equation of equilibrium in terms of $M(x)$ is

$$\frac{d^2M}{dx^2} = -q(x). \tag{4.4}$$

Provided that variable bending stiffness $B(x)$ is twice differentiable then, using (4.3) together with (4.4) the equation of equilibrium in terms of the lateral displacement is

$$B(x)\frac{d^4\eta}{dx^4} + 2B'(x)\frac{d^3\eta}{dx^3} + B''(x)\frac{d^2\eta}{dx^2} = q(x). \tag{4.5}$$

This relates to cylindrical bending with varying bending stiffness. Further details can be found in [24]. In this chapter, the variation in the bending stiffness $B(x)$ is attributable to non-uniformity of Young's modulus, Poisson ratio and/or the area density of the plate, whereas Timoshenko and Woinowsky-Krieger envisage a plate with uniform material properties but varying thickness when deriving their equation. Whilst the varying thickness model may be the most obviously practical one, it is interesting to observe that the mathematical analysis is equally applicable to a plate of constant thickness but varying material, such as an alloy containing changing proportions of metals, and to situations where both thickness and material vary in a suitable way.

Now consider a vibrating plate subject to fluid pressure $q(x,t)$ and with displacement $\eta(x,t)$. The equation governing lateral vibrations follows from (4.5) as

$$\frac{\partial^4\eta}{\partial x^4} + \frac{2B'(x)}{B(x)}\frac{\partial^3\eta}{\partial x^3} + \frac{B''(x)}{B(x)}\frac{\partial^2\eta}{\partial x^2} = -\frac{m(x)}{B(x)}\frac{\partial^2\eta}{\partial t^2} - [p]^+_-, \tag{4.6}$$

where $m(x)$ is the mass per unit area and $[p]^+_-$ the fluid pressure difference across the plate. In the case of motion with harmonic time dependence of angular frequency ω, this becomes

$$\frac{\partial^4\eta}{\partial x^4} + \frac{2B'(x)}{B(x)}\frac{\partial^3\eta}{\partial x^3} + \frac{B''(x)}{B(x)}\frac{\partial^2\eta}{\partial x^2} - \frac{\omega^2 m(x)}{B(x)}\eta = -[p]^+_-. \tag{4.7}$$

The second and third terms of (4.7) vanish when the bending stiffness B is constant. It is thus to be expected that their effect on the mathematical analysis will be greater if $B(x)$ changes rapidly with x.

4.3 The boundary value problem

The boundary-value problem describes a two-dimensional infinite duct occupying the region $0 \le \hat{y} \le \hat{h}$ of a Cartesian coordinate system $(\hat{x}, \hat{y}, \hat{z})$ (see Figure 4.3). Note that, unlike §4.2, dimensional quantities are here and henceforth indicated by a caret $\hat{}$. The lower duct wall, that is at $\hat{y} = 0$, is rigid whilst the upper wall comprises an elastic plate whose material properties vary continuously and monotonically between limiting values which are approached as $\hat{x}$ becomes large in absolute value. A compressible fluid of mean density ρ_0 and sound speed c occupies the interior of the duct whilst the exterior region is *in vacuo*. The dimensional boundary-value-problem is formulated using (4.7) as the plate equation. This is non-dimensionalised with respect to length and time scales k^{-1} and

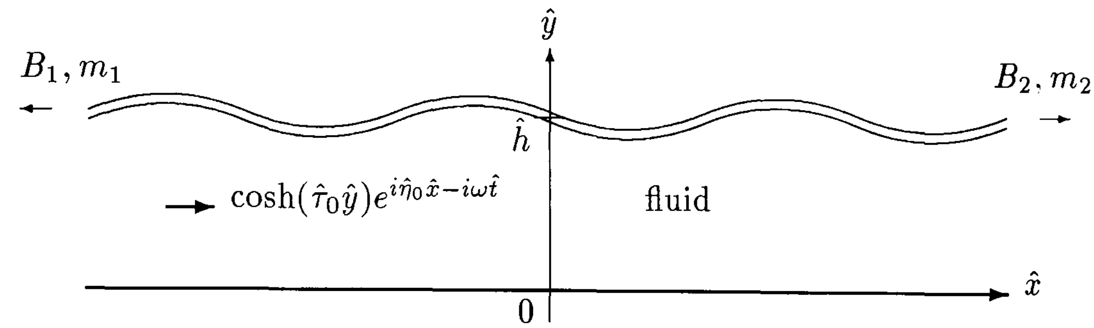

Figure 4.3: *The duct*

ω^{-1} and then modified to represent the situation in which the plate properties vary *slowly* with distance along the plate. The analysis is also applicable to the problem obtained by reflecting the configuration in the plane $\hat{y} = 0$ and removing the rigid surface there. (That is a 2-dimensional duct in which both boundaries comprise elastic plates.)

A fluid-coupled structural wave propagates along the elastic plate and is scattered due to the variation in the plate properties. The incident forcing has the form

$$\phi_0(\hat{x}, \hat{y}, \hat{t}) = A\cosh(\hat{\tau}_0\hat{y})e^{i\hat{\eta}_0\hat{x}-i\omega\hat{t}}$$

where the wavenumbers $\hat{\eta}_0$ and $\hat{\tau}_0$ – or rather their non-dimensional equivalents – are defined later in the text. This incident wave has harmonic time dependence, of angular frequency ω. Both the incident wave and the elastic properties of the plate are independent of $\hat{z}$ and thus fluid velocity potential may be written as $\Phi(\hat{x}, \hat{y}, \hat{t})$. The fluid pressure and plate elevation $\hat{\eta}$ are related to the velocity potential by

$$p(\hat{x}, \hat{y}, \hat{t}) = -\rho_0\frac{\partial\Phi}{\partial\hat{t}}(\hat{x}, \hat{y}, \hat{t}), \qquad \frac{\partial\hat{\eta}}{\partial t} = \frac{\partial\Phi}{\partial y}.$$

A steady state solution is sought and thus the acoustic field may be expressed as

$$\Phi(\hat{x}, \hat{y}, \hat{t}) = \Re\{\hat{\phi}(\hat{x}, \hat{y})e^{-i\omega\hat{t}}\}.$$

For convenience, the harmonic time factor is henceforth suppressed.

The steady state, time-independent potential $\hat{\phi}(\hat{x},\hat{y})$ satisfies the Helmholtz equation

$$\left(\frac{\partial^2}{\partial\hat{x}^2}+\frac{\partial^2}{\partial\hat{y}^2}+k^2\right)\hat{\phi}=0;\quad \Re(k)>0,\ \Im(k)\geq 0, \tag{4.8}$$

where $k=\omega/c$ is the acoustic wavenumber. Although k is a real quantity, it is mathematically convenient to allow it to be complex with a small positive imaginary part. Physically this corresponds to a small dissipation of wave energy with distance. The lower bounding surface is described by the boundary condition

$$\hat{\phi}_{\hat{y}}(\hat{x},0)=0,$$

and the upper one by (4.7) which, expressed in terms of $\hat{\phi}(\hat{x},\hat{y})$, is

$$\left\{\frac{\partial^4}{\partial\hat{x}^4}+\frac{2B'(\hat{x})}{B(\hat{x})}\frac{\partial^3}{\partial\hat{x}^3}+\frac{B''(\hat{x})}{B(\hat{x})}\frac{\partial^2}{\partial\hat{x}^2}-\frac{m(\hat{x})\omega^2}{B(\hat{x})}\right\}\hat{\phi}_{\hat{y}}(\hat{x},\hat{h})=\frac{\rho_0\omega^2}{B(\hat{x})}\hat{\phi}(\hat{x},\hat{h}) \tag{4.9}$$

where ρ_0 is the density of the fluid in the absence of disturbance, $m(\hat{x})$ is the mass per unit area of the plate material and $B(\hat{x})$ its bending stiffness. The bending stiffness and mass per unit area are taken, *cf* (3.7), to have the forms

$$B(\hat{x})=\frac{B_1+B_2e^{\hat{x}/\hat{a}}}{1+e^{\hat{x}/\hat{a}}},\qquad m(\hat{x})=\frac{m_1+m_2e^{\hat{x}/\hat{a}}}{1+e^{\hat{x}/\hat{a}}}, \tag{4.10}$$

where $\hat{a}$ is a positive constant determining the maximum rate of change of the function (which occurs at $\hat{x}=0$). In the case $\hat{a}>>1$ the first and second derivative of $B(\hat{x})$ are small compared to $B(\hat{x})$ itself and this corresponds to *slow* variation of the properties of the plate along its length. In such circumstances a good approximation to the plate equation is obtained by neglecting the second and third terms on the left-hand side. However, this approximation is more widely valid. The reader is referred to the definitions of μ_j and α_j given below equation (4.22). For $\mu_j,\alpha_j>1,\ j=1,2$ it is found that the approximation is valid provided that $a\geq 1$; in fact, for some ranges of the parameters μ_j,α_j it is possible to take smaller values of a. This can be seen by looking at the maximum values of $|B'/B|$ and $|B''/B|$. For example, it is required that

$$\begin{aligned}\mu_j^4 &>> \max\left|\frac{B'(x)}{B(x)}\right| \\ &= \frac{1}{2a}\left|\frac{B_2 - B_1}{B_1 + B_2}\right|\end{aligned}$$

from which it follows that

$$a >> \frac{1}{2\mu_j^4}\left|\frac{B_2 - B_1}{B_1 + B_2}\right|,$$

and a similar expression is obtained for the term $|B''/B|$. This chapter is primarily concerned with the situation in which the second and third terms of the differential operator of (4.9) can be neglected. Note, however, that this approximation is never valid for $a = 0$.

The same radiation condition, (3.8), holds as in chapter 3. That is, with the exception of the incident mode, all disturbances travel out to infinity as though initiating from the point $\hat{x} = 0$. For the geometric constraint $h = \hat{h}k < \pi/2$ with $\alpha_j/\mu_j^4 < \tan(\hat{h}k)$ the fluid velocity potential thus assumes the form

$$\hat{\phi}(\hat{x}, \hat{y}) = \begin{cases} (Ae^{i\hat{\eta}_0\hat{x}} + R_0 e^{-i\hat{\eta}_0\hat{x}})\cosh(\hat{\tau}_0\hat{y}) & \text{as } \hat{x} \to -\infty, \\ T_0\cosh(\hat{\lambda}_0\hat{y})e^{i\hat{\nu}_0\hat{x}} & \text{as } \hat{x} \to +\infty, \end{cases} \tag{4.11}$$

where R_0 (T_0) is the complex reflection (transmission) coefficient of the fundamental mode. The wavenumbers $\hat{\nu}_0$ and $\hat{\lambda}_0$ are associated with the limiting properties of the plate for large positive values of $\hat{x}$ and are defined later in the text.

The boundary-value problem is now expressed in a non-dimensional form by using a length scale of k^{-1} and a time scale of ω^{-1}. Non-dimensional variables, functions, wavenumbers and plate properties are denoted by symbols without carets. For example, $\hat{x}k = x$, $\hat{t}\omega = t$ and $\hat{\phi}k^2/\omega = \phi$. The formulation (4.8)-(4.11) becomes

$$\left(\frac{\partial^2}{\partial x^2} + \frac{\partial^2}{\partial y^2} + 1\right)\phi = 0, \quad 0 \leq y \leq h, \quad -\infty < x < \infty \tag{4.12}$$

$$\phi_y(x,0) = 0, \tag{4.13}$$

$$\left\{\frac{\partial^4}{\partial x^4} - \mu^4(x)\right\}\phi_y(x,h) = \alpha(x)\phi(x,h), \tag{4.14}$$

$$\phi(x,y) = \begin{cases} (Ae^{i\eta_0 x} + R_0 e^{-i\eta_0 x})\cosh(\tau_0 y) & \text{as } x \to -\infty, \\ T_0 \cosh(\lambda_0 y) e^{i\nu_0 x} & \text{as } x \to +\infty, \end{cases} \tag{4.15}$$

where the second and third terms of the plate equation (4.9) are neglected under the assumptions stated above. These assumptions are discussed further in §4.6. The plate wavenumber μ and fluid loading parameter α are defined by

$$\mu^4(x) = \left(\frac{\omega^2}{k^4}\right)\frac{m_1 + m_2 e^{x/a}}{B_1 + B_2 e^{x/a}}, \qquad \alpha(x) = \left(\frac{\rho_0\omega^2}{k^5}\right)\frac{1 + e^{x/a}}{B_1 + B_2 e^{x/a}}. \tag{4.16}$$

Each of these functions has a point of inflection, where the gradient is maximal, at $x = a\log(B_1/B_2)$. Small values of a represent a rapid transition near the points of inflection from the left-hand asymptotic values B_1 and m_1 to the right-hand ones B_2 and m_2; thus in the limit $a \to 0$, when the points of inflection tend to 0, the problem is equivalent to one of standard Wiener–Hopf type, provided that edge conditions are introduced at the position of the discontinuity of material properties. In the special case $B_1 = B_2$, $\alpha(x)$ is constant and no assumptions regarding the relative sizes of μ_j^4 and ka are needed since the second and third terms in (4.9) are zero for all values of a. Further details about the limiting cases $a \to 0$ for $B_1 = B_2$ and $B_1 \neq B_2$ are discussed in §4.6.

A solution of the form

$$\phi(x,y) = \frac{1}{2\pi}\int_C \Phi(s,y)e^{-ixs}\,ds \tag{4.17}$$

is sought, where the wavenumber s is regarded as a complex variable and C is a contour extending from $-\infty$ to ∞ which is chosen so that $\phi(x,y)$ satisfies the radiation condition (4.15). The location of contour C is crucial to the analysis which follows; full details are given in §4.4. It is clear that expression (4.17) satisfies (4.12) provided that

$$\Phi_{yy}(s,y) - (s^2-1)\Phi(s,y) = 0. \tag{4.18}$$

Thus $\Phi(s,y)$ has the general form

$$\Phi(s,y) = A(s)e^{\gamma y} + B(s)e^{-\gamma y},$$

where $\gamma = (s^2-1)^{1/2}$. The boundary condition at the lower duct surface, that is (4.13), implies that $A(s) - B(s) = 0$, so that

$$\Phi(s,y) = 2A(s)\cosh(\gamma y).$$

For convenience $A(s)$ is re-cast as

$$A(s) = \frac{f(s)}{(s^4-\mu_1^4)\gamma\sinh(\gamma h) - \alpha_1\cosh(\gamma h)}$$

where μ_1 and α_1 are the limiting values of the plate wavenumber and fluid loading parameter as $x \to -\infty$, defined by taking the appropriate limits in (4.16) and given explicitly in (4.22). Consequently, (4.17) becomes

$$\phi(x,y) = \frac{1}{2\pi}\int_C \frac{f(s)\cosh(\gamma y)e^{-ixs}\,ds}{(s^4-\mu_1^4)\gamma\sinh(\gamma h) - \alpha_1\cosh(\gamma h)}, \tag{4.19}$$

where $f(s)$ is an unknown meromorphic function. The denominator of the integrand is the dispersion relation appropriate to the plate of uniform properties μ_1 and α_1. Equation (4.19) satisfies the governing equation (4.12) and the boundary condition (4.13). The function $f(s)$ is determined by the need to satisfy (4.14) and (4.15), and is expected to reveal the properties of the transmitted and reflected modes.

4.4 Solution of the boundary value problem

In the expression (4.19) for the velocity potential, the function $f(s)$ and the contour C must be chosen so that the plate and radiation boundary conditions.

(4.14) and (4.15) are satisfied. Using the definitions of $\mu^4(x)$ and $\alpha(x)$ in (4.14).

$$B_1\phi_{yxxxx} - m_1\omega^2\phi_y - \rho_0\omega^2\phi + e^{x/a}(B_2\phi_{yxxxx} - m_2\omega^2\phi_y - \rho_0\omega^2\phi) = 0 \text{ for } y = h. \tag{4.20}$$

On substituting the inverse Fourier integral (4.19) for $\phi(x, y)$ into (4.20), it is found that

$$\begin{aligned} &\frac{1}{2\pi}\int_C \frac{f(s)\{B_1 s^4\gamma\sinh(h\gamma) - m_1\omega^2\gamma\sinh(h\gamma) - \rho_0\omega^2\cosh(h\omega)e^{-ixs}\}}{(s^4-\mu_1^4)\gamma\sinh(h\gamma) - \alpha_1\cosh(h\gamma)}\,ds \\ &+\frac{1}{2\pi}\int_C \frac{f(s)\{B_2 s^4\gamma\sinh(h\gamma) - m_2\omega^2\gamma\sinh(h\gamma) - \rho_0\omega^2\cosh(h\omega)e^{-ix(s+i/a)}\}}{(s^4-\mu_1^4)\gamma\sinh(h\gamma) - \alpha_1\cosh(h\gamma)}\,ds \\ &= 0. \end{aligned} \tag{4.21}$$

This imposes a further constraint on $f(s)$, that is $f(s)$ must be such that both the integrals exist. It is convenient to define.

$$K_j(s) = (s^4 - \mu_j^4)\gamma\sinh(h\gamma) - \alpha_j\cosh(h\gamma), \quad j = 1, 2, \tag{4.22}$$

where

$$\mu_j^4 = \frac{m_j\omega^2}{k^4 B_j}, \quad \alpha_j = \frac{\rho_0\omega^2}{k^5 B_j}.$$

Then (4.21) may be written as

$$\frac{B_1}{2\pi}\int_C f(s)e^{-ixs}\,ds + \frac{B_2}{2\pi}\int_C \frac{K_2(s)}{K_1(s)} f(s)e^{-ix(s+i/a)}\,ds = 0. \tag{4.23}$$

Provided there are no singularities of the integrand lying in the region between the contour C and the contour C' which is everywhere distant $1/a$ above C, the first term in (4.23) can be replaced by

$$\frac{B_1}{2\pi}\int_C f(s)e^{-ixs}\,ds = \frac{B_1}{2\pi}\int_{C'} f(s)e^{-ixs}\,ds = \frac{B_1}{2\pi}\int_C f\left(t+\frac{i}{a}\right)e^{-ix\left(t+\frac{i}{a}\right)}\,dt. \tag{4.24}$$

Then (4.23) becomes

$$\frac{B_1}{2\pi}\int_C f\left(s+\frac{i}{a}\right)e^{-ix(s+i/a)}\,ds + \frac{B_2}{2\pi}\int_C \frac{K_2(s)}{K_1(s)} f(s)e^{-ix(s+i/a)}\,ds = 0. \tag{4.25}$$

It follows that (4.23) will be satisfied if $f(s)$ satisfies the functional difference equation

$$\frac{f\left(s+\frac{i}{a}\right)}{f(s)} = -p(s), \qquad p(s) = \frac{B_2 K_2(s)}{B_1 K_1(s)}. \tag{4.26}$$

There are infinitely many solutions to functional difference equations of this type. The precise form of $f(s)$ is dictated by the need to satisfy (4.15), ensure convergence of the integrals in (4.21) and be pole-free in the (not necessarily straight) strip lying between C and C'. The latter point is essential in view of (4.24) above. The choice of $f(s)$ is thus of paramount importance to the analysis. The solution of (4.26) is outlined below with further details given in Appendix A. For ease of exposition two special cases will be investigated. These are the simplest in that they have the smallest numbers of propagating modes in the scattered acoustic field. The conditions, expressed in terms of the intrinsic fluid loading parameter $\epsilon_1 = \epsilon_1(j) = \alpha_j/\mu_j^4$ denoted by ϵ in Cannell [4] and α in Crighton *et al* [6] $(j = 1, 2)$, are

i) each of the numerator and denominator of $p(s)$ has exactly one pair of real zeros; this requires $h < \pi/2$ and $\epsilon_1 < \tan h$;

ii) each of the numerator and denominator of $p(s)$ has exactly two pairs of real zeros; this happens if either $h < \pi/2$ and $\epsilon_1 > \tan h$ or $3\pi/2 > h > \pi/2$ and $\epsilon_1 < \tan h$.

In (4.26), it is convenient to write $f(s) = f_0(s)f_1(s)f_2(s)$ so that (4.26) is equivalent to the three functional difference equations

$$\frac{f_0\left(s+\frac{i}{a}\right)}{f_0(s)} = -1, \tag{4.27}$$

$$\frac{f_1\left(s+\frac{i}{a}\right)}{f_1(s)} = \frac{B_2}{B_1} \tag{4.28}$$

and

$$\frac{f_2\left(s+\frac{i}{a}\right)}{f_2(s)} = \frac{K_2(s)}{K_1(s)}. \tag{4.29}$$

Solutions of (4.27) are anti-periodic functions, i.e. those which change sign when s is increased by i/a, for example $\sinh\{(2n-1)\pi as\}$. Functions of the form $c(s)e^{-ibs}$, where $b = a\log(B_2/B_1)$ and $c(s)$ is periodic with period i/a, satisfy (4.28). Here, the function $c(s)$ is disregarded, as it can be incorporated in the anti-periodic solution of (4.27). The expression e^{-ibs} will also be omitted in the subsequent analysis, as removing it from the velocity potential (4.19) merely has the effect of translating the y-axis a distance $a\log(B_2/B_1)$ away from the point of inflection of the functions μ^4 and α. Such a shift of coordinates does not affect the physical conclusions.

Equation (4.29) can be solved by writing $p(s)$ as an infinite product over its zeros and poles, which are denoted by $\pm\nu_n$ and $\pm\eta_n$, $n = 0, 1, 2, \ldots$, respectively. Note that η_0 and ν_0 are real (together with η_1 and ν_1 in case (ii) above), and $\Re(\eta_n) \geq 0$, $\Re(\nu_n) \geq 0$, $n = 1, 2, 3, \ldots$. Details of the solution method are given in Appendix A where it is shown that a solution is

$$f_2(s) = \prod_{n=0}^{\infty} \frac{\Gamma\{1 - ia(\eta_n - s)\}\Gamma\{-ia(\nu_n + s)\}}{\Gamma\{1 - ia(\nu_n - s)\}\Gamma\{-ia(\eta_n + s)\}}. \tag{4.30}$$

The poles of functions appearing in the integrand of (4.19), together with zeros of $f_2(s)$, are represented in Figure 4.4. A pole at $-\eta_0$, representing the incident wave, can be introduced by choosing

$$f_0(s) = \frac{H}{\sinh\{\pi a(s + \eta_0)\}}, \tag{4.31}$$

which satisfies (4.27). The constant H will be chosen later to give the incident wave the required amplitude, A in (4.15). The contour C of (4.19) is now chosen to pass below $\pm\eta_0$ and above $-\nu_0$. this choice ensures that $\phi(x, y)$ satisfies the radiation condition (4.15) and also permits the deformation detailed in (4.24).

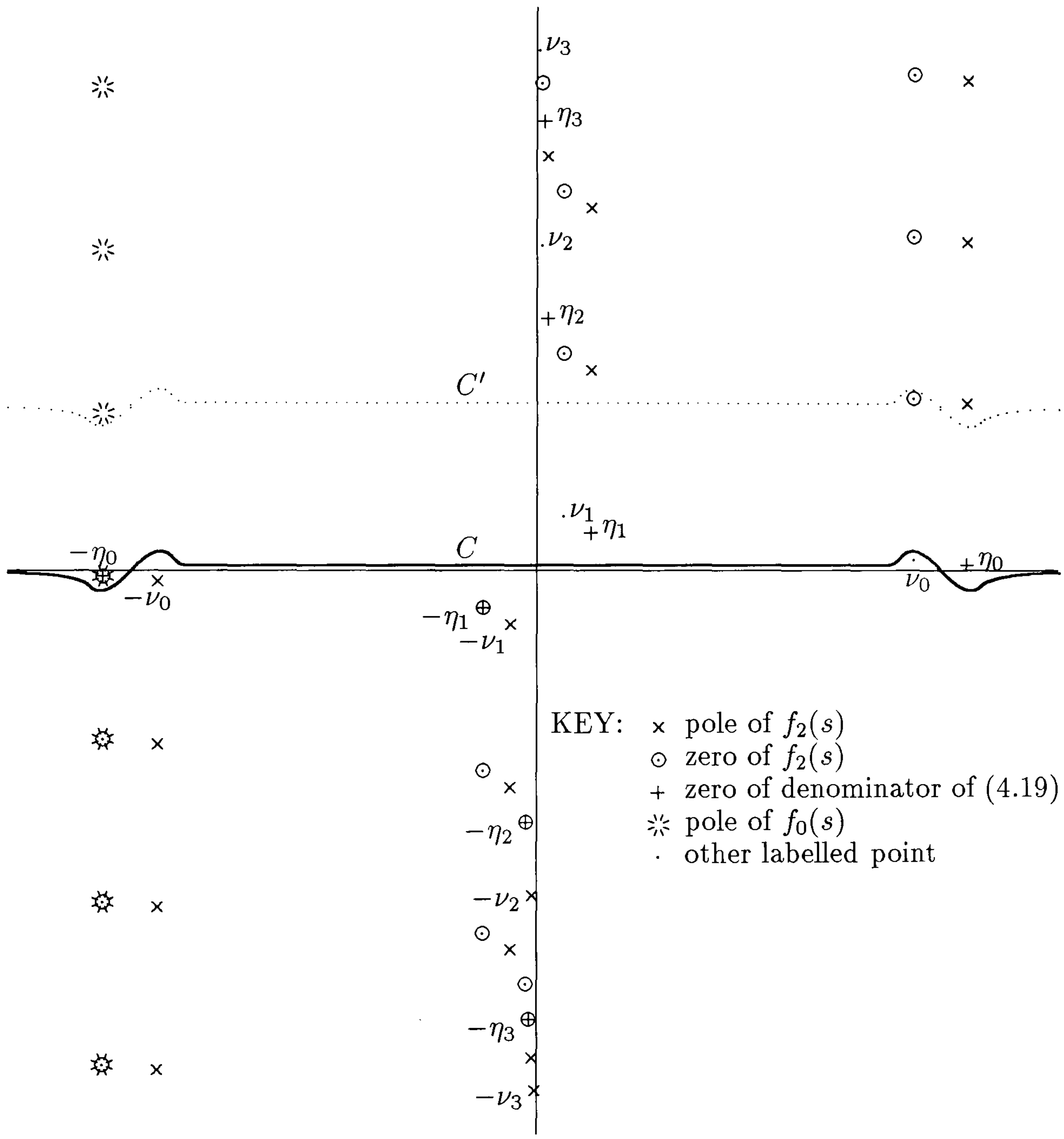

Figure 4.4: *Complex s-plane showing poles of the integrand in (4.19) with the contours C and C′*

That is, no singularities of $f(s)$ lie between the contours C and C', as can be seen in Figure 4.4.

When the poles of the denominator of the integrand of (4.19) are taken into account, the modes which do not attenuate for $x \to \pm\infty$ are seen to be $-\eta_0$ (incident wave), $-\nu_0$ (transmitted wave) and η_0 (reflected wave). Further transmitted and reflected modes may be given by $-\nu_1$, η_1 *etc.* The complete solution to (4.26) is now

$$\begin{aligned} f(s) &= \frac{-iH}{\pi} \cdot \frac{\Gamma\{1+ia(s+\eta_0)\}\Gamma\{1-ia(\eta_0-s)\}\Gamma\{-ia(\nu_0+s)\}}{\Gamma\{1-ia(\nu_0-s)\}} \\ &\quad \times \prod_{n=1}^{\infty} \frac{\Gamma\{1-ia(\eta_n-s)\}\Gamma\{-ia(\nu_n+s)\}}{\Gamma\{1-ia(\nu_n-s)\}\Gamma\{-ia(\eta_n+s)\}}. \end{aligned} \tag{4.32}$$

Expression (4.32) clearly contains three infinite families of poles given by

i) $-\eta_0 + im/a; \quad m = 0, 1, 2, \ldots;$

ii) $\eta_n + im/a; \quad n = 0, 1, 2, \ldots; \quad m = 0, 1, 2, \ldots;$

iii) $-\nu_n - im/a; \quad n = 0, 1, 2, \ldots; \quad m = 1, 2, \ldots;$

and these are represented in Figure 4.4. It should be noted that $f(s)$ does not contain poles at $s = \pm\eta_0$ which correspond to the forcing term and its reflected wave. These terms are present in the denominator of the integral (4.19), that is they are zeros of $K_1(s)$. It is clear that the integral (4.24) is free of poles in the strip $0 \leq \Im(s) \leq 1/a$ provided the contour C passes above the pole at $-\nu_0$. In addition to these requirements, integral (4.19) will have the correct physical composition if and only if C passes below the poles $s = \pm\eta_0$ that arise due to $K_1(s)$.

It is shown in Appendix A that $f(s)$ decays exponentially for $s \to \infty$ in a horizontal strip. This allows the integral (4.19) to converge and provides the final justification for moving the contour in (4.23).

4.5 Reflection and transmission coefficients

The incident wave I is obtained by isolating the residue contribution from (4.19) at $-\eta_0$, on closing the contour in the upper half-plane, to get

$$I = \frac{if(-\eta_0)}{K_1'(-\eta_0)} \cosh(\tau_0 y) e^{i\eta_0 x}, \tag{4.33}$$

where $K_1(s)$ is defined in (4.22). The incident amplitude A in (4.15) is, by comparison with (4.19),

$$A = \frac{if(-\eta_0)}{K_1'(-\eta_0)}. \tag{4.34}$$

Hence, the constant H is related to A by

$$\begin{aligned} H &= \pi A K_1'(-\eta_0) \frac{\Gamma\{1 - ia(\nu_0 + \eta_0)\}}{\Gamma(1 - 2ia\eta_0)\Gamma\{-ia(\nu_0 - \eta_0)\}} \\ &\times \prod_{n=1}^{\infty} \frac{\Gamma\{1 - ia(\nu_n + \eta_0)\}\Gamma\{-ia(\eta_n - \eta_0)\}}{\Gamma\{1 - ia(\eta_n + \eta_0)\}\Gamma\{-ia(\nu_n - \eta_0)\}}. \end{aligned} \tag{4.35}$$

The notation $\tau_n = \gamma(\eta_n)$, $\lambda_n = \gamma(\nu_n)$ is used here, and defines the wavenumbers τ_0 and λ_0 which were used in dimensional form in §4.3.

The first reflected mode is given by the residue contribution at η_0, the contour being closed in the upper half-plane; thus

$$R_0 = \frac{f(\eta_0)}{K_1'(\eta_0)} \tag{4.36}$$

and

$$|R_0| = \left| \frac{f(\eta_0)}{K_1'(\eta_0)} \right|. \tag{4.37}$$

To relate this to (4.34), note that $K_1'(-s) = -K_1'(s)$ since $K_1(s)$ is an even function, so that

$$\begin{aligned} \left|\frac{R_0}{A}\right| &= \left|\frac{f(\eta_0)}{f(-\eta_0)}\right| \\ &= \left|\frac{\Gamma(2ia\eta_0)}{\Gamma(-2ia\eta_0)}\right| \left|\frac{\sinh\{a\pi(\nu_0 - \eta_0)\}}{\sinh\{a\pi(\nu_0 + \eta_0)\}}\right| \\ &\times \prod_{n=1}^{\infty} \left|\frac{\sinh\{a\pi(\eta_n + \eta_0)\} \sinh\{a\pi(\nu_n - \eta_0)\}}{\sinh\{a\pi(\eta_n - \eta_0)\} \sinh\{a\pi(\nu_n + \eta_0)\}}\right|. \end{aligned} \tag{4.38}$$

On the right-hand side the first factor is 1 provided that η_0 is real, and the second factor is less than one for all a. The infinite product is 1 if η_n and ν_n are purely imaginary. This is also true if a pair of roots have the form $\eta_n = iz$, $\eta_{n+1} = i\bar{z}$ which will occur for $\alpha >> 1$. This leads to the alternative forms

$$\left|\frac{R_0}{A}\right| = \begin{cases} \left|\dfrac{\sinh\{a\pi(\nu_0 - \eta_0)\}}{\sinh\{a\pi(\nu_0 + \eta_0)\}}\right|, \eta_0, \nu_0 \in \Re, \\ \left|\dfrac{\sinh\{a\pi(\nu_0 - \eta_0)\} \sinh\{a\pi(\eta_1 + \eta_0)\} \sinh\{a\pi(\nu_1 - \eta_0)\}}{\sinh\{a\pi(\nu_0 + \eta_0)\} \sinh\{a\pi(\eta_1 - \eta_0)\} \sinh\{a\pi(\nu_1 + \eta_0)\}}\right|, \\ \quad \eta_0, \eta_1, \nu_0, \nu_1 \in \Re. \end{cases} \tag{4.39}$$

which are valid for cases (i) and (ii) respectively (see §4.4). In the limit as $a \to 0$, the first of the above expressions, valid for case (i), becomes

$$\left|\frac{R_0}{A}\right| = \left|\frac{\eta_0 - \nu_0}{\eta_0 + \nu_0}\right|, \tag{4.40}$$

which agrees with the reflection coefficient derived from the solution of the limiting Wiener–Hopf problem with continuous edge conditions, *ie* (5.67). In the limit as $a \to \infty$, the first expression in (4.39) tends to zero. This indicates that, even though there may be a substantial difference between the left and right asymptotic bending stiffnesses or thicknesses, the reflected wave has negligible amplitude provided that the material properties change slowly enough.

The first transmitted mode is given by the residue contribution at $-\nu_0$, the contour being closed in the lower half-plane, so that its amplitude is

$$T_0 = \frac{\mathrm{Res}_{s=-\nu_0} f(s)}{K_1(-\nu_0)}, \tag{4.41}$$

where the residue can be expressed as an infinite product by means of (4.32),

$$\begin{aligned} \operatorname*{Res}_{s=-\nu_0} f(s) &= \frac{H}{a\pi} \cdot \frac{\Gamma\{1 + ia(\eta_0 - \nu_0)\}\Gamma\{1 - ia(\eta_0 + \nu_0)\}}{\Gamma(1 - 2ia\nu_0)} \\ &\quad \times \prod_{n=1}^{\infty} \frac{\Gamma\{1 - ia(\eta_n + \nu_0)\}\Gamma\{-ia(\nu_n - \nu_0)\}}{\Gamma\{1 - ia(\nu_n + \nu_0)\}\Gamma\{-ia(\eta_n - \nu_0)\}}. \end{aligned} \tag{4.42}$$

The above, together with the expression for H in (4.35), give T_0 in terms of the gamma function and, for case (i), the limiting forms for small and large a satisfy

$$\lim_{a\to 0}\left|\frac{T_0}{A}\right| = \frac{2\eta_0}{\nu_0+\eta_0}\prod_{n=1}^{\infty}\left|\frac{\eta_n-\eta_0}{\eta_n-\nu_0}\cdot\frac{\nu_n+\eta_0}{\nu_n+\nu_0}\right| \tag{4.43}$$

and

$$\lim_{a\to\infty}\left|\frac{T_0}{A}\right| = \sqrt{\frac{\eta_0}{\nu_0}}\prod_{n=1}^{\infty}\left|\frac{\eta_n-\eta_0}{\eta_n-\nu_0}\cdot\frac{\nu_n+\eta_0}{\nu_n+\nu_0}\right|. \tag{4.44}$$

The first of these expressions agrees with the transmission coefficient derived from the Wiener–Hopf problem mentioned above, *ie* (5.70). It is interesting to note that, whilst $|R_0/A| \to 0$ as $a \to \infty$, there is no simple form for T_0 in this limit. This is to be expected, since the different wavenumbers of the transmitted and incident modes would require different amplitudes to convey the same energy.

The following graphs show the moduli of the fundamental reflection and transmission coefficients for the cases $B_1 = B_2$ and $B_1 \neq B_2$. In the first case the graphs are valid for $a \geq 0$ but for the case $B_1 \neq B_2$ this is not so. Figure 4.5 compares the modulus of the reflection coefficient for $\mu_1 = 0.5$, $\mu_2 = 3.5$ and $\alpha_1 = \alpha_2 = 200$ against the heavy fluid loading case in which $\mu_1 = 5$, $\mu_2 = 15$ and $\alpha_1 = \alpha_2 = 100000$. It is clear, with reference to equation (4.39), that both curves decay exponentially with increasing a, however, although initially larger in magnitude the reflection coefficient for the second set of parameters decays significantly more rapidly. Figure 4.6 shows the modulus of the transmission coefficient for the same two sets of parameters. It is clear that the two curves are very nearly constant albeit at different values. Figure 4.7 compares the modulus of the reflection coefficient for $\mu_1 = 1.5$, $\mu_2 = 3$ and $\alpha_1 = 200$, $\alpha_2 = 1500$ against that for $\mu_1 = 5$, $\mu_2 = 15$ and $\alpha_1 = 1000$, $\alpha_2 = 100000$. In this case the graph is valid only for $a > 0.3$ and it is clear that both curves are extremely small for $a = O(1)$. The transmission coefficient, for the same two sets of parameters, is shown in Figure 4.8 and, clearly, for $a > 0.3$ the curves are constant. From Fig-

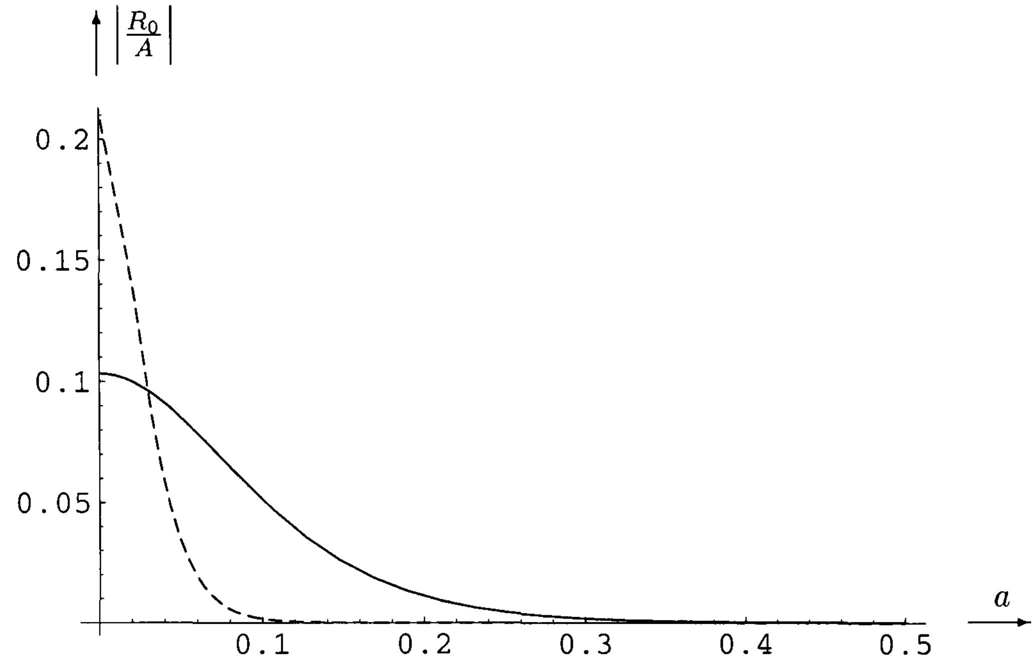

Figure 4.5: *The modulus of the reflection coefficient for the case* $B_1 = B_2$; *continuous line is for* $\mu_1 = 0.5$, $\mu_2 = 3.5$, $\alpha_1 = \alpha_2 = 200$ *and broken line is for* $\mu_1 = 5$, $\mu_2 = 15$ *and* $\alpha_1 = \alpha_2 = 100000$

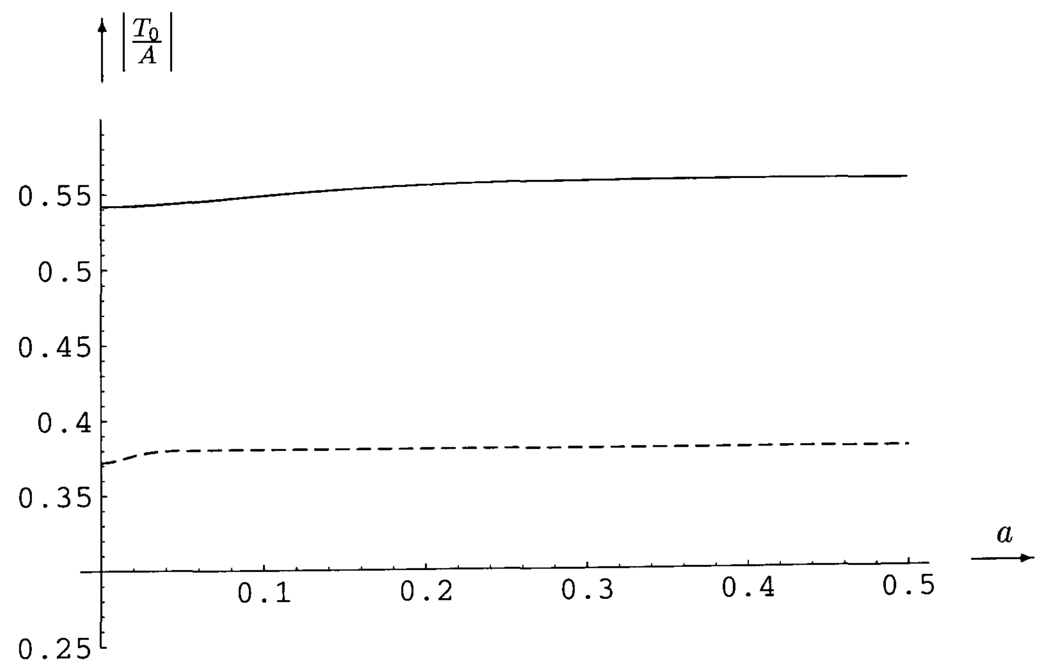

Figure 4.6: *The modulus of the transmission coefficient, evaluated on* $y = h$, *for the case* $B_1 = B_2$; *continuous line is for* $\mu_1 = 0.5$, $\mu_2 = 3.5$, $\alpha_1 = \alpha_2 = 200$ *and broken line is for* $\mu_1 = 5$, $\mu_2 = 15$ *and* $\alpha_1 = \alpha_2 = 100000$

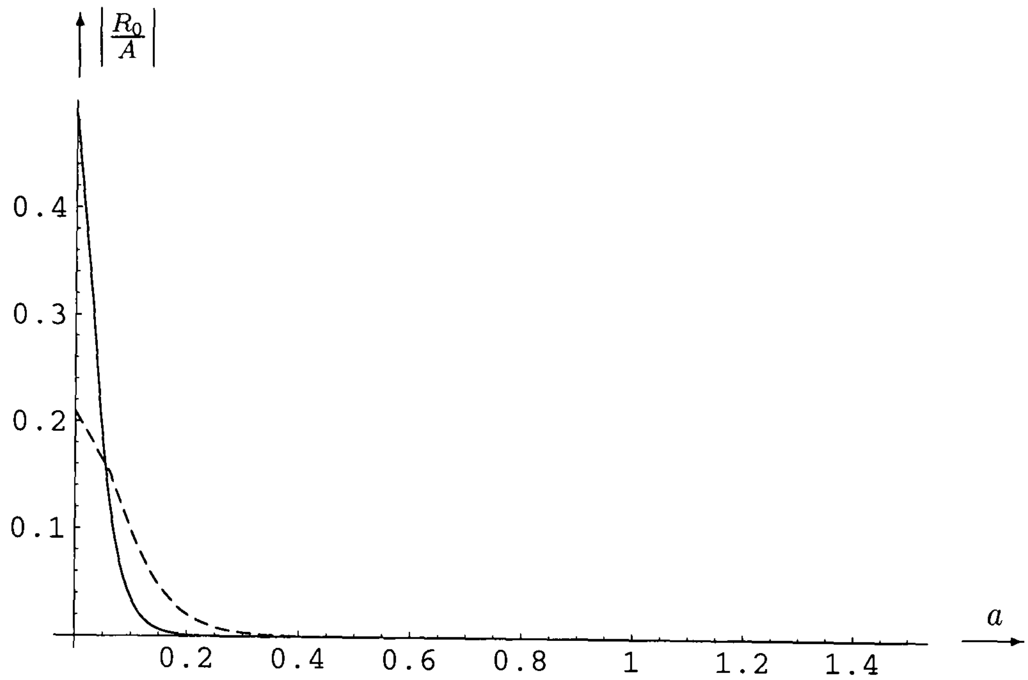

Figure 4.7: *The modulus of the reflection coefficient for the case $B_1 \neq B_2$; continuous line is for $\mu_1 = 1.5$, $\mu_2 = 3$, $\alpha_1 = 200$, $\alpha_2 = 1500$ and broken line is for $\mu_1 = 5$, $\mu_2 = 15$ and $\alpha_1 = 1000$, $\alpha_2 = 100000$*

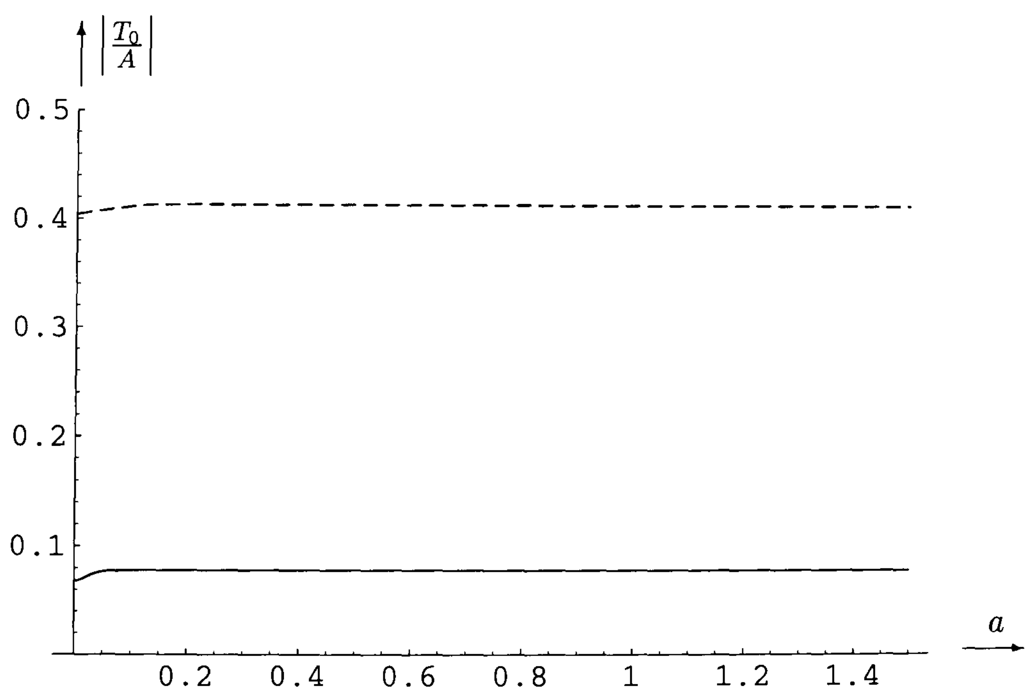

Figure 4.8: *The modulus of the transmission coefficient, evaluated on $y = h$, in the case $B_1 \neq B_2$; continuous line is for $\mu_1 = 1.5$, $\mu_2 = 3$, $\alpha_1 = 200$, $\alpha_2 = 1500$ and broken line is for $\mu_1 = 5$, $\mu_2 = 15$ and $\alpha_1 = 1000$, $\alpha_2 = 100000$*

ures 4.5–4.8 it is clear that the most interesting behaviour for both the reflection and transmission coefficients occurs for $a << 1$. The discussion of section 4.6 centres on a number of different approximations to the full plate equation (4.9) and, in particular, presents a modified version by which results valid for $B_1 \neq B_2$, $a << 1$ may be obtained.

4.6 Discussion and Conclusions

The analysis of §4.3 and §4.4 involves a simplified plate equation, (4.14), which is valid for $|B'/B|, |B''/B| << \mu_j^4, \alpha_j$, $j = 1, 2$ and also for the case $B_1 = B_2$. In this section an alternative modification is presented by which results can be obtained for the cases where (4.14) is not valid and, in particular, for $a << 1$.

The non-dimensional form of the full plate equation (4.9) is

$$\left\{ \frac{\partial^4}{\partial x^4} + \frac{2B'(x)}{B(x)}\frac{\partial^3}{\partial x^3} + \frac{B''(x)}{B(x)}\frac{\partial^2}{\partial x^2} - \mu^4(x) \right\} \phi_y - \alpha(x)\phi = 0, \quad -\infty < x < \infty, \quad y = h. \tag{4.45}$$

For situations in which the constraints discussed above do not apply the *ansatz* of §4.3 can still be applied to the full plate equation. It is found that

$$\begin{aligned}
&\frac{1}{2\pi}\int_C f(s)e^{-ixs}\,ds + \frac{1}{\pi}\int_C f(s)e^{-ix(s+i/a)}\,ds \\
&+ \frac{1}{\pi}\int_C \frac{B_2K_2(s)}{B_1K_1(s)} f(s)e^{-ix(s+2i/a)}\,ds + \frac{1}{2\pi}\int_C \frac{B_2K_2(s)}{B_1K_1(s)} f(s)e^{-ix(s+3i/a)}\,ds \\
&+ \frac{B_2 - B_1}{\pi a^2}\int_C \frac{s^2(2ias+1)\gamma\sinh(h\gamma)f(s)e^{-ix(s+i/a)}}{B_1K_1(s)}ds \\
&+ \frac{B_2 - B_1}{2\pi a^2}\int_C \frac{s^2(2ias-1)\gamma\sinh(h\gamma)f(s)e^{-ix(s+2i/a)}}{B_1K_1(s)}ds \\
&= 0,
\end{aligned} \tag{4.46}$$

where $f(s)$ is the unknown (meromorphic) function contained in the integral representation for $\phi(x, y)$ and the contour C extends from $-\infty$ to $+\infty$ but its full specification is not yet known. In order to obtain a (rather more complicated) functional difference equation from (4.46) it is necessary for all but one of the integrals to shift the path of integration upward a distance m/a, where $m = 1, 2, 3$ depending on the exponent in the integrand. Then the substitution $s = t + im/a$ ensures that each final integral contains the factor $e^{-ix(t+3i/a)}$. The contour C, which can be suitably translated without encountering poles of the integrand, is similar to that shown in Figure 4.4, but with extra detours below the points $-\eta_0$, η_0, η_1 *etc.* Such a contour is possible if $2\Im(\eta_1) > 3/a$, that is if a is suitably large. Otherwise, allowance has to be made for poles which are the wrong side of the contour by adding appropriate residue terms to the right-hand side of (4.46). For $a = O(1)$ or $a << 1$ a contour can be found only if η_1, η_2 *etc* have small real parts as indicated in Figure 4.4. This can be ensured if the wavenumber k is assumed to have a small positive imaginary part as may be seen easily for extreme values of α_1 or α_2, when $\hat{\eta}_l$ and $\hat{\nu}_l$ take the forms

$$\hat{\eta}_n,\ \hat{\nu}_n \sim \begin{cases} \sqrt{k^2 - \dfrac{\pi^2 n^2}{k^2\hat{h}^2}} & (\alpha_j \to 0; j = 1,2), \\ \sqrt{k^2 - \dfrac{\pi^2(n-1/2)^2}{k^2\hat{h}^2}} & (\alpha_j \to \infty). \end{cases}$$

Positive imaginary values of the above expressions acquire small real parts when k is given a small positive imaginary part. There is no loss of generality involved in this assumption provided that $\Im(k) \to 0$ at the end of the analysis.

The full difference equation for $f(s)$ is now

$$\frac{B_2K_2(s)}{B_1K_1(s)}f(s) + \frac{2B_2K_2(s+i/a)}{B_1K_1(s+i/a)}f\Big(s+\frac{i}{a}\Big) + f\Big(s+\frac{i}{a}\Big)$$
$$+ \frac{B_2K_2(s+2i/a)}{B_1K_1(s+2i/a)}f\Big(s+\frac{2i}{a}\Big) + 2f\Big(s+\frac{2i}{a}\Big) + f\Big(s+\frac{3i}{a}\Big)$$
$$+ \frac{\{s+3i/(2a)\}(s+i/a)^2\{B_2K_2(s+i/a) - B_1K_1(s+i/a)\}}{\pi a^2\{(s+i/a)^4 - \sigma^4\}B_1K_1(s+i/a)}f\Big(s+\frac{i}{a}\Big)$$
$$+ \frac{\{s+3i/(2a)\}(s+2i/a)^2\{B_2K_2(s+2i/a) - B_1K_1(s+2i/a)\}}{2\pi a^2\{(s+2i/a)^4 - \sigma^4\}B_1K_1(s+2i/a)}f\Big(s+\frac{2i}{a}\Big)$$

$$= 0, \tag{4.47}$$

where σ is defined by

$$\sigma^4 = \frac{m_2 - m_1}{B_2 - B_1}.$$

The quantity σ plays an important role in the Wiener–Hopf analysis, see [3].

When $\hat{a} >> 1$, the first six terms on the left-hand side predominate, forming a third-order functional difference equation, that is

$$p(s)f(s) + f\left(s + \frac{i}{a}\right) + 2p\left(s + \frac{i}{a}\right) f\left(s + \frac{i}{a}\right) + 2f\left(s + \frac{2i}{a}\right)$$
$$+ p\left(s + \frac{2i}{a}\right) f\left(s + \frac{2i}{a}\right) + f\left(s + \frac{3i}{a}\right) = 0, \tag{4.48}$$

where $p(s)$ denotes $B_2K_2(s)/\{B_1K_1(s)\}$. This can be re-cast as

$$F(s) + 2F(s + i/a) + F(s + 2i/a) = 0 \tag{4.49}$$

where

$$p(s)f(s) + f(s + i/a) = F(s).$$

Its is easily shown that

$$F(s) = \{A(s) + sB(s)\}e^{\pi sa}$$

where the functions $A(s)$ and $B(s)$ are periodic so that, for example, $A(s) = A(s + i/a)$. The solution to (4.48) that has the correct pole structure and for which the integral representation of the velocity potential $\phi(x, y)$ exists is obtained only if $A(s) = B(s) = 0$ whence the results of §4.4 are retrieved. For $\hat{a} << 1$, the last two terms on the left-hand side of (4.47) appear to predominate, but the limiting equation does not provide physically meaningful solutions. This is because the difference between the arguments s and $s + i/a$ tends to infinity as a tends to zero, with the result that the limiting equation no longer has the nature of a difference equation. The increasingly abrupt change in physical properties as $a \to 0$ invalidates assumptions on which the thin plate theory are based. A more productive approach for analysis of the problem when $a << 1$ is to multiply (4.9) throughout by $B(x)$ and then replace the quantities $B'(x)$ and $B''(x)$ by the generalised functions which reflect their limiting properties. The notation $B(x) = B(x; a)$ makes the parameter explicit. It is shown in Appendix C that

$$\lim_{n\to\infty} B'(x; 1/n) = (B_2 - B_1)\delta(x) \tag{4.50}$$

and

$$\lim_{n\to\infty} B''(x; 1/n) = (B_2 - B_1)\delta'(x) \tag{4.51}$$

where $\delta(x)$ here denotes the Dirac delta function. The analysis presented herein is based on the assumption that the velocity potential maintains continuity of displacement, gradient and the next two derivatives with respect to x across $x = 0$, that is

$$\begin{aligned} \phi_y(0-, h) &= \phi_y(0+, h), \\ \phi_{yx}(0-, h) &= \phi_{yx}(0+, h), \\ \phi_{yxx}(0-, h) &= \phi_{yxx}(0+, h), \\ \phi_{yxxx}(0-, h) &= \phi_{yxxx}(0+, h). \end{aligned} \tag{4.52}$$

Under these conditions and for $a << 1$, the terms of interest give rise to forcing functions

$$2B'(x)\frac{\partial^3 \phi_y(x,h)}{\partial x^3} \sim 2(B_2 - B_1)\phi_{yxxx}(x,h)\delta(x) = -A_0\delta(x) \tag{4.53}$$

say and

$$B''(x)\frac{\partial^2 \phi_y(x,h)}{\partial x^2} \sim (B_2 - B_1)\phi_{yxx}(x,h)\delta'(x) = -A_1\delta'(x). \tag{4.54}$$

The boundary condition (4.14) is then replaced by

$$\left\{B(x)\frac{\partial^4}{\partial x^4} - m(x)\right\}\phi_y(x,h) - \rho_0\omega^2\phi(x,h) = A_0\delta(x) + A_1\delta'(x). \tag{4.55}$$

Equation (4.55) permits the theory presented here to be extended to two further situations. Firstly, it approximates the plate boundary condition for the case $B_1 \neq B_2$ with $a << 1$. Secondly, it models the case $B_1 = B_2$, $a > 0$ with the plate constrained so that its displacement and gradient are continuous but specified at $x = 0$ (or at any other x value). In the latter case, the delta functions on the right-hand side of (4.54) are to be viewed as forcing terms (cf [2]) and are not the $a \to 0$ limiting forms of B' and B'' (which are in any case known to be zero for $B_1 = B_2$). Both situations are of interest and the solution of the boundary value problem with (4.55) instead of (4.9) as boundary condition could form the subject of future research. It was noted in §4.3 that $B' = B'' = 0$ for $B_1 = B_2$. Expressions (4.53) and (4.54) are consistent with this since then $A_1 = A_0 = 0$. This special case in which $B_2 = B_1$ arises if the Young's modulus and Poisson's ratio vary with x but $\delta(x)$ also varies in such a way that

$$\frac{E(x)\delta(x)^3}{12(1-\nu(x)^2)} = \text{constant.}$$

It is worthwhile commenting on the Wiener–Hopf problem which arises as $a \to 0$. On multiplying (4.9) through by $B(x)$ and taking this limit in each term it is found that

$$\left[\{B_1 + (B_2 - B_1)H(x)\}\frac{\partial^4}{\partial x^4} - \{m_1 + (m_2 - m_1)H(x)\}\right]\phi_y(x,h) - \rho_0\omega^2\phi(x,h)$$
$$= A_0(x)\delta(x) + A_1(x)\delta'(x) \tag{4.56}$$

where $H(x)$ is the Heaviside step function. The boundary value problem that is obtained on replacing (4.14) with this two-part condition can be solved by recourse to the Wiener–Hopf technique. It should be noted that this is not the Wiener–Hopf problem that is referred to and used for comparison in §4.5. The Wiener–Hopf problem results quoted there arise from the $a \to 0$ limiting case of (4.14), that is, the Wiener–Hopf limit of the $a >> 1$ approximation to (4.9). (The derivation of these results is the subject of chapter 5. Thus, the results presented in §4.5 for the case $B_1 \neq B_2$, although not valid for $a = 0$, are compared with the Wiener–Hopf result as a means of checking algebraic accuracy. The results are, however, valid for $a = 0$ in the case $B_1 = B_2$.

As a final point, it is noted that the special case $m_1 = m_2$ permits some slight simplification of the functional difference equation. This case arises if the density and thickness of the plate material both vary but in such a way that the area density $m = \rho_0\delta$ remains uniform. In this case the quantity σ in (4.47) is zero.

Chapter 5

Scattering in a duct with elastic plate walls that have abrupt change in material property

5.1 Introduction

The boundary-value problem considered here relates to a two-dimensional duct in which the material properties of one wall are discontinuous. The Wiener–Hopf method of analysis is used and the reflection and transmission coefficients are obtained directly from the velocity potential. The problem is similar to that investigated by Brazier-Smith [3] and Norris and Wickham [19] in the nature of the elastic plate. There is some parallel in the formulation and method of solution, but the details of the analysis are quite different because of the characteristic types of duct waves found here.

5.2 The boundary value problem

The boundary-value problem describes a two-dimensional infinite duct occupying the region $0 \leq \hat{y} \leq \hat{h}$ of a Cartesian coordinate system $(\hat{x}, \hat{y}, \hat{z})$ (Figure 5.1). The lower duct wall, that is at $\hat{y} = 0$, is rigid whilst the upper wall comprises

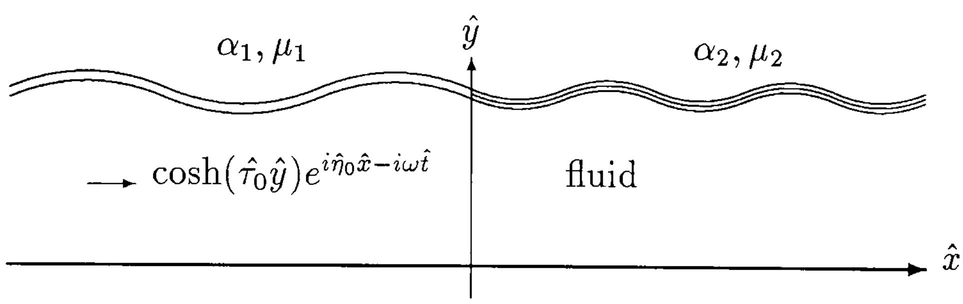

Figure 5.1: *The duct*

two elastic plates with different material properties fixed together along the line $\hat{x} = 0$, $\hat{y} = \hat{h}$. A compressible fluid of density ρ_0 and sound speed c occupies the interior of the duct whilst the exterior region is *in vacuo*. The analysis is also applicable to the problem obtained by reflecting the configuration in the plane $\hat{y} = 0$ and removing the rigid surface there. At the join of the two plates, edge conditions have to be specified depending on the physical join to be modelled, for example welded, clamped, hinged. Some edge conditions are formulated and applied later in the analysis.

A fluid-coupled structural wave propagates along the elastic plate and is scattered due to the variation in the plate properties. The incident forcing has the form

$$\phi_0(\hat{x}, \hat{y}, \hat{t}) = A \cosh(\hat{\tau}_0 \hat{y}) e^{i\hat{\eta}_0 \hat{x} - i\omega\hat{t}} \tag{5.1}$$

where the wavenumbers $\hat{\eta}_0$ and $\hat{\tau}_0$ (or rather their non-dimensional equivalents) are defined on page 84 in terms of zeros of the dispersion functions $K_1(s)$ and $K_2(s)$. This incident wave has harmonic time dependence, of angular frequency ω.

Both the incident wave and the elastic properties of the plate are independent of $\hat{z}$ and thus fluid velocity potential may be written as $\Phi(\hat{x}, \hat{y}, \hat{t})$. The fluid pressure is related to the velocity potential by

$$p(\hat{x}, \hat{y}, \hat{t}) = -\rho_0 \frac{\partial \Phi}{\partial \hat{t}}(\hat{x}, \hat{y}, \hat{t}). \tag{5.2}$$

A steady state solution is sought and thus the acoustic field may be expressed as

$$\Phi(\hat{x}, \hat{y}, \hat{t}) = \Re\{\hat{\phi}(\hat{x}, \hat{y}) e^{-i\omega\hat{t}}\}. \tag{5.3}$$

For convenience, the harmonic time factor is henceforth suppressed.

The time-independent potential $\hat{\phi}(\hat{x}, \hat{y})$ satisfies the Helmholtz equation

$$\left(\frac{\partial^2}{\partial \hat{x}^2} + \frac{\partial^2}{\partial \hat{y}^2} + k^2\right) \hat{\phi} = 0; \quad \Re(k) > 0, \ \Im(k) \geq 0, \tag{5.4}$$

where $k = \omega/c$ is the acoustic wavenumber. The lower bounding surface is described by the boundary condition

$$\hat{\phi}_{\hat{y}}(\hat{x}, 0) = 0,$$

and the upper one by

$$\begin{aligned} \left(B_1 \frac{\partial^4}{\partial \hat{x}^4} - m_1 \omega^2\right) \hat{\phi}_{\hat{y}}(\hat{x}, \hat{h}) &= -[p]_{h-}^{h+}, \ x < 0, \\ \left(B_2 \frac{\partial^4}{\partial \hat{x}^4} - m_2 \omega^2\right) \hat{\phi}_{\hat{y}}(\hat{x}, \hat{h}) &= -[p]_{h-}^{h+}, \ x > 0, \end{aligned} \tag{5.5}$$

where ρ_0 is the density of the fluid in the absence of disturbance, m_j is the mass per unit area of the half-plate material and B_j its bending stiffness. The subscript j is 1 for the left-hand material and 2 for the right-hand material. The bending stiffness is given by

$$B_j = \frac{E_j \delta_j^3}{12(1 - \nu_j^2)},$$

where E_j and ν_j are the Young's modulus and Poisson ratio of the half-plate material and δ_j is the thickness of the half plate. The symbol $[p]_{h-}^{h+}$ represents the pressure difference across the plate which, using (5.2) and (5.3) and noting that the exterior region is *in vacuo*, may be written as

$$[p]_{h_-}^{h_+} = -\rho_0\omega^2\hat{\phi}(\hat{x},\hat{h}). \tag{5.6}$$

The usual radiation condition holds. That is, with the exception of the incident mode, all disturbances propagate to infinity away from the point $x = 0$. For the geometrical restraint $h = \hat{h}k < \pi/2$ with $\alpha_j/\mu_j^4 < \tan(hk)$ (where α_j and μ_j are defined in (5.14)) the dispersion functions (5.24) have one real zero representing a mode in the part of the duct where $x << 0$ and one real zero representing a mode where $x >> 0$. The fluid velocity potential assumes the form

$$\hat{\phi}(\hat{x},\hat{y}) = \begin{cases} (Ae^{i\hat{\eta}_0\hat{x}} + R_0e^{-i\hat{\eta}_0\hat{x}})\cosh(\hat{\tau}_0\hat{y}) & \text{as } \hat{x} \to -\infty, \\ T_0e^{i\hat{\nu}_0\hat{x}}\cosh(\hat{\lambda}_0 y) & \text{as } \hat{x} \to +\infty, \end{cases} \tag{5.7}$$

where $R_0(T_0)$ is the reflection (transmission) coefficient of the fundamental mode. The wavenumbers $\hat{\nu}_0$ and $\hat{\lambda}_0$ are characteristic of the plate lying along $y = h$, $x > 0$ and will be defined on page 84 in terms of zeros of the dispersion function (5.24). The formulation of the boundary-value problem is completed by specifying edge conditions on the line where the two different plates meet. Different edge conditions are introduced in §5.4.

The boundary-value problem is now expressed in a non-dimensional form by using a length scale of k^{-1} and a time scale of ω^{-1}. Non-dimensional variables, functions, wavenumbers and plate properties are denoted by symbols without carets. For example, $\hat{x}k = x, \hat{t}\omega = t$ and $\hat{\phi}k^2/\omega = \phi^{\text{tot}}$. The non-dimensional formulation is for the scattered potential, denoted by ϕ, related to the total potential by

$$\phi^{\text{tot}} = \phi + \frac{\cosh(\tau_0 y)}{\cosh(\tau_0 h)}e^{i\eta_0 x}. \tag{5.8}$$

The incident amplitude A has been given the value $1/\{\cosh(\tau_0 h)\}$ for convenience. Any other incident amplitude would simply introduce a multiplicative constant in the solution obtained below, (5.46). The formulation (5.4–5.7) becomes

$$\left(\frac{\partial^2}{\partial x^2}+\frac{\partial^2}{\partial y^2}+1\right)\phi=0,\quad 0<y<h,-\infty<x<\infty, \tag{5.9}$$

$$\phi_y(x,0)=0, \tag{5.10}$$

$$\left(\frac{\partial^4}{\partial x^4}-\mu_1^4\right)\phi_y(x,h)-\alpha_1\phi(x,h)=0;\ x<0, \tag{5.11}$$

$$\begin{aligned}\left(\frac{\partial^4}{\partial x^4}-\mu_2^4\right)\phi_y(x,h)-\alpha_2\phi(x,h)&\\ +\{(\eta_0^4-\mu_2^4)\tau_0\tanh(\tau_0 h)-\alpha_2\}e^{i\eta_0 x}&=0;\ x\geq 0,\end{aligned} \tag{5.12}$$

$$\phi(x,y)=\begin{cases} R_0e^{-i\eta_0 x}\cosh(\tau_0 y) & \text{as } x\to-\infty,\\ T_0e^{i\nu_0 x}\cosh(\lambda_0 y) & \text{as } x\to+\infty,\end{cases} \tag{5.13}$$

where the plate wavenumbers μ_j and fluid loading parameters α_j are defined by

$$\mu_j^4=\frac{m_j\omega^2}{B_jk^4},\quad \alpha_j=\frac{\rho_0\omega^2}{B_jk^5}. \tag{5.14}$$

The last term on the left-hand side of (5.12) arises from the need to cancel the incident wave in the region $x>0$, where the wavenumbers η_0 and τ_0 cannot exist.

The incident potential, being the last term in (5.8), satisfies (5.11) and (5.9) and use of the scattered potential simply transfers the forcing into (5.12).

The Fourier transform of the scattered potential is

$$\begin{aligned}\Phi(s,y) &= \int_{-\infty}^{\infty}\phi(x,y)e^{isx}\,dx\\ &= \int_0^{\infty}\phi(x,y)e^{isx}\,dx+\int_{-\infty}^{0}\phi(x,y)e^{isx}\,dx\\ &= \Phi^+(s,y)+\Phi^-(s,y),\ \text{say}.\end{aligned}$$

The superscript $^+$ in the name of a function such as Φ^+ in this chapter indicates a plus function, that is one which is analytic in the half-plane above some line $\Im(s)$ = constant. Similarly, $^-$ indicates a minus function, analytic in a lower half-plane. It is clear that the integrals defining $\Phi^\pm$ converge in half-planes above and below the real line.

5.3 Solution of the boundary value problem

The Fourier transform of the governing equation (5.4) is

$$\left(\frac{\partial^2}{\partial y^2} - \gamma^2\right)\Phi = 0, \tag{5.15}$$

where $\gamma = (s^2 - 1)^{1/2}$, and that of the rigid boundary condition (5.10) is

$$\Phi_y(s,0) = \Phi_y^+(s,0) + \Phi_y^-(s,0) = 0. \tag{5.16}$$

The appropriate solution to (5.15) and (5.16) is $\Phi(s,y) = C(s)\cosh(\gamma y)$, with the derivative $\Phi_y(s,y) = \gamma C(s)\sinh(\gamma y)$. In order to take the half-range transforms of (5.11) and (5.12) it is necessary to use

$$\begin{aligned}
&\int_{-\infty}^{0} \phi_{yxxxx} e^{isx}\, dx \\
&= \phi_{yxxx}(0^-,y) - is\phi_{yxx}(0^-,y) - s^2\phi_{yx}(0^-,y) + is^3\phi_y(0^-,y) + s^4\Phi_y^- \\
&= p_1(s,y) + s^4\Phi_y^-(s,y), \text{ say,}
\end{aligned} \tag{5.17}$$

and similarly

$$\begin{aligned}
&\int_{0}^{\infty} \phi_{yxxxx} e^{isx}\, dx \\
&= -\phi_{yxxx}(0^+,y) + is\phi_{yxx}(0^+,y) + s^2\phi_{yx}(0^+,y) - is^3\phi_y(0^+,y) + s^4\Phi_y^+ \\
&= p_2(s,y) + s^4\Phi_y^+(s,y), \text{ say.}
\end{aligned} \tag{5.18}$$

The integrations by parts leading to (5.17) and (5.18) can be justified on assuming that the fluid wavenumber k has a small positive imaginary part. In that case (5.17) and (5.18) hold for s in a horizontal strip of the complex plane that includes the real line.

The following relations between the half-range transforms of ϕ and ϕ_y at $y = h$ can now be written down, making use of (5.11), (5.12) and (5.16):

$$\Phi^+(s,h) + \Phi^-(s,h) = C(s)\cosh(\gamma h), \tag{5.19}$$

$$\Phi_y^+(s,h) + \Phi_y^-(s,h) = \gamma C(s)\sinh(\gamma h), \tag{5.20}$$

$$(s^4 - \mu_1^4)\Phi_y^-(s,h) - \alpha_1\Phi^-(s,h) + p_1(s,h) = 0, \tag{5.21}$$

$$(s^4 - \mu_2^4)\Phi_y^+(s,h) - \alpha_2\Phi^+(s,h) + p_2(s,h) = -i\frac{(\eta_0^4 - \mu_2^4)\tau_0\tanh(\tau_0 h) - \alpha_2}{\eta_0 + s}, \tag{5.22}$$

where γ_0 and τ_0 are the non-dimensional forms of the wavenumbers appearing in the incident wave (5.1) and are defined below. On eliminating $C(s)$, $\Phi^+(s,h)$ and $\Phi^-(s,h)$ it is found that

$$\alpha_1 K_2(s)\Phi_y^+(s,h) + \alpha_2 K_1(s)\Phi_y^-(s,h) = -\gamma\tanh(\gamma h)\left\{p(s) + \frac{i\alpha_1 K_2(\eta_0)}{s+\eta_0}\right\}, \tag{5.23}$$

where

$$K_j(s) = (s^4 - \mu_j^4)\gamma\tanh(\gamma h) - \alpha_j;\ j = 1,2. \tag{5.24}$$

The cubic polynomial $p(s)$ is defined by

$$p(s) = \alpha_2 p_1(s,h) + \alpha_1 p_2(s,h). \tag{5.25}$$

It is evident from (5.23) that the Wiener–Hopf kernel is

$$K(s) = \frac{\alpha_1 K_2(s)}{\alpha_2 K_1(s)}.$$

Let $\eta_n; n = 0,1,2,\ldots;$ be the zeros of $K_2(s)$ and ν_n those of $K_1(s)$. Also define $\tau_n = \gamma(\eta_n)$ and $\lambda_n = \gamma(\nu_n)$. The function γ is given by $\gamma(s) = (s^2-1)^{1/2}$. A product factorization of $K(s)$ can be defined by

$$K(s) = K^+(s)K^-(s)$$

with $K^+(-s) = K^-(s)$. Since $K(s)$ is meromorphic with zeros $\pm\nu_n$ and poles $\pm\eta_n$ it can be written as a product

$$K(s) = K(0)\prod_{n=0}^{\infty}\frac{1 - s^2/\nu_n^2}{1 - s^2/\eta_n^2} = \frac{\alpha_1}{\alpha_2}\prod_{n=0}^{\infty}\frac{s^2 - \nu_n^2}{s^2 - \eta_n^2}, \tag{5.26}$$

where

$$K(0) = \frac{\alpha_1}{\alpha_2} \cdot \frac{\mu_2^4 \tan h - \alpha_2}{\mu_1^4 \tan h - \alpha_1} = \frac{\alpha_1}{\alpha_2} \prod_{n=0}^{\infty} \frac{\nu_n^2}{\eta_n^2}. \tag{5.27}$$

The plus and minus functions can then be defined as

$$\left.\begin{aligned} K^+(s) &= \sqrt{K(0)} \prod_{n=0}^{\infty} \frac{1 + s/\nu_n}{1 + s/\eta_n} = \sqrt{\frac{\alpha_1}{\alpha_2}} \prod_{n=0}^{\infty} \frac{s + \nu_n}{s + \eta_n}, \\ K^-(s) &= \sqrt{K(0)} \prod_{n=0}^{\infty} \frac{1 - s/\nu_n}{1 - s/\eta_n} = \sqrt{\frac{\alpha_1}{\alpha_2}} \prod_{n=0}^{\infty} \frac{s - \nu_n}{s - \eta_n}. \end{aligned}\right\} \tag{5.28}$$

The convergence of the infinite products appearing in (5.26–5.28) is discussed in Appendix D.

On using (5.23) and the relations between $K_1(s)$, $K_2(s)$, $K^+(s)$ and $K^-(s)$, it is possible to derive the alternative Wiener–Hopf equation (see [3])

$$\begin{aligned} &K^+(s)\Phi_y^+(s,h) + \frac{\Phi_y^-(s,h)}{K^-(s)} \\ &= -\frac{K^+(s) - 1/K^-(s)}{s^4(\alpha_1 - \alpha_2) - \alpha_1\mu_2^4 + \alpha_2\mu_1^4} \left\{ p(s) + \frac{i\alpha_1 K_2(\eta_0)}{s + \eta_0} \right\}, \end{aligned} \tag{5.29}$$

which does not contain the functions $\gamma \tanh(\gamma h)$, $K_2(s)$ and $K_1(s)$ that give rise to doubly-infinite sequences of poles. Provided that $\alpha_1 \neq \alpha_2$, it is convenient to write (5.29) as

$$K^+(s)\Phi_y^+(s,h) + \frac{\Phi_y^-(s,h)}{K^-(s)} = \left(K^+(s) - \frac{1}{K^-(s)} \right) v(s) = T(s) \text{ say}, \tag{5.30}$$

where

$$v(s) = -\frac{p(s) + i\alpha_1 K_2(\eta_0)/(s + \eta_0)}{(\alpha_1 - \alpha_2)(s^4 - \sigma^4)} \tag{5.31}$$

and σ is defined by

$$\sigma^4 = \frac{\alpha_1\mu_2^4 - \alpha_2\mu_1^4}{\alpha_1 - \alpha_2}. \tag{5.32}$$

As α_j and μ_j are real, so is σ^4. To avoid ambiguity, σ is chosen so that $\arg \sigma = 0$ or $\pi/4$. The rational function $v(s)$ has poles at σ, $i\sigma$, $-\sigma$, $-i\sigma$ and $-\eta_0$. Since the degree of the numerator is less than that of the denominator, the numerators of the partial fractions are given by the residues and $T(s)$ can be written as the sum of the plus and minus functions

$$T^+(s) = K^+(s)v(s) - R(s), \quad T^-(s) = -\frac{v(s)}{K^-(s)} + R(s) \tag{5.33}$$

with $R(s)$ the rational function defined by

$$\begin{aligned} R(s) \quad = \quad & \frac{K^+(\sigma)\mathrm{Res}_{s=\sigma}v(s)}{s-\sigma} + \frac{K^+(i\sigma)\mathrm{Res}_{s=i\sigma}v(s)}{s-i\sigma} \\ & + \frac{\mathrm{Res}_{s=-\sigma}v(s)}{K^-(-\sigma)(s+\sigma)} + \frac{\mathrm{Res}_{s=-i\sigma}v(s)}{K^-(-i\sigma)(s+i\sigma)} \\ & + \frac{\mathrm{Res}_{s=-\eta_0}v(s)}{K^-(-\eta_0)(s+\eta_0)}. \end{aligned} \tag{5.34}$$

Equation (5.29) can now be arranged as

$$K^+(s)\Phi_y^+(s,h) - T^+(s) = -\frac{\Phi_y^-(s,h)}{K^-(s)} + T^-(s). \tag{5.35}$$

Since there is a strip adjoining the real line in the s-plane in which both members of (5.35) are analytic, both represent the same entire function, $J(s)$ say. To estimate its rate of growth, it is necessary to use the results obtained in Appendix D that $K^+(s) = O(1)$ as $s \to \infty$ in the upper half-plane and $1/K^-(s) = O(1)$ in the lower half-plane.

Since the fluid pressure is finite at $(0, h)$, $\phi_y(x, h)$ has at most an integrable singularity at $x = 0$. Thus

$$\phi_y(x,h) \sim Cx^{\beta^\pm} \text{ as } x \to 0^\pm, \; \beta^\pm > -1. \tag{5.36}$$

On using the Abelian theorem given by Noble [18],

$$\Phi_y^+(s,h) \sim B^+ s^{-\beta^+ -1}$$

as $s \to \infty$ in the upper half-plane and

$$\Phi_y^-(s,h) \sim B^- s^{-\beta^- -1}$$

as $s \to \infty$ in the lower half-plane. It is now evident from (5.31), (5.33), (5.34) and (5.35) that $J(s) \to 0$ as $s \to \infty$, so by Liouville's theorem $J(s)$ is zero.

The half-range transforms $\Phi^+(s,h)$ and $\Phi^-(s,h)$ are expressed in terms of functions already determined by first putting

$$\Phi(s,h) = \frac{\Phi_y(s,h)}{\gamma \tanh(\gamma h)}, \tag{5.37}$$

which follows from (5.19) and (5.20), and then obtaining two equations by using the fact that both members of (5.35) are zero:

$$K^+(s)\Phi_y^+(s,h) - T^+(s) = 0,$$

$$-\frac{\Phi_y^-(s,h)}{K^-(s)} + T^-(s) = 0.$$

From these two equations can be obtained a representation for $\Phi(s,h)$, as shown below. However, this representation involves the functions $R(s)$ and $T(s)$ which in turn depend on the polynomial $p(s)$ which has as coefficients edge values such as $\phi_{yxxx}(0^-,y)$. Hence the solution is not completely determined until the edge conditions are specified and applied, as is done later in this chapter.

On using the representations of $T^+(s)$ and $T^-(s)$ in (5.33) and adding $\Phi_y^+(s,h)$ and $\Phi_y^-(s,h)$, $\Phi_y(s,h)$ is seen to take the form

$$\begin{aligned}
\Phi_y(s,h) &= R(s)\left\{K^-(s) - \frac{1}{K^+(s)}\right\} && (5.38)\\
&= \frac{R(s)\{K(s)-1\}}{K^+(s)} && (5.39)\\
&= R(s)\left\{1 - \frac{1}{K(s)}\right\}K^-(s). && (5.40)
\end{aligned}$$

The last two forms are useful in the upper and lower half-planes respectively. They also show that the poles of $R(s)$ at $\pm\sigma$ and $\pm i\sigma$ are cancelled because $K(s) = 1$ at those points. From (5.37) and (5.38),

$$\Phi(s,h) = \frac{\Phi_y(s,h)}{\gamma \tanh(\gamma h)} = \frac{R(s)}{\gamma \tanh(\gamma h)} \frac{K(s)-1}{K^+(s)},$$

and, from the definition of $K(s)$,

$$\frac{1}{\gamma\tanh(\gamma h)} = \frac{1}{K(s)-1}\left\{\frac{(s^4-\mu_1^4)K(s)}{\alpha_1} - \frac{s^4-\mu_2^4}{\alpha_2}\right\}.$$

It follows that

$$\Phi(s,h) = R(s)\left\{\frac{(s^4-\mu_1^4)K^-(s)}{\alpha_1} - \frac{s^4-\mu_2^4}{\alpha_2 K^+(s)}\right\}. \tag{5.41}$$

The poles of $R(s)$ at $\pm\sigma$ and $\pm i\sigma$ are cancelled by zeros of the bracketed expression as can be seen by using, for example, $K^+(\sigma)K^-(\sigma) = 1$ and the definition of σ, which implies that $(\sigma^4-\mu_2^4)/\alpha_2 = (\sigma^4-\mu_1^4)/\alpha_1$.

The residues of $v(s)$ at $\pm\sigma$ and $\pm i\sigma$ can be expressed as linear combinations of the edge values $\phi_{yxxx}(0\pm,h)$, $\phi_{yxx}(0\pm,h)$, $\phi_{yx}(0\pm,h)$ and $\phi_y(0\pm,h)$ *via* the polynomials $p_1(s,h)$ and $p_2(s,h)$ in the following way.

$$\begin{aligned}
\operatorname*{Res}_{s=\sigma} v(s) &= -\frac{p(\sigma)+i\alpha_1K_2(\eta_0)/(\sigma+\eta_0)}{4\sigma^3(\alpha_1-\alpha_2)},\\
\operatorname*{Res}_{s=i\sigma} v(s) &= -\frac{p(i\sigma)+i\alpha_1K_2(\eta_0)/(i\sigma+\eta_0)}{-4i\sigma^3(\alpha_1-\alpha_2)},\\
\operatorname*{Res}_{s=-\sigma} v(s) &= -\frac{p(-\sigma)+i\alpha_1K_2(\eta_0)/(-\sigma+\eta_0)}{-4\sigma^3(\alpha_1-\alpha_2)},\\
\operatorname*{Res}_{s=-i\sigma} v(s) &= -\frac{p(-i\sigma)+i\alpha_1K_2(\eta_0)/(-i\sigma+\eta_0)}{4i\sigma^3(\alpha_1-\alpha_2)},\\
\operatorname*{Res}_{s=-\eta_0} v(s) &= -\frac{i\alpha_1K_2(\eta_0)}{(\alpha_1-\alpha_2)(\eta_0^4-\sigma^4)}.
\end{aligned} \tag{5.42}$$

From (5.38) the transformed potential for general y is given by

$$\Phi(s,y) = \frac{\cosh(\gamma y)}{\gamma\sinh(\gamma h)}\left\{K^-(s) - \frac{1}{K^+(s)}\right\}R(s), \tag{5.43}$$

$$\Phi_y(s,y) = \frac{\sinh(\gamma y)}{\sinh(\gamma h)}\left\{K^-(s) - \frac{1}{K^+(s)}\right\}R(s). \tag{5.44}$$

An alternative to (5.43) can be obtained from (5.41),

$$\Phi(s,y) = \frac{\cosh(\gamma y)}{\cosh(\gamma h)}\left\{\frac{(s^4-\mu_1^4)K^-(s)}{\alpha_1} - \frac{s^4-\mu_2^4}{\alpha_2 K^+(s)}\right\}R(s). \tag{5.45}$$

The scattered potential is the inverse transform of (5.43), namely

$$\phi(x,y) = \frac{1}{2\pi}\int_{-\infty}^{\infty} \frac{\cosh(\gamma y)}{\gamma \sinh(\gamma h)} \left\{ K^-(s) - \frac{1}{K^+(s)} \right\} R(s) e^{-ixs} ds. \tag{5.46}$$

The incident mode mode should cancel the residue contribution at $-\eta_0$, which is

$$\begin{aligned} I &= \frac{-i\cosh(\tau_0 y)}{\tau_0 \sinh(\tau_0 h)} e^{i\eta_0 x} K^-(-\nu_0) \operatorname*{Res}_{s=-\eta_0} R(s) \\ &= \frac{-i\cosh(\tau_0 y)}{\tau_0 \sinh(\tau_0 h)} \operatorname*{Res}_{s=-\eta_0} v(s) e^{-\eta_0 x} \\ &= -\frac{\cosh(\tau_0 y)}{\tau_0 \sinh(\tau_0 h)} \frac{e^{i\eta_0 x} \alpha_1 K_2(\eta_0)}{(\alpha_1 - \alpha_2)(\eta_0^4 - \sigma^4)} \\ &= -\frac{\cosh(\tau_0 y)}{\cosh(\tau_0 h)} e^{i\eta_0 x}. \end{aligned}$$

This cancels the incident wave in (5.8).

5.4 Application of the edge conditions

The subsequent analysis depends on the form of the rational function $R(s)$, which is determined by the edge conditions where the two plates meet. Several sets of edge conditions may be imposed, each modelling some some kind of physical join. Four relations between eight constants are specified by any set of edge conditions; for example for a welded join the lateral displacement and its first derivative are continuous across the edge, and so are the bending moment and shear force, so that

$$\begin{aligned} \phi_y(0^-,h) &= \phi_y(0^+,h), \\ \phi_{yx}(0^-,h) &= \phi_{yx}(0^+,h), \\ \alpha_2 \phi_{yxx}(0^-,h) &= \alpha_1 \phi_{yxx}(0^+,h), \\ \alpha_2 \phi_{yxxx}(0^-,h) &= \alpha_1 \phi_{yxxx}(0^+,h). \end{aligned} \tag{5.47}$$

Each set of join conditions can be specified concisely in terms of the quantities

$$\begin{aligned}
g_1 &= \phi_y(0^-,h) - \phi_y(0^+,h), \\
g_2 &= \phi_{yx}(0^-,h) - \phi_{yx}(0^+,h), \\
g_3 &= \phi_{yxx}(0^-,h) - \phi_{yxx}(0^+,h), \\
g_4 &= \phi_{yxxx}(0^-,h) - \phi_{yxxx}(0^+,h), \\
h_1 &= \alpha_2\phi_y(0^-,h) - \alpha_1\phi_y(0^+,h), \\
h_2 &= \alpha_2\phi_{yx}(0^-,h) - \alpha_1\phi_{yx}(0^+,h), \\
h_3 &= \alpha_2\phi_{yxx}(0^-,h) - \alpha_1\phi_{yxx}(0^+,h), \\
h_4 &= \alpha_2\phi_{yxxx}(0^-,h) - \alpha_1\phi_{yxxx}(0^+,h).
\end{aligned} \tag{5.48}$$

The sets

$$g_1 = g_2 = g_3 = g_4 = 0, \quad \textit{smooth join}, \tag{5.49}$$

$$g_1 = g_2 = h_3 = h_4 = 0, \quad \textit{welded join} \tag{5.50}$$

and

$$g_1 = g_2 = h_1 = h_2 = 0, \quad \textit{clamped join} \tag{5.51}$$

will be considered in what follows. The polynomial $p(s)$ can be written as

$$p(s) = h_4 - ih_3 s - h_2 s^2 + ih_1 s^3, \tag{5.52}$$

and is evidently linear for a clamped join, and cubic for the other types of join.

Four more relations in addition to the four given by one of (5.49)–(5.51) are needed to determine the eight edge values completely. From (5.21) and (5.22).

$$\begin{aligned}
\Phi_y(s,h) &= -\frac{p_1(s,h) - p_2(s,h)}{s^4} + O(s^{-5}) \text{ as } s \to \infty \\
&= \frac{ig_1}{s} - \frac{g_2}{s^2} - \frac{ig_3}{s^3} + \frac{g_4}{s^4} + O(s^{-5}).
\end{aligned} \tag{5.53}$$

On the other hand, from (5.38),

$$\Phi_y(s,h) = \frac{R(s)\{K(s)-1\}}{K^+(s)}$$

$$\begin{aligned}
&= \frac{R(s)\{\alpha_1 K_2(s) - \alpha_2 K_1(s)\}}{\alpha_2 K_1(s) K^+(s)} \\
&= \frac{(\alpha_1 - \alpha_2)(s^4 - \sigma^4) R(s)}{\alpha_2[s^4 - \mu_1^4 - \alpha_1/\{\gamma \tanh(\gamma h)\}]K^+(s)} \\
&= \frac{(\alpha_1/\alpha_2 - 1)R(s)\{1 + O(s^{-4})\}}{K^+(s)} \quad \text{as } s \to \pm\infty. \qquad (5.54)
\end{aligned}$$

The large-s expansion of $1/K^+(s)$ can be derived from (5.28). Details are given in Appendix D.

$$\frac{1}{K^+(s)} = \sqrt{\frac{\alpha_2}{\alpha_1}}\left(1 + \frac{b_1}{s} + \frac{b_2}{s^2} + \frac{b_3}{s^3}\right) + O(s^{-4}), \qquad (5.55)$$

$$\text{where } b_1 = a_1,\ b_2 = a_2 + \frac{a_1^2}{2},\ b_3 = a_3 + a_1 a_2 + \frac{a_1^3}{6},$$

$$a_r = (-1)^{r-1} \sum_{n=0}^{\infty} \frac{\eta_n^r - \nu_n^r}{r};\ r = 1, 2, 3.$$

An alternative expression for a_r is

$$a_r = \frac{(-1)^{r-1}}{r!} \frac{d^r}{ds^r} \log K^-\left(\frac{1}{s}\right)\bigg|_{s=0}. \qquad (5.56)$$

Also, from (5.34),

$$R(s) = \frac{1}{4\sigma^3(\alpha_2 - \alpha_1)}\left(\frac{L_1}{s - \sigma} + \frac{L_2}{s - i\sigma} + \frac{L_3}{s + \sigma} + \frac{L_4}{s + i\sigma} + \frac{L_5}{s + \eta_0}\right),$$

where

$$\begin{aligned}
L_1 &= K^+(\sigma)\left\{p(\sigma) + \frac{i\alpha_1 K_2(\eta_0)}{\eta_0 + \sigma}\right\}, \\
L_2 &= iK^+(i\sigma)\left\{p(i\sigma) + \frac{i\alpha_1 K_2(\eta_0)}{\eta_0 + i\sigma}\right\}, \\
L_3 &= -K^+(-\sigma)\left\{p(-\sigma) + \frac{i\alpha_1 K_2(\eta_0)}{\eta_0 - \sigma}\right\}, \\
L_4 &= -iK^+(-i\sigma)\left\{p(-i\sigma) + \frac{i\alpha_1 K_2(\eta_0)}{\eta_0 - i\sigma}\right\}, \\
L_5 &= \frac{4i\alpha_1 K_2(\eta_0)\sigma^3}{(\eta_0^4 - \sigma^4)K^-(-\eta_0)}. \qquad (5.57)
\end{aligned}$$

On using the expansion $1/(s-a) = \sum_{j=1}^{\infty} a^{j-1}/s^j$,

$$\begin{aligned} R(s) &= \frac{1}{4\sigma^3(\alpha_2-\alpha_1)}\left\{\frac{L_1+L_2+L_3+L_4+L_5}{s}\right. \\ &+ \frac{(L_1+iL_2-L_3-iL_4)\sigma - L_5\eta_0}{s^2} \\ &+ \frac{(L_1-L_2+L_3-L_4)\sigma^2 + L_5\eta_0^2}{s^3} \\ &+ \left.\frac{(L_1-iL_2-L_3+iL_4)\sigma^3 - L_5\eta_0^3}{s^4}\right\} + O(s^{-5}) \text{ as } s \to \infty \\ &= \frac{c_1}{s} + \frac{c_2}{s^2} + \frac{c_3}{s^3} + \frac{c_4}{s^4} + O(s^{-5}), \end{aligned} \tag{5.58}$$

say. The expression (5.54) can be expanded in negative powers of s in terms of the coefficients b_i and c_i to give

$$\begin{aligned} \Phi_y(s,h) &= \sqrt{\frac{\alpha_2}{\alpha_1}}\left(1-\frac{\alpha_1}{\alpha_2}\right) \\ &\times \left(\frac{c_1}{s} + \frac{b_1c_1+c_2}{s^2} + \frac{b_2c_1+b_1c_2+c_3}{s^3} + \frac{b_3c_1+b_2c_2+b_1c_3+c_4}{s^4}\right) \\ &+ O(s^{-5}). \end{aligned} \tag{5.59}$$

The four remaining relations between the eight edge values of (5.48) are obtained by equating coefficients in (5.53) and (5.59).

$$g_1 = -i\sqrt{\frac{\alpha_2}{\alpha_1}}\left(1-\frac{\alpha_1}{\alpha_2}\right)c_1, \tag{5.60}$$

$$g_2 = -\sqrt{\frac{\alpha_2}{\alpha_1}}\left(1-\frac{\alpha_1}{\alpha_2}\right)(b_1c_1+c_2), \tag{5.61}$$

$$g_3 = i\sqrt{\frac{\alpha_2}{\alpha_1}}\left(1-\frac{\alpha_1}{\alpha_2}\right)(b_2c_1+b_1c_1+c_3), \tag{5.62}$$

$$g_4 = \sqrt{\frac{\alpha_2}{\alpha_1}}\left(1-\frac{\alpha_1}{\alpha_2}\right)(b_3c_1+b_2c_2+b_1c_3+c_4). \tag{5.63}$$

The quantities g_1 to g_4 and c_1 to c_4 depend on the edge values by way of (5.48), (5.58), (5.57) and (5.52).

In the following subsections three different edge conditions are applied, the appropriate form of the rational function $R(s)$ being derived in each case.

I Smooth join

For a smooth join the relations (5.49), substituted in (5.60)–(5.63), imply that $c_1 = c_2 = c_3 = c_4 = 0$. This gives, by comparison of coefficients in (5.58), a set of four linear equations which can be solved to give L_1 to L_4 in terms of other quantities. The values $p(\sigma)$, $p(i\sigma)$, $p(-\sigma)$ and $p(-i\sigma)$ are simple functions of L_1 to L_4 by (5.57) and a further set of four linear equations give h_1 to h_4 by using (5.52). In this way all of g_1 to g_4 and h_1 to h_4 may be found and the eight edge values, only four of which are distinct in this case because of continuity, can be determined from (5.48).

Furthermore, (5.58) shows that $R(s) = O(s^{-5})$ for these edge conditions. Since $R(s)$ is a rational function with constant numerator and quintic denominator, it must be

$$\begin{aligned} R(s) &= \frac{\mathrm{Res}_{s=-\eta_0} v(s)\ (-\eta_0-\sigma)(-\eta_0-i\sigma)(-\eta_0+\sigma)(-\eta_0+i\sigma)}{K^-(-\eta_0)(s-\sigma)(s-i\sigma)(s+\sigma)(s+i\sigma)(s+\eta_0)} \\ &= \frac{i\alpha_1 K_2(\eta_0)}{(\alpha_1-\alpha_2)K^+(\eta_0)(s^4-\sigma^4)(s+\eta_0)}. \end{aligned} \tag{5.64}$$

II Clamped join

The clamped join relations (5.51) imply that $c_1 = c_2 = 0$ and $p(s) = h_4 - ih_3 s$. Equations (5.62) and (5.63) express g_3 and g_4 in terms of c_3 and c_4. (The quantity b_1 is known, as it is ultimately a function of the physical parameters.) By comparison of coefficients in (5.58), four relations are obtained between L_1 to L_4 and c_3 to c_4. Because of the form of $p(s)$, L_1 to L_4 are dependent on the two unknown coefficients h_3 and h_4 only. Hence the four relations in question furnish a set of four linear equations for g_3, g_4, h_3 and h_4. These quantities are sufficient to determine the four non-zero edge values $\phi_{yxx}(0^{\pm}, h)$ and $\phi_{yxxx}(0^{\pm}, h)$ by means of (5.48). The difficult quantity b_1 ($= a_1$) does not appear in the solutions for h_3 and h_4, so it is also not in $R(s)$.

In this case, (5.58) shows that $R(s) = O(s^{-3})$ and it must have the form

$$R(s) = \frac{Fs^2 + Gs + H}{(s^4 - \sigma^4)(s + \eta_0)}. \qquad (5.65)$$

By standard partial-fraction techniques it can be shown that

$$\begin{aligned} F &= 2\sigma^2(C_2 + C_1) + (\eta_0^2 + \sigma^2)C_3, \\ G &= 2\sigma^2\eta_0(C_2 + C_1) + 2\sigma^3(C_1 - C_2), \\ H &= 2\sigma^3\eta_0(C_1 - C_2) - (\eta_0^2 + \sigma^2)\sigma^2 C_3, \end{aligned}$$

where

$$C_1 = \frac{L_1}{4\sigma^3(\alpha_2 - \alpha_1)}, \; C_2 = \frac{L_3}{4\sigma^3(\alpha_2 - \alpha_1)}, \; C_3 = \frac{L_5}{4\sigma^3(\alpha_2 - \alpha_1)}.$$

III Welded join

The welded join relations (5.50) imply that $c_1 = c_2 = 0$ and $p(s) = -h_2 s^2 + i h_1 s^3$. As in the case of the clamped join, equations (5.62) and (5.63) express g_3 and g_4 in terms of c_3 and c_4. By comparison of coefficients in (5.58), four relations are obtained between L_1 to L_4 and c_3 to c_4, but L_1 to L_4 are dependent on the two unknown coefficients h_1 and h_2 only. Hence a set of four linear equations for g_3, g_4, h_1 and h_2 is obtained. Together with the four equations (5.50), eight linear equations for the eight edge values $\phi_{yxx}(0^\pm, h)$ and $\phi_{yxxx}(0^\pm, h)$ are given by (5.48).

As for the clamped join, $R(s) = O(s^{-3})$ and (5.65) gives the form of $R(s)$. Again, the expression for $R(s)$ does not contain b_1.

5.5 The reflection coefficient

The first reflected mode is given by the residue contribution to (5.46) at η_0, namely

$$\frac{i\cosh(\tau_0 y)}{\tau_0 \sinh(\tau_0 h)} e^{-i\eta_0 x} \operatorname*{Res}_{s=\eta_0} K^-(s) \; R(\eta_0). \qquad (5.66)$$

This is the only real reflected mode provided that $h < \pi/2$ and $\alpha_1/\mu_1^4 > \tan h$. Under these conditions η_0 is real, whilst η_1, η_2 *etc* are purely imaginary apart possibly for some complex pairs (η_m, η_n) such that $\eta_m + \eta_n$ is purely imaginary.

I Smooth join

On using (5.13) and (5.64), together with the relation

$$\tau_0 \tanh(\tau_0 h) = \frac{\alpha_1 K_2(\eta_0)}{(\alpha_1 - \alpha_2)(\eta_0^4 - \sigma^4)}$$

(which follows from the definition of $K(s)$) the reflection coefficient can be written in the form

$$R_0 = \frac{1}{\cosh(\tau_0 h)} \times \frac{\mathrm{Res}_{s=\eta_0} K^-(s)}{2\eta_0 K^+(\eta_0)}.$$

If the product forms for $K^+(s)$ and $K^-(s)$ are substituted, the reflection coefficient can be written as

$$R_0 = \frac{1}{\cosh(\tau_0 h)} \times \frac{\eta_0 - \nu_0}{\eta_0 + \nu_0} \prod_{n=1}^{\infty} \left(\frac{\eta_0 - \nu_n}{\eta_0 - \eta_n} \cdot \frac{\eta_0 + \eta_n}{\eta_0 + \nu_n} \right).$$

The radiation condition (5.13) is satisfied if η_0 and ν_0 are real, whilst the other η_n and ν_n are purely imaginary. In this case the modulus of the reflection coefficient takes the form

$$|R_0| = \left| \frac{\eta_0 - \nu_0}{\eta_0 + \nu_0} \right| \times \frac{1}{\cosh(h\tau_0)}. \tag{5.67}$$

As can be seen from (5.7) and (5.8), the amplitude of the incident wave is $|A| = 1/\cosh(h\tau_0)$. The ratio $|R_0|/|A|$ agrees with the expression already obtained in (4.40) by letting $a \to 0$ in the continuously-varying problem.

II Clamped join

The real reflected mode is given by (5.66), where $R(\eta_0)$ takes the form (5.65) with values of F, G and H calculated as described in subsection II of §5.4. The reflection coefficient is

$$R_0 = \frac{1}{\cosh(\tau_0 h)} \times \frac{i(\alpha_1 - \alpha_2)(F\eta_0^2 + G\eta_0 + H)\mathrm{Res}_{s=\eta_0} K^-(s)}{2\eta_0 \alpha_1 K_2(\eta_0)}. \tag{5.68}$$

The full form of R_0 in terms of the problem parameters together with η_0 and σ is not given here on account of its complexity. It was obtained by computer algebra and used when the reflection and transmission coefficients were evaluated numerically.

III Welded join

The real reflected mode is given by (5.66), where $R(\eta_0)$ takes the form (5.65) with values of F, G and H calculated as in subsection III of §5.4. Again the reflection coefficient has the form (5.68).

5.6 The transmission coefficient

The first transmitted mode is given by the residue contribution to (5.46) at $-\nu_0$, namely

$$-\frac{i\cosh(\lambda_0 y)}{\lambda_0 \sinh(\lambda_0 h)} e^{i\nu_0 x} \left\{ \operatorname*{Res}_{s=-\nu_0} \frac{1}{K^+(s)} \right\} R(-\nu_0). \tag{5.69}$$

This is the only real transmitted mode provided that $h < \pi/2$ and $\alpha_2/\mu_2^4 > \tan h$. Under these conditions ν_0 is real, whilst ν_1, ν_2 *etc* are purely imaginary apart possibly for some complex pairs (ν_m, ν_n) such that $\nu_m + \nu_n$ is purely imaginary.

I Smooth join

On using (5.13) and (5.64), together with the relation

$$\lambda_0 \tanh(\lambda_0 h) = -\frac{\alpha_2 K_1(\nu_0)}{(\alpha_1 - \alpha_2)(\nu_0^4 - \sigma^4)}$$

(which follows from the definition of $K(s)$) the transmission coefficient can be written in the form

$$T_0 = \frac{-1}{\cosh(\lambda_0 h)} \times \frac{\alpha_1 K_2(\eta_0) \operatorname{Res}_{s=-\nu_0}\{1/K^+(s)\}}{\alpha_2 K_1(\nu_0) K^+(\eta_0)(\eta_0 - \nu_0)}.$$

Thus, using product forms of $K_1(s), K_2(s)$ and $K^+(s)$, it is found that

$$T_0 = \frac{1}{\cosh(\tau_0 h)} \times \frac{-2i\eta_0}{\eta_0 + \nu_0} \prod_{n=1}^{\infty} \left(\frac{\eta_0 - \nu_n}{\nu_0 + \eta_n} \cdot \frac{\eta_0 + \eta_n}{\nu_0 - \nu_n} \right). \tag{5.70}$$

The ratio $|T|/|A|$ is equal to the expression already obtained in (4.43) by letting $a \to 0$ in the continuously-varying problem. This can be seen if it is borne in mind that all η_n and ν_n for $n > 0$ are purely imaginary, whilst η_0 and ν_0 are real. Hence, for example, $|\eta_0 - \nu_n|$ in (5.70) is equal to $|\nu_n + \eta_0|$ in (4.43).

II Clamped join

The real transmitted mode is given by (5.69), where $R(-\nu_0)$ takes the form (5.65) with values of F, G and H calculated as described in subsection II of §5.4. The transmission coefficient is

$$T_0 = \frac{1}{\cosh(\lambda_0 h)} \times \frac{i(\alpha_1 - \alpha_2)(F\nu_0^2 - G\nu_0 + H)\operatorname{Res}_{s=-\nu_0}\{1/K^+(s)\}}{\alpha_2(\nu_0 + \eta_0)K_1(\nu_0)}. \tag{5.71}$$

III Welded join

The real transmitted mode is given by (5.69), where $R(\nu_0)$ takes the form (5.65) with values of F, G and H calculated as in subsection III of §5.4. Again the reflection coefficient has the form (5.71).

Chapter 6

Discussion

Two boundary-value problems have been analysed, both modelling waveguides in which the physical properties of a wall vary in one spatial direction. In both cases the limiting configuration, where the variation is replaced by an abrupt change, has been analysed independently by the Wiener–Hopf technique as a check. In chapter 3.1 the limiting case gives rise to a standard type of Wiener–Hopf problem, which however does not seem to have been solved before in the literature. In chapter 4, the limiting problem has a boundary condition of an unusual type, with a discontinuous coefficient in the differential operator (see (4.6)).

In analytical terms the most striking difference between the cases of smooth change and abrupt change in properties is the presence of doubly-infinite sequences of duct modes in the former case, which reduce to simple infinite sequences in the latter. However, all of the many extra modes have significant imaginary parts so that they are not propagated any distance from the centre of the region of variation ($x = 0$ in the coordinate system of the problems). Of more importance physically is the fact that the amount of reflected energy is small when the variation in properties is gradual. This can be seen clearly in the graphs of reflected and transmitted amplitudes presented in chapter 4.

For simplicity the analysis has generally been for the case of a single propagating reflected mode within the waveguide and a single transmitted mode. If the problem parameters are varied, for example by increasing the duct height, more propagating modes will be present. For example, to consider the second mode, it would be necessary to replace a radiation condition such as (3.8) by

$$\phi(x,y) \sim \begin{cases} (Ae^{i\beta_0 x} + R_0 e^{-i\beta_0 x})\cosh(\tau_0 y) + R_1 e^{-i\beta_1 x}\cosh(\tau_1 y), & x \to -\infty, \\ T_0 e^{i\alpha_0 x}\cosh(y\lambda_0) + T_1 e^{i\alpha_1 x}\cosh(y\lambda_1), & x \to \infty, \end{cases} \tag{6.1}$$

The extra reflected mode, with amplitude R_1, is due to the wavenumber α_1, the second positive real root of equation (3.12) taking $\eta = \eta_1$. The root α_1 is greater than α_0. The condition for real α_1 is $\pi/2 < h < 3\pi/2$ with $\Im(\eta) < \tan h$; or $h < \pi/2$ with $\Im(\eta) > \tan h$. The extra transmitted mode corresponds to β_1 which is a root of (3.12) when $\eta = \eta_2$. With these extra real roots, the contour of integration, C, in figure 3.3 would have to pass below the real pole for the reflected mode β_1 and above that for the transmitted mode $-\alpha_1$ in addition to the usual indentations discussed in chapter 3.

Several features complicated the analysis in the elastic-plate problem (chapters 4 and 5). Firstly, the duct walls, being elastic, carry waves which in the steady state are coupled to harmonic waves in the fluid. In the limit of light fluid loading all the wave energy is in the duct wall and the fluid properties are immaterial. In the limit of heavy fluid loading the elastic plate is totally compliant and behaves like a membrane.

Secondly, there are several different edge conditions that can be applied in the limiting case of discontinuity, each with a physical interpretation. It is evident, (since the analysis of chapter 4 relies on ϕ and all its derivatives being continuous) that the "continuous" edge conditions have to be applied at the join in the limiting problem. There are similarities between the Wiener–Hopf problem of chapter 5 and the case of an elastic plate with an abrupt change in properties and surrounded by fluid, which is analysed by Brazier-Smith [3] and Norris and Wickham [19]. Although the analysis for the waveguide is algebraically similar in some places, the type of scattering is quite different, comprising waves which can travel in two directions only. There is no radiation of sound outside the duct as $y \to \pm\infty$. The wavenumbers appear as an infinite number of zeros of transcendental functions $K_1(s)$ and $K_2(s)$ (5.24), rather than of a polynomial.

Thirdly, the fourth-order boundary condition due to the elastic plate contains a linear operator which, in general, has fourth-, third-, second- and first-order terms (see equation (4.45)). This leads to a functional difference equation of the third order (4.48). Simplifying assumptions were needed to reduce the order of the difference equation, and the implication of these was discussed in chapter 4.

The two-part elastic plate, that is made of two materials with a transition region between them, is amenable to the functional-difference equation method. The same principle could be applied to a three-part configuration, where there are two transition regions. For simplicity consider the impedance problem of chapter 3. A suitable three-part impedance function would be

$$\eta(x) = \frac{\eta_2\{e^{(x-b)/a} + e^{(x+b)/a}\} + \eta_1\{1 + e^{2x/a}\}}{1 + e^{(x-b)/a} + e^{(x+b)/a} + e^{2x/a}}. \tag{6.2}$$

This has the asymptotic value η_1 for large x both positive and negative, but is approximately η_2 in a region around $x = 0$. It was constructed from functions of the tanh type in order to give rise to a simple functional difference equation. In fact, when (6.2) is substituted for (3.7) in the problem of chapter 3, the impedance boundary condition takes the form

$$\phi_y - ik\eta_1\phi + De^{x/a}(\phi_y - ik\eta_2\phi) + e^{2x/a}(\phi_y - ik\eta_1\phi) = 0, \tag{6.3}$$

where $D = e^{-b/a} + e^{b/a}$. This corresponds to (3.14) in the analysis of chapter 3. The analysis continues as in chapter 3 by changing the variable in a contour integral and then translating the contour back through the pole-free region $-1/a \leq \Im(s) \leq 1/a$. The functional difference equation which has to be satisfied by the function $f(s)$ in the velocity potential integral is in this case

$$f(s + i/a) + Df(s) + f(s - i/a) = 0. \tag{6.4}$$

This is a second-order linear equation, and because of its homogenous form it can be transformed into a Ricatti equation. On dividing (6.4) and defining

$$g(s) = \frac{f(s + i/a)}{f(s)},$$

the first-order non-linear Ricatti equation

$$g(s) + \frac{1}{g(s - i/a)} = -D \tag{6.5}$$

is obtained. This may be solved numerically by an iterative method. However, it is unclear just how useful such a solution would be since it is by no means apparent that the strip $-1/a \leq \Im(s) \leq 1/a$ can be clear of poles.

The functional difference equation method could be applied to other problems where material properties vary continuously in one space dimension. Further work could include applying the method to a single plate embedded in fluid, rather like that studied by Brazier-Smith [3], although in this case the dispersion relation, instead of taking the form

$$(s^4 - \mu_j^4)\gamma \tanh(h\gamma) - \alpha_j = 0,$$

which is obtained from (4.22), would be

$$(s^4 - \mu_j^4)\gamma - \alpha_j = 0.$$

This last relation is an odd function of γ and so has branch points, and it is likely that this would make the analysis more difficult.

Appendix A

This appendix applies the method of §3.8 to the functional difference equation (4.29) in chapter 4. The equation

$$\frac{f(z+1)}{f(z)} = h(z) = h_1(z)h_2(z) \tag{A.1}$$

has the formal solution

$$f(z) = \frac{\prod_{n=1}^{\infty} h_1(z-n)}{\prod_{n=0}^{\infty} h_2(z+n)} = \frac{1}{h_2(z)} \prod_{n=1}^{\infty} \frac{h_1(z-n)}{h_2(z+n)}, \tag{A.2}$$

as may be seen by substituting and treating infinite products as absolutely convergent. The numerator and denominator in (A.2) are both adapted from Nörlund's *principal solution* [16]. In a particular case, $h_1(z)$ and $h_2(z)$ need to be chosen so that the solution given by (A.2) contains an absolutely convergent infinite product which defines a meromorphic functional solution to (A.1).

For the functional difference equation (4.29), suitable functions $h_1(s)$ and $h_2(s)$ can be defined in much the same way as the plus and minus functions employed in the Wiener-Hopf method. A product representation of $p(s)$, which is defined by (4.26), is

$$p(s) = p(0) \prod_{n=0}^{\infty} \frac{1 - s^2/\nu_n^2}{1 - s^2/\eta_n^2}, \tag{A.3}$$

where

$$p(0) = \frac{\mu_2^4 \tan h - \alpha_2}{\mu_1^4 \tan h - \alpha_1} = \prod_{n=0}^{\infty} \frac{\nu_n^2}{\eta_n^2}, \tag{A.4}$$

the last equality following from the fact that $\lim_{s\to\infty} p(s) = 1$, which may be deduced from (4.26). The infinite product in (A.3) converges because both ν_n and η_n are asymptotically $\pi i n/h$ as $n \to \infty$. The infinite product in (A.4) converges because $\nu_n - \eta_n = O(n^{-5})$, which follows from (B.7). Separating the zeros and poles of $p(s)$ into two sets, $\{\eta_n\} \cup \{\nu_n\}$ and $\{-\eta_n\} \cup \{-\nu_n\}$, $p(s)$ can be factorised as $p(s) = h_1(s)h_2(s)$, where

$$h_1(s) = \sqrt{p(0)} \prod_{n=0}^{\infty} \frac{1 - s/\nu_n}{1 - s/\eta_n}, \quad h_2(s) = \sqrt{p(0)} \prod_{n=0}^{\infty} \frac{1 + s/\nu_n}{1 + s/\eta_n}. \tag{A.5}$$

The products converge absolutely for all s because, using (B.7) and (B.6), $\nu_n^{-1} - \eta_n^{-1} = O(n^{-7})$ as $n \to \infty$.

By (A.2), (4.29) has a solution

$$f_2(s) = \frac{1}{h_2(s)} \prod_{m=1}^{\infty} \frac{h_1\left(s - \frac{im}{a}\right)}{h_2\left(s + \frac{im}{a}\right)},$$

provided that the product converges. With $h_1(s)$ $h_2(s)$ are given by (A.5), the product does converge and can be reduced to the form

$$f_2(s) = \prod_{n=0}^{\infty} \frac{\Gamma\{1 - ia(\eta_n - s)\}\Gamma\{-ia(\nu_n + s)\}}{\Gamma\{1 - is(\nu_n - s)\}\Gamma\{-ia(\eta_n + s)\}} \tag{A.6}$$

where the infinite product representation for $\Gamma(z)$ has been utilised. In order to examine the behaviour of $f(s)$ as $|s| \to \infty$ it is useful to recast $f_2(s)$ as

$$\begin{aligned} f_2(s) &= \frac{1}{h_2(s)} \prod_{m=1}^{\infty} \prod_{n=0}^{\infty} \left(\frac{1 - \frac{s}{\eta_n + \frac{im}{a}}}{1 - \frac{s}{\nu_n + \frac{im}{a}}} \cdot \frac{1 + \frac{s}{\nu_n + \frac{im}{a}}}{1 + \frac{s}{\eta_n + \frac{im}{a}}} \right) & \text{(A.7)} \\ &= \frac{1}{h_2(s)} \prod_{k=0}^{\infty} \left(\frac{1 - s/y_k}{1 - s/x_k} \cdot \frac{1 + s/x_k}{1 + s/y_k} \right), & \text{(A.8)} \end{aligned}$$

where x_k (with $k = 0, 1, 2, \ldots$) are the numbers $\nu_n + im/a$ arranged in order of increasing imaginary part and y_k are the numbers $\eta_n + im/a$ similarly arranged. Note that

$$\left.\begin{aligned} |x_k| &\sim \sqrt{2\pi k/ha} && \text{as } k \to \infty, \\ |y_k| &\sim \sqrt{2\pi k/ha} && \text{as } k \to \infty, \\ x_k - y_k &= O(k^{-7/2}) && \text{as } k \to \infty. \end{aligned}\right\} \tag{A.9}$$

The complete solution to (4.26) can now be written in the form

$$f(s) = \frac{He^{-ibs}}{h_2(s)\sinh\{\pi a(s+\nu_0)\}} \prod_{k=0}^{\infty} \left(\frac{1 - s/y_k}{1 - s/x_k} \cdot \frac{1 + s/x_k}{1 + s/y_k} \right). \tag{A.10}$$

The roots η_n and ν_n become purely imaginary and increasing in modulus for large n. It follows that x_k and y_k are both purely imaginary for all large enough k, and so the infinite product and the function $h_2(s)$ in (A.10) are bounded as $s \to \infty$ in a horizontal strip. The complete function $f(s)$ therefore decays exponentially for such s, provided that $B_1 < e^{\pi} B_2$, and certainly if the factor e^{ibs} is omitted, as explained in §4.4.

Appendix B

In this appendix an asymptotic expansion is derived, in negative powers of the index n, for the roots of the dispersion relation in chapter 4. Let $\pm\eta_n$ be the roots of $K_1(s) = (s^4 - \mu_1^4)\gamma \tanh(\gamma h) - \alpha_1 = 0$, and $\pm\nu_n$ those of $K_2(s) = (s^4 - \mu_2^4)\gamma \tanh(\gamma h) - \alpha_2 = 0$. Apart from a finite number, say $2m_1$ and $2m_2$, the roots of each equation are purely imaginary. So for large n, η_n and ν_n are those roots which are closest to $\pi i(n - m_j + 1)/h$ respectively ($j = 1, 2$). In what follows it can be assumed without loss of generality that $m_1 = m_2 = m$.

An asymptotic expression for η_n in powers of n^{-1} can be obtained by the method given by Olver [20]. For simplicity of notation expressions are derived for the case $m = 1$. Using the notation $\tau_n = \gamma(\eta_n)$, define

$$\epsilon_n = h\tau_n + \pi i n \tag{B.1}$$

and write the defining equation as

$$\epsilon_n = \tanh^{-1} \frac{\alpha_1}{(\eta_n^4 - \mu_1^4)\tau_n}. \tag{B.2}$$

From (B.1),

$$\epsilon_n = -h\eta_n \left(1 - \frac{1}{\eta_n^2}\right)^{\frac{1}{2}} + \pi i n,$$

choosing an appropriate branch of γ,

$$= \quad -h\eta_n + \pi i n + \frac{h}{2\eta_n} + \frac{h}{8\eta_n^3} + \frac{h}{16\eta_n^5} + \frac{5h}{128\eta_n^7} + \frac{7h}{256\eta_n^9} + \frac{21h}{1024\eta_n^{11}}$$

$$+ O(\eta_n^{-13}) \text{ as } n \to \infty. \tag{B.3}$$

On the other hand, from (B.2),

$$\begin{aligned} \epsilon_n &= \tanh^{-1}\left\{-\frac{\alpha_1}{\eta_n^5}\left(1-\frac{\mu_1^4}{\eta_n^4}\right)^{-1}\left(1-\frac{1}{\eta_n^2}\right)^{-\frac{1}{2}}\right\} \\ &= -\frac{\alpha_1}{\eta_n^5}-\frac{\alpha_1}{2\eta_n^7}-\frac{\alpha_1}{\eta_n^9}\left(\mu_1^4+\frac{3}{8}\right)-\frac{\alpha_1}{\eta_n^{11}}\left(\frac{\mu_1^4}{2}+\frac{5}{16}\right) \\ &\quad + O(\eta_n^{-13}). \end{aligned} \tag{B.4}$$

Combining (B.3) and (B.4),

$$\begin{aligned} h\eta_n &= \pi i n + \frac{h}{2\eta_n} + \frac{h}{8\eta_n^3} + \left(\frac{h}{16}+\alpha_1\right)\frac{1}{\eta_n^5} + \left(\frac{5h}{128}+\frac{\alpha_1}{2}\right)\frac{1}{\eta_n^7} \\ &\quad + \left(\frac{7h}{256}+\alpha_1\mu_1^4+\frac{3\alpha_1}{8}\right)\frac{1}{\eta_n^9} + \left(\frac{21h}{1024}+\frac{\alpha_1\mu_1^4}{2}+\frac{5\alpha_1}{16}\right)\frac{1}{\eta_n^{11}} \\ &\quad + O(\eta_n^{-13}). \end{aligned} \tag{B.5}$$

Starting with

$$\eta_n = \frac{\pi i n}{h} + O(n^{-1})$$

and repeatedly substituting for η_n in the right-hand side, the following expression is obtained

$$\begin{aligned} \eta_n &= \frac{\pi i n}{h} - \frac{ih}{2\pi n} - \frac{ih^3}{8\pi^3 n^3} - \left(\frac{1}{16}+\frac{\alpha_1}{h}\right)\frac{ih^5}{\pi^5 n^5} - \left(\frac{5}{128}+\frac{5\alpha_1}{2h}\right)\frac{ih^7}{\pi^7 n^7} \\ &\quad - \left\{\frac{7}{256}+(\mu_1^4+4)\frac{\alpha_1}{h}\right\}\frac{ih^9}{\pi^9 n^9} + O(n^{-11}). \end{aligned} \tag{B.6}$$

The expression for ν_n is the same except that α_2 and μ_2 replace α_1 and μ_1. When $m > 1$, the expression on the right-hand side of (B.6) represents η_{n+m-1} or ν_{n+m-1} rather than η_n or ν_n. Subtracting,

$$\begin{aligned} \eta_{n+m-1} - \nu_{n+m-1} &= (\alpha_2-\alpha_1)\frac{ih^4}{\pi^5 n^5} + (\alpha_2-\alpha_1)\frac{5ih^7}{\pi^7 n^7} \\ &\quad + \{4(\alpha_2-\alpha_1)+\mu_2^4-\mu_1^4\}\frac{ih^9}{\pi^9 n^9} \\ &\quad + O(n^{-11}) \text{ as } n \to \infty. \end{aligned} \tag{B.7}$$

Appendix C

This appendix is concerned with the limiting case of discontinuous bending properties, in which an elastic plate has an abrupt change of properties. This generalised-function argument is needed for the discussion of chapter 5. The bending stiffness as a function of x is denoted by

$$B(x;a) = \frac{B_1 + B_2 e^{x/a}}{1 + e^{x/a}} \tag{C.1}$$

where B_1, B_2 and a are positive parameters and x is real. As $a \to 0$, the pointwise limits are

$$\lim_{a \to 0} B(x;a) = B_1 + (B_2 - B_1)H(x), \tag{C.2}$$

where $H(x)$ is the Heaviside step function with $H(0) = 1/2$. On differentiating (C.1),

$$B'(x;a) = \frac{(B_2 - B_1)}{4a\cosh^2(x/2a)}. \tag{C.3}$$

It will be shown here that *the sequence $B'(x;1/n)$ defines the generalised function $(B_2 - B_1)\delta(x)$ where*

$$\int_{-\infty}^{\infty} \delta(x)F(x)\,dx = F(0), \tag{C.4}$$

for any good function $F(x)$ in the sense of [15]. The small parameter a has been replaced by $1/n$ and following [15]:

$$\left| \int_{-\infty}^{\infty} B'(x;1/n)F(x)\,dx - F(0) \right|$$

$$
\begin{aligned}
&= \left| \int_{-\infty}^{\infty} \frac{n}{4} \operatorname{sech}^2 \frac{nx}{2} \, F(x)\, dx - F(0) \right| \\
&= \left| \int_{-\infty}^{\infty} \frac{n}{4} \operatorname{sech}^2 \frac{nx}{2} \, \{F(x) - F(0)\}\, dx \right| \\
&\leq \max |F'(\xi)| \int_{-\infty}^{\infty} \frac{n|x|}{4} \operatorname{sech}^2 \frac{nx}{2} \, dx, -\infty < \xi < \infty \qquad \text{(C.5)}
\end{aligned}
$$

where the last step is accomplished by recourse to the mean value theorem of the differential calculus.

It remains to be shown that the value of the integral in (C.5) tends to zero as $n \to \infty$. this is done by writing

$$
\begin{aligned}
&\int_{-\infty}^{\infty} \frac{n|x|}{4} \operatorname{sech}^2 \frac{nx}{2} \, dx \\
&\quad = \frac{n}{2} \int_{0}^{\infty} x \operatorname{sech}^2 \frac{nx}{2} \, dx \\
&\quad = \frac{1}{2n} \int_{0}^{\infty} t \operatorname{sech}^2 \frac{t}{2} \, dt \\
&\quad \to 0 \text{ as } n \to \infty.
\end{aligned}
$$

It follows that

$$B'(x; 1/n) \sim (B_2 - B_1)\delta(x)$$

and, by the consistency properties proved in [15] page 18,

$$B''(x; 1/n) \sim (B_2 - B_1)\delta'(x).$$

Appendix D

In this appendix the function K^+, obtained by a product split in the course of chapter 4, is shown to have an asymptotic expansion in negative powers of the variable s. From the definition of $K^+(s)$, (5.28),

$$K^+(s) = \sqrt{\frac{\alpha_1}{\alpha_2}} \prod_{n=0}^{\infty} \frac{s+\eta_n}{s+\nu_n} = \sqrt{\frac{\alpha_1}{\alpha_2}} \prod_{n=0}^{\infty} \left(1 + \frac{\eta_n - \nu_n}{s+\nu_n}\right). \tag{D.1}$$

If $|s| > 1 + |\nu_0|$ and $\Im(s) \geq 0$,

$$\begin{aligned} K^+(s) &\leq \sqrt{\frac{\alpha_1}{\alpha_2}} \prod_{n=0}^{\infty} \left(1 + \frac{|\eta_n - \nu_n|}{|s+\nu_n|}\right) \\ &\leq \sqrt{\frac{\alpha_1}{\alpha_2}} (1 + |\eta_0 + \nu_0|) \prod_{n=1}^{\infty} \left(1 + \frac{|\eta_n - \nu_n|}{\Im(\nu_n)}\right) \end{aligned}$$

where the product converges. It follows that $K^+(s) = O(1)$ as $s \to \infty$ in the upper half-plane and by a similar argument that $1/K^-(s) = O(1)$ in the lower half-plane. By the symmetry of the definitions, it is evident that similar arguments are valid for $1/K^+(s)$ in the upper half plane and $K^-(s)$ in the lower half plane.

It is possible to go further than this and obtain asymptotic expansions for the above functions in negative powers of s. For example, from (D.1),

$$K^+(s) = \sqrt{\frac{\alpha_1}{\alpha_2}} \prod_{n=0}^{\infty} \frac{1 + \frac{\eta_n}{s}}{1 + \frac{\nu_n}{s}}$$

$$= \sqrt{\frac{\alpha_2}{\alpha_1}} \exp \sum_{n=0}^{\infty} \left(\frac{\eta_n - \nu_n}{s} - \frac{\eta_n^2 - \nu_n^2}{2s^2} + \frac{\eta_n^3 - \nu_n^3}{3s^3} \right)$$

$$\times \prod_{n=0}^{\infty} \frac{\left(1+\frac{\eta_n}{s}\right) e^{-\frac{\eta_n}{s}+\frac{\eta_n^2}{2s^2}-\frac{\eta_n^3}{3s^3}}}{\left(1+\frac{\nu_n}{s}\right) e^{-\frac{\nu_n}{s}+\frac{\nu_n^2}{2s^2}-\frac{\nu_n^3}{3s^3}}} \tag{D.2}$$

$$= \sqrt{\frac{\alpha_2}{\alpha_1}}\, e^{\frac{a_1}{s}+\frac{a_2}{s^2}+\frac{a_3}{s^3}}\, e^{o(s-3)} \text{ as } s \to \infty$$

$$= \sqrt{\frac{\alpha_2}{\alpha_1}} \left(1+\frac{b_1}{s}+\frac{b_2}{s^2}+\frac{b_3}{s^3}\right) + o(s^{-3}), \tag{D.3}$$

where $b_1 = a_1$, $b_2 = a_2 + a_1^2/2$, $b_3 = a_3 + a_1 a_2 + a_1^3/6$,

$$a_r = (-1)^{r-1} \sum_{n=0}^{\infty} \frac{\nu_n^r - \eta_n^r}{r};\ r = 1, 2, 3.$$

Bibliography

[1] Abrahams I.D., 1986, *Diffraction by a semi-infinite membrane in the presence of a vertical barrier*, J. Sound Vib., **111**, 191–207.

[2] Abrahams, I.D. and Lawrie, J.B., 1995, *Travelling waves on a membrane: reflection and transmission at a corner of arbitrary angle. I*, Proc. R. Soc. Lond., **A451**, 657–683.

[3] Brazier-Smith, P.R., 1987, *The acoustic properties of two co-planar half plates*, Proc. R. Soc. Lond., **A409**, 115–139.

[4] Cannell, P.A., 1975, *Edge scattering of aerodynamic sound by a lightly loaded elastic half plane*, Proc. R. Soc. Lond., **A347**, 213–238.

[5] Cannell, P.A., 1976, *Acoustic edge scattering by a heavily loaded elastic half plane*, Proc. R. Soc. Lond., **A350**, 71–89.

[6] Crighton, D.G.*et al*, 1992, *Modern methods in analytical acoustics*, Springer-Verlag, London

[7] Crighton, D.G. and Oswell, J., 1991, *Fluid loading with mean flow. I. Response of an elastic plate to localized excitation*, Phil. Trans. R. Soc. Lond., **A335**, 557–592.

[8] Evans, D.V., 1985, *A solution of a class of boundary-value problems with smoothly-varying boundary conditions*, Q. Jl Mech. appl. Math. **38**, 521–536.

[9] Fernyhough, M. and Evans, D.V., 1996, *Comparison of a step approximation to an exact solution of acoustic scattering in a uniform-width pipe with nonuniform wall impedance*, Q. Jl Mech. appl. Math., **49**, 419–437.

[10] Fernyhough, M., 1994, *Applications of the residue and modified residue calculus method in linear acoustic and water wave theory*, PhD thesis, University of Bristol

[11] Gradshteyn, J. S. and Ryzhik, I. M., *Tables of Integrals, Series and Products,* 1965, Academic Press

[12] Grant, A.D. and Lawrie, J.B., 2000, *Propagation of fluid-loaded structural waves along a duct with smoothly-varying bending characteristics*, Q. Jl Mech. appl. Math., **52**, 299–321

[13] Koiter, W.T., 1955, *On the diffusion of load from a stiffener into a sheet*, Q Jl Mech. appl. Math., **8**, 164–178

[14] Korn, A. K. and Korn, T. M., *Mathematical Handbook for Scientists and Engineers*, 1968, McGraw-Hill

[15] Lighthill, M.J., 1958, *Introduction to Fourier analysis and generalised functions*, Cambridge University Press.

[16] Milne-Thompson, L.M., 1933, *The calculus of finite differences*, Macmillan and Co., London.

[17] Morse P. M. and Feshbach, H., *Methods of Theoretical Physics*, 1953, McGraw-Hill

[18] Noble, B., 1988, *Methods based on the Wiener-Hopf technique*, Chelsea Publishing Coy., New York.

[19] Norris, A.N. and Wickham, G.R., 1995, *Acoustic diffraction from the junction of two flat plates*, Proc. R. Soc. Lond., **A451**, 631–655.

[20] Olver, F.W.J., *Asymptotics and special functions*, 1974, Academic Press, New York.

[21] Osipov, A.V. and Norris, A.N. 1997, *Acoustic diffraction by a fluid-loaded membrane corner*, Proc. R. Soc. Lond., **A453**, 43–64.

[22] Rawlins, A., 1999, *Diffraction by, or diffusion into a penetrable wedge*, Proc. R. Soc. Lond., **A455**, 2655–2686.

[23] Roseau, M., 1976, *Asymptotic Wave Theory*, North-Holland, Amsterdam.

[24] Timoshenko and Woinowsky-Krieger, *Theory of Plates and Shells*, 1959, McGraw-Hill, New York.

[25] Warren, D.P., Lawrie, J.B. and Mohamed, I.M., *Acoustic scattering in waveguides that are discontinuous in geometry and material property*, 2002, Submitted to Wave Motion.

[26] Whittaker, E.T. and Watson, G.N., 1927, *Modern Analysis*, 4th edition, Cambridge University Press